UNIVERSITY OF CALIFORNIA
RIVERSIDE

The Role of G Protein Signaling Components in Growth and Development of the Filamentous Fungus, *Neurospora crassa*

A Dissertation submitted in partial satisfaction
of the requirements for the degree of

Doctor of Philosophy

in

Genetics, Genomics and Bioinformatics

by

Ilva Esther Cabrera

December 2015

Dissertation Committee:
Dr. Katherine A. Borkovich, Chairperson
Dr. Jason E. Stajich
Dr. Bir Bhanu

The Dissertation of Ilva Esther Cabrera is approved:

_____

_____

_____

Committee Chairperson

University of California, Riverside

Acknowledgements:

The journey through life could not be accomplished without the assistance of many individuals throughout the way. I am extremely indebted with the teachers who made an impact in sparking the passion of science. First and foremost, I have to thank my undergraduate Professor, Dr. Lisa Klig for being such a great mentor and for accepting me in her research group at an early stage during my undergraduate career. Experiencing scientific research gave me the passion to explore life to its fullest. Dr. Klig always supported me in anything I did. She was my strongest supporter when I decided to go to graduate school to pursue a Ph.D. I could have not done it without her!

I am thankful for all my Professors in graduate school. They have advanced my knowledge and undertstanding in Science. Dr. David Carter, for all the technical support provided in microscopy. The time and training you have committed to help has not gone unnoticed. I am intensely grateful to my committee members, Dr. Jason Stajich and Dr. Bir Bhanu. Thank you for taking the time out of your extremely busy schedules to mentor me throughout my Ph.D. Thank you Dr. Bhanu for giving me the opportunity to be a part of the Video Bioinformatics program. I have gained irreplaceable knowledge. Thank You Dr. Stajich for all the many collaborations and the encouraging words when I needed them the most. I owe my graduate school success to my dissertation mentor, Dr. Katherine Borkovich. Thank you for supporting me in every obstacle that came my way. You have been very supportive. You have made me the scientist I am today.

I have to give a special thanks to my “unofficial” mentor, Maria Franco-Aguilar in graduate division. I can recall countless hours of encouragement. You have been the only person who truly understands. Thank you for being you!

A big thanks to Dr. Mead, who has helped me in the latter part of my graduate career.

I thank all my laboratory mates, past and present, for making the lab productive and fun at the same time. They are; Gyungsoon Park, Sara Wright, James Kim, Fitz-Gerald Diala, Carla Eaton, Jackie Servin, Asharie Campbell, Shouqiang Ouyang, Patrick Schacht, Alexander Michkov, Amruta Garud, Arit Ghosh, Caleb Hubbard and Alex Carrillo. Although not a Borkovich lab member, Steven Ahrendt was a fantastic friend in all the many years in graduate school. I will miss our intellectual conversations that we had walking to get coffee. I have made amazing friends throughout the process of graduate school.

I would like to thank my friends and family. At times, I couldn't make it to many family/friends functions, thank you for understanding my busy schedule. I would like to thank my grandfather, Ito, for buying me an encyclopedia set, and for showing me lots of love. Although you are not physically present, you will always be present in my heart.

I would especially like to thank my one true love, my husband Samuel Meleika. Thank you for always being there, and supporting me every step of the way.

Lastly, I would like to thank God for everything. Sometimes I do not understand why things happen, but I do know that all things are planned for Your glory.

Dedication:

I dedicate this dissertation to my husband, Sam.

ABSTRACT OF THE DISSERTATION

The Role of G Protein Signaling Components in Growth and Development of the Filamentous Fungus, *Neurospora crassa*

by

Ilva Esther Cabrera

Doctor of Philosophy, Graduate Program in Genetics, Genomics and Bioinformatics
University of California, Riverside, December 2015
Dr. Katherine A. Borkovich, Chairperson

The G protein signaling pathway is very important in relaying information for growth and development. The main objectives of this dissertation are to: 1. Generate novel image processing tools with the aid of video bioinformatics, 2. Decipher the role of G protein signaling on development and growth through phenotypic analysis and localization studies, and 3. Confirm functions amongst proteins implicated in the Erk1/2 MAPK pathways in *Neurospora crassa.*

In Chapter 2, I used video bioinformatics and image processing tools to develop algorithms that allowed for the analysis of vegetative cell compartment size, conidia size, and growth rate. I used the hyphal compartment size program and found that Δ*gna-1* and Δ*ric8* had smaller length and diameter, whereas Δ*rgs-3*, Δ*rgs-4*, and Δ*rgs-5* had larger compartment sizes. Morphological assays were also conducted on the G signaling components. The results in Chapter 2, suggests that Δ*gna-1* and Δ*ric8* regulate cell compartment size and growth rate in *N. crassa*. In Chapter 3, the phenotypic analysis of available G protein coupled receptor (GPCR) mutants were performed in a collaborative manner, with a majority of contributions by undergraduate students at UCR. All available

GPCR mutants were phenotyped using classical morphological assays, as well as tested on chemicals for resistance or sensitivity on that tested chemical. Publically available gene expression data was obtained in order to compare expression patterns of the GPCR's during growth and development. The results obtained in Chapter 3 improved our knowledge on GPCRs, especially on the Pth-11 related pathogenic receptors. In Chapter 4, the Gα subunits were fluorescently tagged, and their subcellular localization assayed during early development. In Chapter 4, my results demonstrated that all three Gα proteins localize to the plasma membrane in ungerminated conidia and young germlings, with GNA-1 also localizing on septa, and GNA-3 localizing on distinct patches on germlings. Lastly, Chapter 5 examined downstream effectors, specifically the MAK-1 and MAK-2, mitogen-activated protein kinase (MAPK) cascades in two G protein signaling component mutants, *ric8* and *ste50*. The experiments revealed that *ste50* is necessary for phosphorylation of MAK-2 in 16 hr VM liquid cultures and MAK-1 and MAK-2 in 6 day old VM plate cultures. However, MAK-1 and MAK-2 were phosphorylated to wild-type levels in cultures grown on low nitrogen medium (SCM) in Δ*ste50* mutants. The objective of this dissertation was to shed light and expand the knowledge on G protein signaling components and their effects on growth and development in *N. crassa*.

Table of Contents

Title page……..i

Copyright page…….ii

Approval page…….iii

Abstract of the dissertation……...…..vii

Table of contents……..…...ix

List of Tables…..……..…..xii

Table of Figures...……..xiii

Chapter 1. Introduction

Neurospora crassa: Background and Significance to Science....…….……1

Neurospora crassa Life Cycle……...2

Heterotrimeric G protein Signaling in *Neurospora crassa*……...….5

Downstream Effectors of the G Protein Pathway in *Neurospora crassa*….....9

Hypothesis and Objectives…….....11

References……...…….....17

Chapter 2: Quantitative analyses during growth and development in the filamentous fungus, *Neurospora crassa*

Abstract…….....27

Introduction……...…….….27

Materials and Methods…….……...30

Results…….....34

Discussion……...37

References……..…….....60

Chapter 3. Global Analysis of protein coupled receptor genes in the filamentous fungus *Neurospora crassa*

Abstract……...…63

Introduction……...…….…….64

Materials and Methods…….……...67

Results…….....70

Discussion……...91

References……...……...111

Chapter 4. The guanine nucleotide exchange factor RIC8 regulates conidial germination through Gα proteins in *Neurospora crassa*

Abstract……..119

Introduction……...…….....120

Materials and Methods…….…….....123

Results……127

Discussion…….....130

References……...…….....141

Chapter 5. The guanine nucleotide exchange factor RIC8 and STE50 influence Erk class mitogen activated protein kinase activity in *Neurospora crassa*

Abstract……..…….…...144

Introduction……...…….145

Materials and Methods…….……..147

Results…….....151

Discussion……..154

References……..……...…....166

Chapter 6. Conclusions and Future Directions…….……...169

References……...……...…....173

Appendix A: Phenotypic analyses on the regulators of G protein signaling mutants..174

Appendix B: Prediction of gene functions using phenomics in the model filamentous fungus, *Neurospora crassa*……..……...……..…..…….186

List of Tables

Chapter 2

Table 2.1 *N. crassa s*trains used in Chapter 2……..…....40

Table 2.2 Quantitative data for hyphal growth rate and aerial hyphae height……..42

Table 2.3 Conidiation and sexual development phenotypes ……....43

Table 2.4 Results from hyphal cell compartment size video bioinformatics program.....47

Table 2.5 Results of *Δgna-1* and wild type conidial spore size…….....53

Chapter 3

Table 3.1 *Neurospora crassa* G protein coupled receptor gene families and summary of growth/developmental and chemical sensitivity/nutrition phenotypes…….....95

Table 3.2 G protein coupled receptor mutants with chemical sensitivity phenotypes.....100

Chapter 4

Table 4.1 *N. crassa s*trains used in Chapter 4…….....133

Chapter 5

Table 5.1 *N. crassa s*trains used in Chapter 5…….……...158

Table 5.2 Co-immunoprecipitation conditions…….…….…….165

Appendix A

Table A.1 Summary of double mutants…….…….……..……..183

Table A.2 Primers used for confirmation PCRs…….…….…….…...184

Appendix B

Table B.1 Total variance for each component…….…….……..……191

List of Figures

Chapter 1

Figure 1.1 Overall representation of the Heterotrimeric G protein cycle in *N. crassa*…….14

Figure 1.2 Diagram of MAPK pathways in *N. crassa*……..16

Chapter 2

Figure 2.1 Predicted protein topology for RGS 1-5…….41

Figure 2.2 Female fertility assay/plates...……..…….44

Figure 2.3 Female fertility assay/microscopic examination of perithecia ……..…….45

Figure 2.4 Automated analysis of hyphal cell compartments…….…….46

Figure 2.5 Colony edge hyphae stained with calcoflour white……...…….48

Figure 2.6 Conidial spore image processing example…….……...…….52

Figure 2.7 Hyphal growth rate video extraction…….……...…….…….54

Figure 2.8 Determination of hyphal growth rate…….……...…….……55

Figure 2.9 Venn diagram displaying G protein component mutants with phenotypes in growth and development…….....……...…….…….57

Figure 2.10 Proposed pathway in regulating hyphal growth…….…….58

Figure 2.11 Proposed pathway in regulating cell size…….....…….…….59

Chapter 3

Figure 3.1 Venn diagram displaying GPCR mutants with phenotypes in growth and development…….....…….……...…….……..102

Figure 3.2 Perithecial development in *Δgpr-1*, *Δgpr-2* and *Δgpr-3* mutants lacking CRL Class GPCRs…….....…….……..…….……...103

Figure 3.3 Clustering and heatmap generation of mRNA expression data for *N. crassa* GPCR genes during a time course of sexual development……...……...……..…...104

Figure 3.4 GPCR genes during time courses of colony growth and asexual development (conidiation) ……....……...…….....106

Figure 3.5 Expression patterns for 40 predicted GPCR genes on two different carbon sources…….……....……...……..108

Figure 3.6 Phylogenetic analysis of Pth11-related proteins in *N. crassa*……...……..109

Chapter 4

Figure 4.1 Western blot detection of Gα-TagRFP fusion proteins..……...……..134

Figure 4.2 Localization of Gα proteins in germinating conidia..……...…….…..135

Figure 4.3 All three Gα proteins localize to vacuoles……....……...…….…..137

Figure 4.4 Localization of GNA-1-TagRFP and GNA-3-TagRFP with RIC8-GFP in germinating conidia..……...……...…….…..139

Chapter 5

Figure 5.1 Flask morphology of mutants in *N. crassa*..……...…….…..159

Figure 5.2 Colony morphology of mutants in *N. crassa*..……....…….160

Figure 5.3 Lysing enzymes MAPK assay..……..……....……162

Figure 5.4 MAPK assay on VM and SCM plate cultures..…….....164

Appendix A

Figure A.1 Growth analysis assay..……..……....……178

Figure A.2 Spore germination analysis..……..……....……179

Figure A.3 Schematic of the centrifugation process used to obtain the plasma membrane fraction...……..……....……..181

Figure A.4 Gα Protein levels...…….....……..182

Appendix B

Figure B.1 Score plot of all mutants...…….....……..192

Chapter 1

Neurospora crassa: Background and Significance to Science

Neurospora crassa is a multicellular eukaryote belonging to the phylum Ascomycota. *N. crassa* has been designated as the model organism for filamentous fungi by the National Institutes of Health. Achieving this title has been result of extensive work with this organism. *N. crassa* was initially identified as a contaminant in French bakeries in the 1800's (Davis, 2000). Who would have thought that this "red bread mold" would become such a highly studied organism in genetics and biochemistry? Drs. George W. Beadle and Edward L. Tatum were awarded the Nobel Prize in Physiology or Medicine in 1958 for their discovery of the "one gene, one enzyme" theory using *N. crassa* (Beadle & Tatum, 1941). Hallmark discoveries in genetics, such as mechanistic details of meiosis, have been extensively studied using the genetically tractable octad system (Case, M.E. and Giles, 1958). In addition, the strength of *N. crassa* as a genetic system has resulted in the isolation of tens of thousands of mutants from forward and more recently, reverse, genetic screens. Strains containing multiple mutations can be easily isolated simply by crossing the single mutants. This highly studied organism has built and maintained a community that has contributed to scientific advancements. *N. crassa* genome was sequenced in 2003, revealing a 43Mb genome containing approximately 10,000 genes within 7 linkage groups (chromosomes) (Galagan *et al.*, 2003; Borkovich *et al.*, 2004).

The discovery of *mus-51* and *mus- 52*, two genes homologous to *KU70* and *KU80* in humans which are responsible for non-homologous end joining, has facilitated the production of gene deletion mutants (Ninomiya, 2004) Utilization of these two genetic

backgrounds, Δ*mus 51* and Δ*mus 52*, ensures a nearly 100% recombination rate using the hygromycin resistance cassette (*hph*) to replace the target gene (Ninomiya, 2004; Colot *et al.*, 2006). To date, approximately 90% of nuclear genes have been replaced with *hph* and placed in the Fungal Genetics Stock Center (FGSC) where they are available to the scientific community.

Neurospora crassa Life Cycle

The lifecycle of *N. crassa* includes three different developmental pathways: two asexual and one sexual. This complex life-cycle gives *N. crassa* over 28 tissue types (Bistis, 2003). The major tissue type in the organism is hyphae, as it is produced during all phases of the life cycle. Hyphae are the tube-like structures that allows for *N. crassa* to increase its surface area and perform its specialized function as it grows. Hyphae develop cellular compartments, separated by incomplete cell walls (septa) (Harris, 2001). The septal wall contains a pore that allows for cytoplasmic communication and movement of organelles between the cell (Hickey *et al.*, 2002). Six out of the 28 tissue types are specialized hyphae that encompass the asexual and sexual pathways (Riquelme *et al.*). The six specialized hyphal types are leading hyphae, trunk hyphae, aerial hyphae, enveloping hyphae, trichogyne, and ascogenous hyphae (Riquelme *et al.*; Robertson, 1965; Raju, 1980; Bistis, 1981; Read, 1983; Raju, 1992; Read, 1994; Bistis, 2003; Glass *et al.*, 2004; Roca *et al.*, 2005).

N. crassa grows by polar extension, branching, and fusion of hyphae (Buller, 1933; Glass *et al.*, 2004). All three mechanisms of growth involve polarization of the

hyphal tip (Riquelme *et al.*). Hyphae grow in a polar manner, eventually branching and fusing with neighboring vegetative hyphae; ultimately forming the web-like mycelial mat (Davis, 2000). Growth is an essential process required for colonization of dead and decaying plant material by *N. crassa*. In fungal animal and plant pathogens, tip-based (polarized) growth is used for invasion of the host and defects in hyphal morphogenesis compromise the virulence of pathogens (Nichols *et al.*, 2004; Castillo-Lluva *et al.*, 2007).

N. crassa is one of the most rapidly growing filamentous fungi, extending at a rate of 5 mm/hr on solid medium (Ryan *et al.*, 1943; Perkins and Davis, 2000). In filamentous fungi, the complex hypothesized to be responsible for hyphal polarized growth is the Spitzenkorper. The Spitzenkorper is the vesicle organization site, from which vesicles containing components needed for cell wall degradation and synthesis are shuttled (Harris *et al.*, 2005). Cell-wall-synthesizing activity occurs at the hyphal apex to promote hyphal extension (Bartnicki-Garcia *et al.*, 1995). In addition, the position of the Spitzenkorper correlates with the local direction of growth (Reynaga-Pena *et al.*, 1997). Tracking the polarized hyphal tip of *N. crassa* can also be applied to other fungi that grow the same manner. The cytoskeleton is also important for polarized growth. The absence of actin filaments blocks polarized growth and prevents septum formation (Riquelme *et al.*, 1998; Torralba *et al.*, 1998). Microtubules, another component of the cytoskeleton, have also been proposed to play a role during polarized growth. The absence of microtubules leads to loss of directed extension of hyphae and irregular growth patterns (Konzack *et al.*, 2005; Takeshita *et al.*, 2008).

The major asexual sporulation developmental pathway is known as macroconidiation. Macroconidia (conidia) are multinucleate, with 3 to 5 nuclei per cell (Kolmark and Westergaard, 1949). The average diameter of a conidium is 5-10μm (Greenwald *et al.*). Conidia production is initiated by the desiccation of the mycelial mat (Berlin and Yanofsky, 1985). Aerial hyphae begins to grow upwardly, perpendicular to the mycelial mat. Conidia develop in chains at the end of aerial hyphae and are easily dispersed into the environment upon maturation (Greenwald *et al.*).

The second asexual sporulation pathway is microconidiation (Grigg, 1960; Horowitz, 1960). Microconidia, contain only one nucleus and develop from basal vegetative hyphae (Barratt and Garnjobst, 1949). Microconidia spans a diameter of 1μm (Greenwald *et al.*). Due to its small diameter, one can use a ≤ 5μm filtration device to separate microconidia, from conidia and/or hyphae. Ebbole and Sachs described the optimal environmental conditions as; 0.1% synthetic crossing media (SCM), 0.5% sucrose, 2% agar, and 1mM iodoacetate to induce microconidia production from culture (Ebbole, 1990). These conditions will favor the production of homokaryotic microconidia without going through the sexual cycle.

The third type of spore, the ascospore, is produced during sexual reproduction. Sexual reproduction in *N. crassa* involves the fusion of cells from the two mating types, *mat A* and *mat a* (Metzenberg and Glass, 1990; Nelson and Metzenberg, 1992). Either *mat A* and *mat a* can serve as the female (Raju and Leslie, 1992). Nitrogen starvation induces the production of female reproductive structures termed protoperithecia (Read, 1994; Nelson, 1996). The presence of an asexual spore (male) of opposite mating type in

the vicinity will cause a hypha from the protoperithecium to grow towards the male and fuse (Bistis, 1981). This event will cause the uptake of the male nucleus into the protoperithecium. Fertilization and meiosis occur and the female structure then enlarges to form a fruiting body (perithecium) containing the progeny (ascospores) (Raju, 1992; Perkins, 1996). Ascospores are ejected from the mature perithecium into the environment, and are able to germinate, when activated, to form a colony (Lindegren, 1932).

Heterotrimeric G protein signaling in *Neurospora crassa*

Heterotrimeric (αβγ) G proteins are essential components of signal transduction pathways that regulate environmental sensing, growth, and development in eukaryotes (Li *et al.*, 2007). Figure 1.1 provides a schematic overview of the G-protein signaling pathway. Heterotrimeric G proteins are associated with the plasma membrane through G protein coupled receptors (GPCRs). GPCRs are seven transmembrane helix receptors that serve as guanine nucleotide exchange factors (GEFs) for Gα subunits. When a ligand binds to the GPCR a conformational change causes GDP to be exchanged for GTP on the Gα subunit. Subsequently, the Gα dissociates from Gβγ heterodimer (Lambright *et al.*, 1994). Both the Gα–GTP and Gβγ dimer proceed to regulate downstream effectors, such as mitogen activated protein kinase (MAPK) cascades, ion channels, adenylyl cyclases, phosphodiesterases, and phospholipases (Neves *et al.*, 2002; Kays and Borkovich, 2004; Goldsmith and Dhanasekaran, 2007). The Gα subunit contains native GTPase activity, thus hydrolyzes GTP to return to the inactive Gα-GDP form. The process of G protein

hydrolyzing GTP to GDP is considered the rate-limiting step in the cycle (Hamm, 1998). The process of inactivation of the Gα subunit is accelerated via Regulator of G protein Signaling (RGS) proteins, which function as GTPase activating proteins (GAPs) (Neves *et al.*, 2002). Recent studies have identified a cytosolic protein (RIC8) that is able to bypass the GPCR mechanism, and change Gα-GDP to Gα –GTP directly (Miller *et al.*, 2000; Tall *et al.*, 2003; Afshar *et al.*, 2004; Couwenbergs *et al.*, 2004; David *et al.*, 2005; Wright *et al.*, 2011). RIC8 is required for asymmetric cell division in zygotes and priming of synaptic vesicles in *Caenorhabditis elegans* (Miller *et al.*, 2000; Miller and Rand, 2000). In *Drosophila* RIC8 is also required for asymmetrical cell division (Hampoelz *et al.*, 2005). A RIC8 homologue is found in fungi (Gong *et al.*; Kwon *et al.*; Li *et al.*; Wright *et al.*, 2011). Interestingly, a RIC8 homolog are not found in *Saccharomyces cerevisiae*, *Arabidopsis thaliana*, and *Dictyostelium discoideum* (Wilkie and Kinch, 2005). There is one copy of RIC8 in the *N. crassa* genome (Wright *et al.*, 2011). In *N. crassa,* RIC8 plays an essential role in growth and development, as it is needed during spore germination, polar growth, and proper aerial hyphae maintenance (Wright *et al.*, 2011; Eaton *et al.*, 2012). Mutants lacking *ric8* hyper-branch and inappropriately produce conidia in liquid cultures (Wright *et al.*, 2011).

N. crassa provides a robust system for studying the G protein signaling pathway, as it contains three Gα proteins (GNA-1, GNA-2, and GNA-3), one Gβ protein (GNB-1), one Gγ protein (GNG-1), five RGS proteins (RGS-1-5), one RIC8 protein, and 43 predicted GPCRs (Kays and Borkovich, 2004; Li *et al.*, 2007; Cabrera, 2015). The first Gα proteins from filamentous fungi were identified in *N. crassa* (Turner and Borkovich,

1993). Removing *gna-1* and *gna-3* from the genome of *N. crassa* has drastic effects on growth and development. Specifically, studies have found that in Δ*gna-1* mutants are female sterile, and grow more poorly than wild type (Ivey *et al.*, 2002; Kays and Borkovich, 2004). Δ*gna-3* mutants have shorter aerial hyphae and inappropriately conidiate in submerged culture (Kays *et al.*, 2000). Δ*gna-2* mutants do not exhibit a visible phenotype, but when combined with any of the other two Gα mutations, the phenotype is more pronounced than any of the single mutants (Baasiri *et al.*, 1997; Kays and Borkovich, 2004). A Δ*gna-1* Δ*gna- 3* double mutant or a triple mutant lacking all three Gα genes shows severe defects in hyphal extension and very little aerial hyphae (Kays and Borkovich, 2004).

The Gβ subunit plays an important role in Gα protein stability, as deletion of *gnb-1* decreases the protein levels of all three Gαs (GNA-1, GNA-2, and GNA-3) (Yang *et al.*, 2002). Both Δ*gnb-1* and Δ*gng-1* mutants do not differ significantly from wild type in regards to apical extension of basal hyphae (Krystofova and Borkovich, 2005). However, both mutants are female-sterile and inappropriately conidiate in liquid culture (Yang *et al.*, 2002; Krystofova and Borkovich, 2005). These findings suggest the importance of G protein subunits in growth and development.

RGS proteins have not been characterized in *N. crassa*. At the time of this study, *N. crassa* contained five putative RGS genes within its genome: NCU08319 (*rgs-1*), NCU05435 (*rgs-2*), NCU08343 (*rgs-3*), NCU03937 (*rgs-4*), and NCU09983 (*rgs-5*). In 2013, two additional RGS genes were suggested: NCU03153 and NCU09415 (Wang *et al.*, 2013). Functions for these *rgs* genes are unknown (Wang *et al.*, 2013).

RGS proteins must contain an RGS box, which is approximately 130 amino acids in length (Ross and Wilkie, 2000). RGS proteins have been studied in other fungi. *Aspergillus nidulans* and *Saccharomyces cerevisiae* are known to have four and five *rgs* genes respectively (Wang *et al.*, 2013). *Aspergillus nidulans* flbA has been extensively studied (Yu *et al.*, 1996). FlbA is required for development, hyphal growth, and biosynthesis of secondary metabolites (Han *et al.*, 2004; Yu, 2006). In the yeast, *Saccharomyces cerevisiae*, the RGS- Sst2, is a negative regulator during the pheromone response (Chan and Otte, 1982). The Sst2 is homologous to the RGS-1 protein in *N. crassa*. Rgs2 is known to accelerate the hydrolysis of the alpha, Gpa2 (Versele *et al.*, 1999). Rgs2 is homologous to RGS-2 in *N. crassa*. Rax1 is suggested to play a role in the establishment and maintenance of cell polarity (Fujita *et al.*, 2004). The last RGS in yeast is Mdm1, which is required for correct nuclear and mitochondrial inheritance in the presence of high temperatures (McConnell *et al.*, 1990; Fisk and Yaffe, 1997).

There are 43 predicted GPCR's in the *N. crassa* genome (Cabrera, 2015). The predicted *N. crassa* GPCRs fall into twelve of the thirteen classes (I-XII) described for *Verticillium* and *Trichoderma* fungal species (Zheng *et al.*, 2010; Gruber *et al.*, 2013), with a fourteenth class belonging to that containing the pathogenic receptor, Pth11-related (Kulkarni *et al.*, 2005). Currently, five of the 43 predicted *N. crassa* putative GPCR genes have been characterized. Classes I and II contain the pheromone response receptors PRE-2 and PRE-1 (Kim and Borkovich, 2004; Kim *et al.*, 2012). These two GPCRs have been demonstrated to interact with peptide pheromones to regulate female fertility in a mating-type dependent manner (Kim *et al.*, 2002; Kim and Borkovich, 2004,

2006; Kim *et al.*, 2012). The *N. crassa* Class III GPCR is GPR-4, which regulates growth on poor carbon sources (Li and Borkovich, 2006). Class V is the cAMP receptor-like (CRL) group containing GPR-1, GPR-2 and GPR-3 (Borkovich *et al.*, 2004; Krystofova and Borkovich, 2006), which are similar to chemoattractant GPCRs found in *Dictyostelium discoideum* (Klein *et al.*, 1988). There is no evidence that fungal CRLs bind cAMP. *N. crassa* GPR-1 is localized in female reproductive structures and is required for normal formation of perithecial beaks and spore discharge from female fruiting bodies (Krystofova and Borkovich, 2006). Class IX includes the microbial opsins NOP-1 and ORP-1. Heterologous experiments showed that NOP-1 is a light-activated proton pump (Bieszke *et al.*, 1999). Loss of *nop-1* leads to subtle alterations in conidiation and expression of conidiation-specific genes in *N. crassa* (Bieszke *et al.*, 1999; Bieszke *et al.*, 2007). There is no known function for ORP-1.

Downstream effectors of the G protein pathway in *Neurospora crassa*

MAPK pathways are key components in signal transduction, relaying important information in the cell. STE50 is a conserved adaptor protein that regulates MAP kinase signaling. In *Saccharomyces cerevisiae*, ScSte50p is required for the mating repsonse, filamentous growth and osmosensing (Rad *et al.*, 1992; Posas and Saito, 1998; Ramezani Rad *et al.*, 1998). STE50 weakly and transiently interacts with heterotrimeric G proteins, Gαβγ, bound to the pheromone receptor (Ramezani-Rad, 2003). In *Cryptococcus neoformans,* STE50 is required for the pheromone response MAPK pathway (Jung *et al.*, 2011). In *Aspergillus nidulans,* STE50 is responsible for development and secondary

metabolite production (Bayram *et al.*, 2012). *N. crassa* contains one STE50 homolog (NCU00455). Recent studies found that STE50 interacts with NRC-1, the MAPKK, in order to activate of the MAK-2 pathway in *N. crassa* (Dettmann *et al.*, 2014). Thus, STE50 plays an important function in MAPK pathways in fungi.

There are three major MAPK pathways in *N. crassa*: cell wall integrity, cell fusion, and the osmoregulation (Zhang *et al.*, 2002; Borkovich *et al.*, 2004; Pandey *et al.*, 2004; Park *et al.*, 2008). All three pathways are required for female fertility (Park *et al.*, 2011). Figure 1.2 depicts the three MAPK pathways in *N. crassa*. Two of the pathways contain Erk class MAP kinases (MAK-1 and MAK-2; (Pandey *et al.*, 2004; Li *et al.*, 2005; Maerz *et al.*, 2008; Park *et al.*, 2008), while the third cascade has a terminal p38 MAP kinase (OS-2) (Zhang *et al.*, 2002). The MAK-1 and MAK-2 pathways are implicated in control of cell growth and integrity, formation of aerial hyphae and conidia, fusion of conidial anastomosis tubes (CATs), and production of protoperithecia (Pandey *et al.*, 2004; Li *et al.*, 2005; Roca *et al.*, 2005; Maerz *et al.*, 2008; Park *et al.*, 2008; Fu *et al.*, 2011). The MAK-2 pathway plays an important role during homing and fusion of vegetative hyphae (Pandey *et al.*, 2004). The OS-2 cascade is essential for resistance to hyperosmotic stress, resistance to certain fungicides, cell integrity and production of protoperithecia (Fujimura *et al.*, 2000; Zhang *et al.*, 2002; Jones *et al.*, 2007).

Another major downstream signaling pathway is the adenylyl cyclase cascade. G protein signaling regulates the adenylyl cyclase cascade, which is responsible for converting ATP to cAMP (Neves *et al.*, 2002). cAMP can now act upon the catalytic subunit of cAMP- dependent protein kinase (PKA), therefore allowing for

phosphorylation of downstream effectors (Lengeler *et al.*, 2000). *N. crassa* has one adenylyl cyclase protein CR-1 (Ivey *et al.*, 1999). A multitude of studies in *N. crassa* have demonstrated the connection between the G protein signaling pathway with the adenylyl cyclase cascade. Mutants lacking *gna-1*, *gna-3*, *gnb-1*, and *gng-1* genes have low cAMP levels (Ivey *et al.*, 1999; Yang *et al.*, 2002; Krystofova and Borkovich, 2005) and GNA-1 has been demonstrated to directly activate adenylyl cyclase activity (Ivey, Kays).

Hypothesis and Objectives

The G protein signaling pathway plays a vital role in growth and development in the filamentous fungus, *Neursopora crassa*. Due to the complexity of signal transduction, only partial information is known, and the connections between activation of the GEF with downstream effectors remain elusive. The hypothesis of this thesis is that different components of the G protein signaling pathway affect growth in *N. crassa* at different developmental stages. In this thesis, I utilize genetic, molecular biology, microscopy, and bioinformatics tools to elucidate how the G protein components influence growth and development in *N. crassa*.

Aim 1: Obtain quantitative and qualitative information on G protein signaling components during growth and development

There are a number of quantitative and qualitative assays utilized to assay the impact of gene knockouts (Turner, 2011). In addition to these assays performed on the

G protein component mutants, the development of novel computational methods will be accomplished. These methods include measuring colony establishment using video bioinformatics. The development of these tools will streamline the phenotypic analysis, which in turn will give quantitative data in a time saving manner.

Aim 2: Obtain morphological/chemical phenotypes on gene deletion strains and expression data during development for G protein coupled receptors

G protein coupled receptors (GPCRs) are responsible for a plethora of functions, including growth, development and environmental sensing in eukaryotes. The *N. crassa* genome predicts 43 GPCR genes, but only five have been functionally characterized. In this chapter, the remaining available GPCR mutants are characterized morphologically using quantitative and qualitative parameters. In addition, chemicals are utilized to extract any additional phenotypes. Lastly, there is abundant publically available expression data for these genes. Expression data will be analyzed during growth and development.

Aim 3: Determine localization of Gα proteins during conidial germination

Fungal Gα subunits have not been visualized during conidial spore germination. Manipulating fluorescent tagging of proteins will facilitate the visualization of protein localization during conidial development. Localization of the three Gα proteins during conidial germination was probed through analysis of cells expressing fluorescently tagged proteins. Functional TagRFP fusions of each of the three Gα subunits were

constructed through insertion of TagRFP in a conserved loop region of the Gα subunits. Time course studies will reveal localization, and the changes over time will imply functions for the Gα proteins.

Aim 4: Determine the effects of the guanine nucleotide exchange factor, RIC8, and MAPK adaptor protein, STE50, on the MAPK pathways in *Neurospora crassa*

Studies in other fungi have implicated STE50 in MAPK pathways. A potential protein-protein interaction between RIC8 and STE50 was demonstrated using a yeast-2-hybrid screen. Analyzing downstream effects on the MAPK pathways in the single and double mutants will give insight to the network of communication during development.

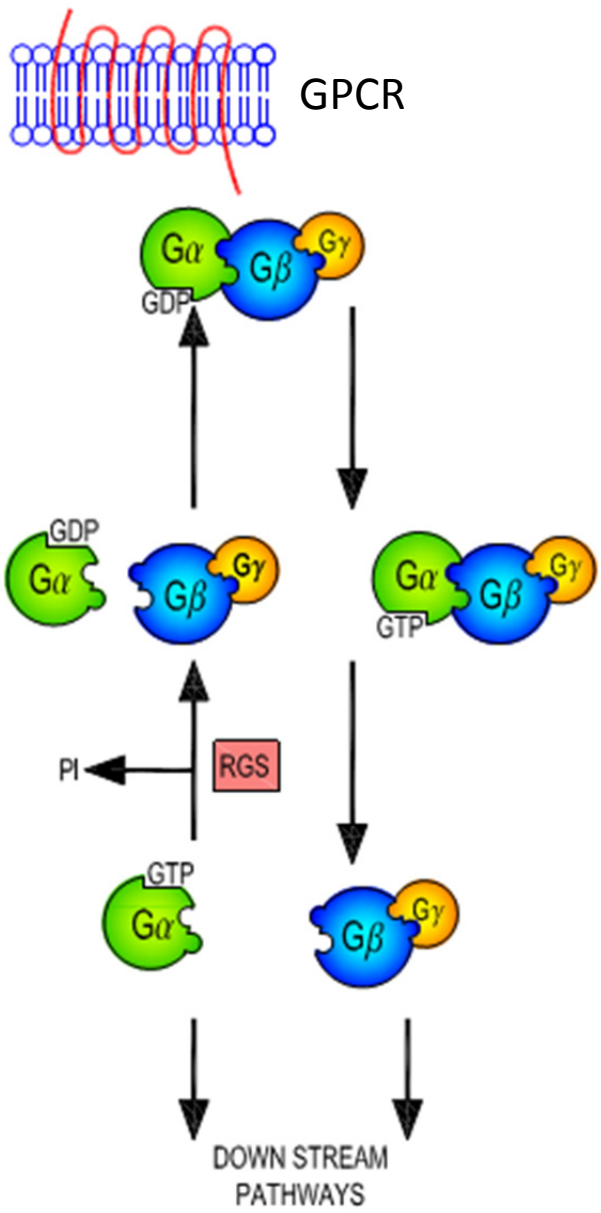
GPCR
Gα
Gβ
Gγ
GDP
GDP
Gα
Gβ
Gγ
Gα
Gβ
Gγ
GTP
PI
RGS
GTP
Gα
Gβ
Gγ
DOWN STREAM
PATHWAYS

Figure 1.1 Overall representation of the Heterotrimeric G protein cycle in *N. crassa*.

An extracellular ligand binds to the G protein coupled receptor (GPCR), causing exchange of GDP for GTP on the Gα subunit. Gα-GTP and Gβɣ dissociate from the GPCR and act on downstream effectors. Gα-GTP will be hydrolyzed to Gα-GDP by the intrinsic GTPase activity of the Gα or by a RGS protein. This Gα-GDP will re-associate with the Gβɣ and the GPCR.

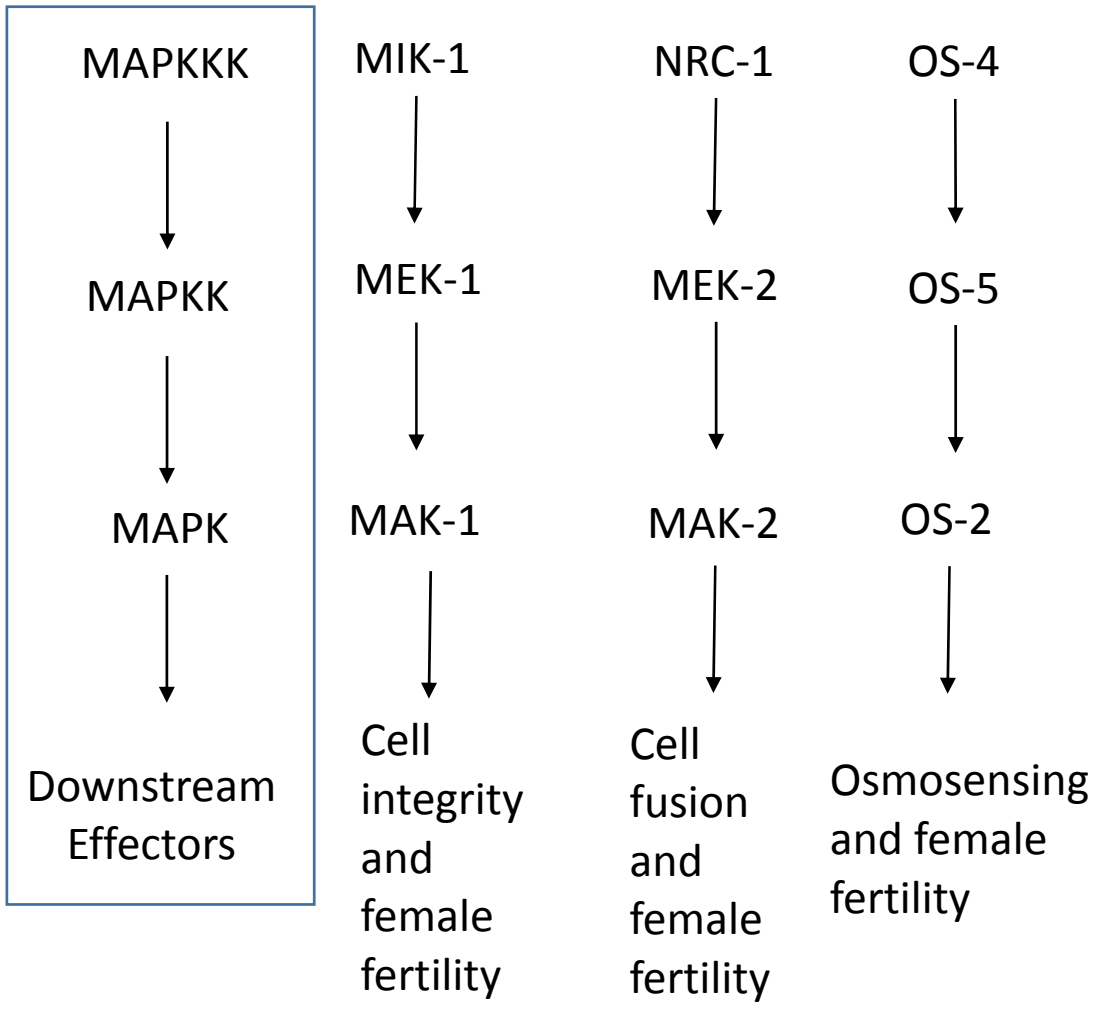

Figure 1.2 Diagram of MAPK pathways in *N. crassa*

N. crassa has genes encoding components for three MAPK pathways within its genome (see schematic on left). These are the cell integrity, cell fusion, and osmosensing pathways. All three pathways are required for female fertility.

References

Afshar, K., Willard, F.S., Colombo, K., Johnston, C.A., McCudden, C.R., Siderovski, D.P., and Gonczy, P. (2004). RIC-8 is required for GPR-1/2-dependent Galpha function during asymmetric division of *C. elegan*s embryos. Cell *119*, 219-230.

Baasiri, R.A., Lu, X., Rowley, P.S., Turner, G.E., and Borkovich, K.A. (1997). Overlapping functions for two G protein alpha subunits in *Neurospora crassa*. Genetics *147*, 137-145.

Barratt, R.W., and Garnjobst, L. (1949). Genetics of a colonial microconidiating mutant strain of *Neurospora crassa*. Genetics *34*, 351-369.

Bartnicki-Garcia, S., Bartnicki, D.D., Gierz, G., Lopez-Franco, R., and Bracker, C.E. (1995). Evidence that Spitzenkorper behavior determines the shape of a fungal hypha: A test of the hyphoid model. Experimental mycology *19*, 153-159.

Bayram, O., Bayram, O.S., Ahmed, Y.L., Maruyama, J., Valerius, O., Rizzoli, S.O., Ficner, R., Irniger, S., and Braus, G.H. (2012). The Aspergillus nidulans MAPK module AnSte11-Ste50-Ste7-Fus3 controls development and secondary metabolism. PLoS Genet *8*, e1002816.

Berlin, V., and Yanofsky, C. (1985). Protein changes during the asexual cycle of *Neurospora crassa*. Mol Cell Biol *5*, 839-848.

Bieszke, J., Li, L., and Borkovich, K. (2007). The fungal opsin gene *nop-1* is negatively-regulated by a component of the blue light sensing pathway and influences conidiation-specific gene expression in *Neurospora crassa*. Curr Genet *52*, 149-157.

Bieszke, J.A., Braun, E.L., Bean, L.E., Kang, S., Natvig, D.O., and Borkovich, K.A. (1999). The *nop-1* gene of *Neurospora crassa* encodes a seven transmembrane helix retinal-binding protein homologous to archaeal rhodopsins. Proc Natl Acad Sci U S A *96*, 8034-8039.

Bistis, G.N. (1981). Chemotropic interactions between trichogynes and conidia of opposite mating-type in *Neurospora crassa*. Mycologia, 959-975.

Bistis, G.N., Perkins, D.D., and Nick D. Read. (2003). Different cell types in *Neurospora crassa*. Fungal Genet. Newsl. , 17-19.

Borkovich, K.A., Alex, L.A., Yarden, O., Freitag, M., Turner, G.E., Read, N.D., Seiler, S., Bell-Pedersen, D., Paietta, J., Plesofsky, N., Plamann, M., Goodrich-Tanrikulu, M., Schulte, U., Mannhaupt, G., Nargang, F.E., Radford, A., Selitrennikoff, C., Galagan, J.E., Dunlap, J.C., Loros, J.J., Catcheside, D., Inoue, H., Aramayo, R., Polymenis, M., Selker,

E.U., Sachs, M.S., Marzluf, G.A., Paulsen, I., Davis, R., Ebbole, D.J., Zelter, A., Kalkman, E.R., O'Rourke, R., Bowring, F., Yeadon, J., Ishii, C., Suzuki, K., Sakai, W., and Pratt, R. (2004). Lessons from the genome sequence of *Neurospora crassa*: tracing the path from genomic blueprint to multicellular organism. Microbiol Mol Biol Rev *68*, 1-108.

Buller, A.H.R. (1933). Researches on Fungi: Longman, London.

Cabrera, I.E., Itallia V. Pacentine , Andrew Lim , Nayeli Guerrero , Svetlana Krystofova , LIande Li , Alexander V. MIchkov , Jacqueline A. Servin , Mr. Steven R. Ahrendt , Alexander J. Carrillo , Liza M. Davidson , Andrew H. Barsoum , Jackie Cao , Ronald Castillo , Wan-Ching Chen , Alex Dinkchian , Stephanie Kim , Sho M. Kitada , Taffani H. Lai , Ashley Mach , Cristin Malekyan , Toua R. Moua , Carlos Rojas Torres , Alaina Yamamoto, and Katherine A. Borkovich. (2015). Global analysis of predicted G protein coupled receptor genes in the filamentous fungus, *Neurospora crassa*. Submitted.

Castillo-Lluva, S., Alvarez-Tabares, I., Weber, I., Steinberg, G., and Perez-Martin, J. (2007). Sustained cell polarity and virulence in the phytopathogenic fungus *Ustilago maydis* depends on an essential cyclin-dependent kinase from the Cdk5/Pho85 family. Journal of cell science *120*, 1584-1595.

Chan, R.K., and Otte, C.A. (1982). Isolation and genetic analysis of Saccharomyces cerevisiae mutants supersensitive to G1 arrest by a factor and alpha factor pheromones. Mol Cell Biol *2*, 11-20.

Colot, H.V., Park, G., Turner, G.E., Ringelberg, C., Crew, C.M., Litvinkova, L., Weiss, R.L., Borkovich, K.A., and Dunlap, J.C. (2006). A high-throughput gene knockout procedure for *Neurospora* reveals functions for multiple transcription factors. Proc Natl Acad Sci U S A *103*, 10352-10357.

Couwenbergs, C., Spilker, A.C., and Gotta, M. (2004). Control of embryonic spindle positioning and Galpha activity by *C. elegans* RIC-8. Curr Biol *14*, 1871-1876.

David, N.B., Martin, C.A., Segalen, M., Rosenfeld, F., Schweisguth, F., and Bellaiche, Y. (2005). Drosophila Ric-8 regulates Galphai cortical localization to promote Galphai-dependent planar orientation of the mitotic spindle during asymmetric cell division. Nat Cell Biol *7*, 1083-1090.

Davis, R. (2000). *Neurospora*: Contributions of a Model Organism. Oxford University Press: New York, N.Y.

Dettmann, A., Heilig, Y., Valerius, O., Ludwig, S., and Seiler, S. (2014). Fungal communication requires the MAK-2 pathway elements STE-20 and RAS-2, the NRC-1 adapter STE-50 and the MAP kinase scaffold HAM-5. PLoS Genet *10*, e1004762.

Eaton, C.J., Cabrera, I.E., Servin, J.A., Wright, S.J., Cox, M.P., and Borkovich, K.A. (2012). The guanine nucleotide exchange factor RIC8 regulates conidial germination through Galpha proteins in *Neurospora crassa*. PLoS One *7*, e48026.

Ebbole, D.a.M.S.S. (1990). A rapid and simple method of isolation of *Neurospora crassa* homokaryons using microconidia. Fungal Genet. Newslett. , 17-18.

Fisk, H.A., and Yaffe, M.P. (1997). Mutational analysis of Mdm1p function in nuclear and mitochondrial inheritance. J Cell Biol *138*, 485-494.

Fu, C., Iyer, P., Herkal, A., Abdullah, J., Stout, A., and Free, S.J. (2011). Identification and characterization of genes required for cell-to-cell fusion in *Neurospora crassa*. Eukaryot Cell *10*, 1100-1109.

Fujimura, M., Ochiai, N., Ichiishi, A., Usami, R., Horikoshi, K., and Yamaguchi, I. (2000). Fungicide resistance and osmotic stress sensitivity in *os* mutants of *Neurospora crassa*. Pestic. Biochem. Physiol. *67*, 125-133.

Fujita, A., Lord, M., Hiroko, T., Hiroko, F., Chen, T., Oka, C., Misumi, Y., and Chant, J. (2004). Rax1, a protein required for the establishment of the bipolar budding pattern in yeast. Gene *327*, 161-169.

Galagan, J.E., Calvo, S.E., Borkovich, K.A., Selker, E.U., Read, N.D., Jaffe, D., FitzHugh, W., Ma, L.J., Smirnov, S., Purcell, S., Rehman, B., Elkins, T., Engels, R., Wang, S., Nielsen, C.B., Butler, J., Endrizzi, M., Qui, D., Ianakiev, P., Bell-Pedersen, D., Nelson, M.A., Werner-Washburne, M., Selitrennikoff, C.P., Kinsey, J.A., Braun, E.L., Zelter, A., Schulte, U., Kothe, G.O., Jedd, G., Mewes, W., Staben, C., Marcotte, E., Greenberg, D., Roy, A., Foley, K., Naylor, J., Stange-Thomann, N., Barrett, R., Gnerre, S., Kamal, M., Kamvysselis, M., Mauceli, E., Bielke, C., Rudd, S., Frishman, D., Krystofova, S., Rasmussen, C., Metzenberg, R.L., Perkins, D.D., Kroken, S., Cogoni, C., Macino, G., Catcheside, D., Li, W., Pratt, R.J., Osmani, S.A., DeSouza, C.P., Glass, L., Orbach, M.J., Berglund, J.A., Voelker, R., Yarden, O., Plamann, M., Seiler, S., Dunlap, J., Radford, A., Aramayo, R., Natvig, D.O., Alex, L.A., Mannhaupt, G., Ebbole, D.J., Freitag, M., Paulsen, I., Sachs, M.S., Lander, E.S., Nusbaum, C., and Birren, B. (2003). The genome sequence of the filamentous fungus *Neurospora crassa*. Nature *422*, 859-868.

Glass, N.L., Rasmussen, C., Roca, M.G., and Read, N.D. (2004). Hyphal homing, fusion and mycelial interconnectedness. Trends Microbiol *12*, 135-141.

Goldsmith, Z.G., and Dhanasekaran, D.N. (2007). G protein regulation of MAPK networks. Oncogene *26*, 3122-3142.

Gong, J., Grodsky, J.D., Zhang, Z., and Wang, P. A Ric8/synembryn homolog promotes Gpa1 and Gpa2 activation to respectively regulate cyclic AMP and pheromone signaling in *Cryptococcus neoformans*. Eukaryot Cell *13*, 1290-1299.

Greenwald, C.J., Kasuga, T., Glass, N.L., Shaw, B.D., Ebbole, D.J., and Wilkinson, H.H. Temporal and spatial regulation of gene expression during asexual development of *Neurospora crassa*. Genetics *186*, 1217-1230.

Grigg, G.W. (1960). The control of conidial differentiation in *Neurospora crassa*. J Gen Microbiol *22*, 662-666.

Gruber, S., Omann, M., and Zeilinger, S. (2013). Comparative analysis of the repertoire of G protein-coupled receptors of three species of the fungal genus Trichoderma. BMC microbiology *13*, 108.

Hamm, H.E. (1998). The many faces of G protein signaling. J Biol Chem *273*, 669-672.
Hampoelz, B., Hoeller, O., Bowman, S.K., Dunican, D., and Knoblich, J.A. (2005). *Drosophila* Ric-8 is essential for plasma-membrane localization of heterotrimeric G proteins. Nat Cell Biol *7*, 1099-1105.

Han, K.H., Seo, J.A., and Yu, J.H. (2004). Regulators of G-protein signalling in *Aspergillus nidulans*: RgsA downregulates stress response and stimulates asexual sporulation through attenuation of GanB (Galpha) signalling. Mol Microbiol *53*, 529-540.

Harris, S.D. (2001). Septum formation in *Aspergillus nidulans*. Curr Opin Microbiol *4*, 736-739.

Harris, S.D., Read, N.D., Roberson, R.W., Shaw, B., Seiler, S., Plamann, M., and Momany, M. (2005). Polarisome meets spitzenkorper: Microscopy, genetics, and genomics converge. Eukaryotic cell *4*, 225-229.

Hickey, P.C., Jacobson, D., Read, N.D., and Glass, N.L. (2002). Live-cell imaging of vegetative hyphal fusion in Neurospora crassa. Fungal Genet Biol *37*, 109-119.

Horowitz, N.H.a.H.M. (1960). The DNA content of *Neurospora* nuclei. Microbial Genet. Bull. *17*, 6-7.

Ivey, F.D., Kays, A.M., and Borkovich, K.A. (2002). Shared and independent roles for a Galpha(i) protein and adenylyl cyclase in regulating development and stress responses in *Neurospora crassa*. Eukaryot Cell *1*, 634-642.

Ivey, F.D., Yang, Q., and Borkovich, K.A. (1999). Positive regulation of adenylyl cyclase activity by a galphai homolog in *Neurospora crassa*. Fungal Genet Biol *26*, 48-61.

Jones, C.A., Greer-Phillips, S.E., and Borkovich, K.A. (2007). The response regulator RRG-1 functions upstream of a mitogen-activated protein kinase pathway impacting asexual development, female fertility, osmotic stress, and fungicide resistance in *Neurospora crassa*. Mol Biol Cell *18*, 2123-2136.

Jung, K.W., Kim, S.Y., Okagaki, L.H., Nielsen, K., and Bahn, Y.S. (2011). Ste50 adaptor protein governs sexual differentiation of Cryptococcus neoformans via the pheromone-response MAPK signaling pathway. Fungal Genet Biol *48*, 154-165.

Kays, A.M., and Borkovich, K.A. (2004). Severe impairment of growth and differentiation in a *Neurospora crassa* mutant lacking all heterotrimeric G alpha proteins. Genetics *166*, 1229-1240.

Kays, A.M., Rowley, P.S., Baasiri, R.A., and Borkovich, K.A. (2000). Regulation of conidiation and adenylyl cyclase levels by the Galpha protein GNA-3 in *Neurospora crassa.* Mol Cell Biol *20*, 7693-7705.

Kim, H., and Borkovich, K.A. (2004). A pheromone receptor gene, *pre-1*, is essential for mating type-specific directional growth and fusion of trichogynes and female fertility in *Neurospora crassa*. Mol Microbiol *52*, 1781-1798.

Kim, H., and Borkovich, K.A. (2006). Pheromones are essential for male fertility and sufficient to direct chemotropic polarized growth of trichogynes during mating in *Neurospora crassa*. Eukaryot Cell *5*, 544-554.

Kim, H., Metzenberg, R.L., and Nelson, M.A. (2002). Multiple functions of *mfa-1*, a putative pheromone precursor gene of *Neurospora crassa*. Eukaryot Cell *1*, 987-999.

Kim, H., Wright, S.J., Park, G., Ouyang, S., Krystofova, S., and Borkovich, K.A. (2012). Roles for receptors, pheromones, G proteins, and mating type genes during sexual reproduction in *Neurospora crassa*. Genetics *190*, 1389-1404.

Klein, P.S., Sun, T.J., Saxe, C.L., 3rd, Kimmel, A.R., Johnson, R.L., and Devreotes, P.N. (1988). A chemoattractant receptor controls development in *Dictyostelium discoideum*. Science *241*, 1467-1472.

Kolmark, G., and Westergaard, M. (1949). Induced back-mutations in a specific gene of *Neurospora crassa*. Hereditas *35*, 490-506.

Konzack, S., Rischitor, P.E., Enke, C., and Fischer, R. (2005). The role of the kinesin motor KipA in microtubule organization and polarized growth of *Aspergillus nidulans*. Molecular biology of the cell *16*, 497-506.

Krystofova, S., and Borkovich, K.A. (2005). The heterotrimeric G-protein subunits GNG-1 and GNB-1 form a Gbetagamma dimer required for normal female fertility, asexual development, and galpha protein levels in *Neurospora crassa*. Eukaryot Cell *4*, 365-378.

Krystofova, S., and Borkovich, K.A. (2006). The predicted G-protein-coupled receptor GPR-1 is required for female sexual development in the multicellular fungus *Neurospora crassa*. Eukaryot Cell *5*, 1503-1516.

Kulkarni, R.D., Thon, M.R., Pan, H., and Dean, R.A. (2005). Novel G-protein-coupled receptor-like proteins in the plant pathogenic fungus *Magnaporthe grisea*. Genome biology *6*, R24.

Kwon, N.J., Park, H.S., Jung, S., Kim, S.C., and Yu, J.H. The putative guanine nucleotide exchange factor RicA mediates upstream signaling for growth and development in *Aspergillus*. Eukaryot Cell *11*, 1399-1412.

Lambright, D.G., Noel, J.P., Hamm, H.E., and Sigler, P.B. (1994). Structural determinants for activation of the [alpha]-subunit of a heterotrimeric G protein. Nature *369*, 621-628.

Lengeler, K.B., Davidson, R.C., D'Souza, C., Harashima, T., Shen, W.C., Wang, P., Pan, X., Waugh, M., and Heitman, J. (2000). Signal transduction cascades regulating fungal development and virulence. Microbiol Mol Biol Rev *64*, 746-785.

Li, D., Bobrowicz, P., Wilkinson, H.H., and Ebbole, D.J. (2005). A mitogen-activated protein kinase pathway essential for mating and contributing to vegetative growth in *Neurospora crassa*. Genetics *170*, 1091-1104.

Li, L., and Borkovich, K.A. (2006). GPR-4 is a predicted G-protein-coupled receptor required for carbon source-dependent asexual growth and development in *Neurospora crassa*. Eukaryot Cell *5*, 1287-1300.

Li, L., Wright, S.J., Krystofova, S., Park, G., and Borkovich, K.A. (2007). Heterotrimeric G protein signaling in filamentous fungi. Annu Rev Microbiol *61*, 423-452.

Li, Y., Yan, X., Wang, H., Liang, S., Ma, W.B., Fang, M.Y., Talbot, N.J., and Wang, Z.Y. MoRic8 Is a novel component of G-protein signaling during plant infection by the rice blast fungus *Magnaporthe oryzae*. Mol Plant Microbe Interact *23*, 317-331.

Lindegren, C.C. (1932). The genetics of *Neurospora* I. The inheritance of response to heat-treatment. Bull Torrey Botanicals Club, 85-102.

Maerz, S., Ziv, C., Vogt, N., Helmstaedt, K., Cohen, N., Gorovits, R., Yarden, O., and Seiler, S. (2008). The nuclear Dbf2-related kinase COT1 and the mitogen-activated protein kinases MAK1 and MAK2 genetically interact to regulate filamentous growth, hyphal fusion and sexual development in *Neurospora crassa*. Genetics *179*, 1313-1325.

McConnell, S.J., Stewart, L.C., Talin, A., and Yaffe, M.P. (1990). Temperature-sensitive yeast mutants defective in mitochondrial inheritance. J Cell Biol *111*, 967-976.

Metzenberg, R.L., and Glass, N.L. (1990). Mating type and mating strategies in *Neurospora*. BioEssays *12*, 53-59.

Miller, K.G., Emerson, M.D., McManus, J.R., and Rand, J.B. (2000). RIC-8 (Synembryn): a novel conserved protein that is required for G(q)alpha signaling in the *C. elegans* nervous system. Neuron *27*, 289-299.

Miller, K.G., and Rand, J.B. (2000). A role for RIC-8 (Synembryn) and GOA-1 (G(o)alpha) in regulating a subset of centrosome movements during early embryogenesis in *Caenorhabditis elegans*. Genetics *156*, 1649-1660.

Nelson, M.A. (1996). Mating systems in ascomycetes: a romp in the sac. Trends Genet *12*, 69-74.

Nelson, M.A., and Metzenberg, R.L. (1992). Sexual development genes of *Neurospora crassa*. Genetics *132*, 149-162.

Neves, S.R., Ram, P.T., and Iyengar, R. (2002). G protein pathways. Science *296*, 1636-1639.

Nichols, C.B., Fraser, J.A., and Heitman, J. (2004). PAK kinases Ste20 and Pak1 govern cell polarity at different stages of mating in *Cryptococcus neoformans*. Molecular biology of the cell *15*, 4476-4489.

Ninomiya, Y., K. Suzuki, C. Ishii, and H. Inoue. . (2004). Highly efficient gene replacements in*Neurospora* strains deficient for nonhomologous end-joining. *Neurospora* strains deficient for nonhomologous end-joining. . Proc Natl Acad Sci U S A, 12248-12253

Pandey, A., Roca, M.G., Read, N.D., and Glass, N.L. (2004). Role of a mitogen-activated protein kinase pathway during conidial germination and hyphal fusion in *Neurospora crassa*. Eukaryot Cell *3*, 348-358.

Park, G., Pan, S., and Borkovich, K.A. (2008). Mitogen-activated protein kinase cascade required for regulation of development and secondary metabolism in *Neurospora crassa*. Eukaryot Cell *7*, 2113-2122.

Park, G., Servin, J.A., Turner, G.E., Altamirano, L., Colot, H.V., Collopy, P., Litvinkova, L., Li, L., Jones, C.A., Diala, F.G., Dunlap, J.C., and Borkovich, K.A. (2011). Global analysis of serine-threonine protein kinase genes in *Neurospora crassa*. Eukaryot Cell *10*, 1553-1564.

Perkins, D.D. (1996). Details for collection of asci as unordered groups of eight projected ascospores. *Neurospora* Newsl. *9*, 11.

Perkins, D.D., and Davis, R.H. (2000). *Neurospora* at the millennium. Fungal genetics and biology : FG & B *31*, 153-167.

Posas, F., and Saito, H. (1998). Activation of the yeast SSK2 MAP kinase kinase kinase by the SSK1 two-component response regulator. EMBO J *17*, 1385-1394.

Rad, M.R., Xu, G., and Hollenberg, C.P. (1992). STE50, a novel gene required for activation of conjugation at an early step in mating in *Saccharomyces cerevisiae*. Mol Gen Genet *236*, 145-154.

Raju, N.B. (1980). Meiosis and ascospore genesis in *Neurospora*. European Journal of Cell Biology *23*, 208-223.

Raju, N.B. (1992). Genetic control of the sexual cycle in *Neurospora*. Mycologia Research *96*, 241-262.

Ramezani-Rad, M. (2003). The role of adaptor protein Ste50-dependent regulation of the MAPKKK Ste11 in multiple signalling pathways of yeast. Curr Genet *43*, 161-170.

Ramezani Rad, M., Jansen, G., Buhring, F., and Hollenberg, C.P. (1998). Ste50p is involved in regulating filamentous growth in the yeast *Saccharomyces cerevisiae* and associates with Ste11p. Mol Gen Genet *259*, 29-38.

Read, N.D. (1983). A scanning electron microscopic study of the external features of perithecium development in *Sordaria humana*. Canadian Journal of Botany, 3217-3229.

Read, N.D. (1994). Cellular nature and multicellular morphogenesis of higher fungi. Academic Press: London.

Reynaga-Pena, C.G., Gierz, G., and Bartnicki-Garcia, S. (1997). Analysis of the role of the Spitzenkorper in fungal morphogenesis by computer simulation of apical branching in *Aspergillus niger*. Proc Natl Acad Sci U S A *94*, 9096-9101.

Riquelme, M., Reynaga-Pena, C.G., Gierz, G., and Bartnicki-Garcia, S. (1998). What determines growth direction in fungal hyphae? Fungal genetics and biology : FG & B *24*, 101-109.

Riquelme, M., Yarden, O., Bartnicki-Garcia, S., Bowman, B., Castro-Longoria, E., Free, S.J., Fleissner, A., Freitag, M., Lew, R.R., Mourino-Perez, R., Plamann, M., Rasmussen, C., Richthammer, C., Roberson, R.W., Sanchez-Leon, E., Seiler, S., and Watters, M.K. Architecture and development of the *Neurospora crassa* hypha - a model cell for polarized growth. Fungal Biol *115*, 446-474.

Robertson, N.F. (ed.) (1965). The mechanism of cellular extension and branching. Academic Press: New York.

Roca, M.G., Arlt, J., Jeffree, C.E., and Read, N.D. (2005). Cell biology of conidial anastomosis tubes in Neurospora crassa. Eukaryot Cell *4*, 911-919.

Ross, E.M., and Wilkie, T.M. (2000). GTPase-Activating Proteins for heterotrimeric G proteins: Regulators of G protein signaling (RGS) and RGS-like proteins. Annu Rev Biochem, 795-827.

Ryan, F.J., Beadle, G.W., and Tatum, E.L. (1943). The tube method of measuring the growth rate of *Neurospora*. Amer J Bot *30*, 784-799.

Takeshita, N., Higashitsuji, Y., Konzack, S., and Fischer, R. (2008). Apical sterol-rich membranes are essential for localizing cell end markers that determine growth directionality in the filamentous fungus *Aspergillus nidulans*. Molecular biology of the cell *19*, 339-351.

Tall, G.G., Krumins, A.M., and Gilman, A.G. (2003). Mammalian Ric-8A (synembryn) is a heterotrimeric Galpha protein guanine nucleotide exchange factor. J Biol Chem *278*, 8356-8362.

Torralba, S., Raudaskoski, M., Pedregosa, A.M., and Laborda, F. (1998). Effect of cytochalasin A on apical growth, actin cytoskeleton organization and enzyme secretion in *Aspergillus nidulans*. Microbiology *144 (Pt 1)*, 45-53.

Turner, G.E. (2011). Phenotypic analysis of *Neurospora crassa* gene deletion strains. Methods Mol Biol *722*, 191-198.

Turner, G.E., and Borkovich, K.A. (1993). Identification of a G protein alpha subunit from *Neurospora crassa* that is a member of the Gi family. J Biol Chem *268*, 14805-14811.

Versele, M., de Winde, J.H., and Thevelein, J.M. (1999). A novel regulator of G protein signalling in yeast, Rgs2, downregulates glucose-activation of the cAMP pathway through direct inhibition of Gpa2. EMBO J *18*, 5577-5591.

Wang, Y., Geng, Z., Jiang, D., Long, F., Zhao, Y., Su, H., Zhang, K.Q., and Yang, J. (2013). Characterizations and functions of regulator of G protein signaling (RGS) in fungi. Appl Microbiol Biotechnol *97*, 7977-7987.

Wilkie, T.M., and Kinch, L. (2005). New roles for Galpha and RGS proteins: communication continues despite pulling sisters apart. Curr Biol *15*, R843-854.

Wright, S.J., Inchausti, R., Eaton, C.J., Krystofova, S., and Borkovich, K.A. (2011). RIC8 is a guanine-nucleotide exchange factor for Galpha subunits that regulates growth and development in *Neurospora crassa*. Genetics *189*, 165-176.

Yang, Q., Poole, S.I., and Borkovich, K.A. (2002). A G-protein beta subunit required for sexual and vegetative development and maintenance of normal G alpha protein levels in *Neurospora crassa*. Eukaryot Cell *1*, 378-390.

Yu, J.H. (2006). Heterotrimeric G protein signaling and RGSs in *Aspergillus nidulans*. J Microbiol *44*, 145-154.

Yu, J.H., Wieser, J., and Adams, T.H. (1996). The *Aspergillus* FlbA RGS domain protein antagonizes G protein signaling to block proliferation and allow development. EMBO J *15*, 5184-5190.

Zhang, Y., Lamm, R., Pillonel, C., Lam, S., and Xu, J.R. (2002). Osmoregulation and fungicide resistance: the Neurospora crassa os-2 gene encodes a HOG1 mitogen-activated protein kinase homologue. Appl Environ Microbiol *68*, 532-538.

Zheng, H., Zhou, L., Dou, T., Han, X., Cai, Y., Zhan, X., Tang, C., Huang, J., and Wu, Q. (2010). Genome-wide prediction of G protein-coupled receptors in *Verticillium spp*. Fungal biology *114*, 359-368.

Chapter 2

Quantitative analyses during growth and development in the filamentous fungus, *Neurospora crassa*

Abstract

G-protein signaling plays essential roles during many processes in eukaryotic cells. In this study, we have analyzed several components of G-protein signaling using phenotypic assays, as well as novel methods that extract quantitative data from images and videos. Phenotypic data was extracted from images from many developmental stages, specifically during the formation of a colony. We are the first to analyze the asexual spore (conidia) size, hyphal compartment size, and hyphal growth rate in an automated manner using image processing algorithms. The growth rates from wild type and mutants were extracted from videos captured using phase microscopy. This automated method is time saving, eliminates subjectivity, and allows for high-throughput analysis.

Introduction

N. crassa grows very rapidly through polar extension of tube-like structures called hyphae. Hyphae are a major tissue type that is essential during the colonization process. As hyphae grow, septa are laid down between cell compartments. The average diameter for *N. crassa* are about 4-12μm (Mclean, 1987).

N. crassa uses three different developmental pathways to produce three different types of spores. The major asexual sporulation developmental pathway is known as macroconidiation. Macroconidia, also referred to as conidia, are multinucleate, containing 3 to 5 nuclei per cell (Kolmark and Westergaard, 1949). These conidia develop in chains at the end of aerial hyphae and are easily dispersed into the environment upon maturation. Spores produced during the second asexual sporulation pathway, microconidia, contain only one nucleus and develop from basal vegetative hyphae (Barratt and Garnjobst, 1949). The third type of spore is produced during sexual reproduction. Ascospores are ejected from the mature perithecium into the environment, and are able to germinate to form a colony upon heat activation (Lindegren, 1932).

Studies suggest that perturbation of components in the G protein signaling pathway results in altered growth and development in *N. crassa*. *N. crassa* contains three Gα proteins (GNA-1, GNA-2, and GNA-3), one cytosolic guanine nucleotide exchange factor (GEF; RIC8), one Gβ protein (GNB-1), one Gγ protein (GNG-1) and five Regulators of G protein signaling (RGS) proteins (RGS-1-5). The RGS proteins are negative regulators in the G protein signaling pathway that have not been characterized in *N. crassa*. RGS proteins can accelerate hydrolysis of GTP bound to the Gα subunit more than 2000 times fold faster than the native Gα GTPase activity (Ross and Wilkie, 2000). All five RGS proteins contain a highly conserved RGS box. In addition, RGS-3, RGS-4 and RGS-5 contain a transmembrane domain (Figure 2.1). Interestingly, RGS-5 contains a seven-transmembrane domain resembling a GPCR.

Conventionally, data is gathered via manual analysis by multiple experts who would repeat the same measurements multiple times for the same image in order to increase the accuracy of the results. Cell compartment properties are quantified by examining morphology. Diameter and length can be taken manually, however measuring the area and perimeter will be much more difficult, not to mention time consuming. Conidial spore size can be estimated by taking manual measurements, but will be very tedious and time consuming. Extracting information from videos are nearly impossible to do manually. Therefore, developing a program that can automate these processes was a high priority. In collaboration with graduate students and faculty in the Video Bioinformatics, NSF-IGERT program, at the University of California, Riverside, we have developed a graphical user interphase (GUI) for cell compartment analysis. MATLAB code was develop for conidial spore area as well as hyphal growth rate. As more data is collected, they can be ran through these algorithms in order to obtain quantifiable results. An automated program not only removes the user's subjectivity on the analysis process, but also saves time. The major focus of this research project is the analysis via quantitative and qualitative methods of components of G protein signaling during development and growth.

The text of Chapter two of this dissertation contains reprint of material published in "Video Bioinformatics - From Live Imaging to Knowledge", Springer 2016. ISBN: 978-3-319-23723-7 with the title "Quantitative analyses using Video Bioinformatics and image analysis tools during growth and development in the multicellular fungus *Neurospora crassa*," with additions to include the G protein pathway mutants. I was

responsible for obtaining data and optimizing the conditions needed to proceed with the video bioinformatics program. Images for cell compartment size were obtained by undergraduate students, Caleb Hubbard and Alexander Carrillo under my supervision. Assistance with phenotyping G- protein mutants was provided by Alexander Carrillo, again under my supervision. All analysis was conducted independently. I would like to acknowledge Asongu Tambo for the development of the growth rate program and the assistance with optimizing the conidia cell size program; Dr. Albert Cruz for the development of the hyphal compartment size program and Benjamin Guan for the assistance with removing the halo produced from the phase microscopy images using MATLAB for the conidia size program. I would also like to acknowledge Drs. Bir Bhanu and Katherine A. Borkovich, who contributed assistance and supervision.

Materials and Methods

Growth and developmental phenotypes:

N. crassa strains used in this study are listed in Table 2.1. Conidia from 5-7 day old flask or slant cultures were used to inoculate all media. Phenotypic assays were conducted as described (Park *et al.*, 2011; Turner, 2011; Ghosh *et al.*, 2014). Manual growth rate analysis was measured using 25 ml plastic disposable pipets containing 13 ml of solid Vogel's Minimal (VM) medium (Vogel, 1964; White and Woodward, 1995). For asexual phenotypic assays, 2 ml of VM liquid medium or 2 ml of liquid VM

supplemented with 2% yeast extract were inoculated with a small amount of conidia or hyphae. Tubes were incubated stationary in the dark at 30°C for three days. For sexual development assays, strains were inoculated on slants containing 6 ml synthetic crossing medium agar [SCM; (Westergaard and Mitchell, 1947)]. These slants were then incubated under constant light for one week at room temperature. Protoperithecia were scored 7 days after inoculation. Cultures were fertilized using conidia from a wild type strain of opposite mating type at seven days post-inoculation. Formation of perithecia was scored one week after fertilization and beak morphology and ascospore ejection two weeks after fertilization. Wild type strain (FGSC 4200; *mat a*) was used as a control.

Video bioinformatics analyses:

For obtaining hyphal compartment size, conidia were inoculated in the center of a 100 x 15mm petri plate containing 12 ml of VM with 1% agar as a solidifying agent (Vogel, 1964). Cultures were incubated for 20-22 hour at 30°C in the dark to allow formation of hyphae. Vegetative hyphae were stained using a 1:1 ratio of Calcoflour White in VM liquid medium (Elorza *et al.*, 1983). The "inverted agar block method" described in (Hickey *et al.*, 2004) was used to visualize the sample using an Olympus IX71 inverted microscope (Olympus America, Center Valley, PA) with a 40x phase objective. Several images (10-15) were collected for each mutant strain.

For the cell compartment size program, pixel intensity value with a probabilistic framework, and a normal distribution in computation was used to find the region of

interest (ROI) (Gopinath *et al.*, 2008), a normal distribution is applied as a point spread function and segmentation (Su *et al.*, 2013). These operations were performed using MATLAB software (2010).

To quantify conidia area, conidia from 5-7 day old 2 ml VM slant cultures were collected using 1 ml of sterile water. The suspension was diluted 1:50 and visualized using an Olympus IX71 inverted microscope (Olympus America, Center Valley, PA) with a 40x phase objective. Several images were collected for analysis.

The algorithm to detect the conidia uses a Gabor filter to enhance the effect of the halo, produced by phase microscopy, for cell region detection (Mehrotra *et al.*, 1992). After filtering, a simple thresholding by Otsu's method is used for segmenting out cell regions from non-cell regions (Otsu, 1979). These operations are performed using MATLAB software (2010).

For hyphal growth video microcopy analysis, cultures, 5-7 day old, were used in this study. The "inverted agar block method" described in (Hickey *et al.*, 2004) was used to visualize the sample using an Olympus IX71 inverted microscope (Olympus America, Center Valley, PA) with a 100x phase objective. Frames were captured at a speed of one frame every second for five minutes (300 seconds).

Video analysis for quantifying growth rate was performed using MATLAB software (2010). For each image in the video sequence, image segmentation was performed to distinguish the hypha (foreground) from the medium (background). This process was achieved using an edge-based active contour model as outlined in (Li *et al.*,

2010). The algorithm was provided with an initial contour that it collapses using gradient-descend to find the shape of the hypha. The result of this process was a binary image where the foreground pixels have a value of 1 and the background pixels are 0. The extracted shape of the hypha is further collapsed inward using gradient descend and the distance transform image to find the internal line of symmetry of the hypha. The tip of the line is projected to intersect with the contour of shape to form the complete line of symmetry. This line is used to compute the length of the hypha via Euclidean distance.

Statistical image analysis:

For quantitative growth and developmental assays (apical extension rate and aerial hyphae height), mutant replicate data was compared to its corresponding wild type using a t-test in Excel (2013).

Manual analysis of the length and diameter were also performed (data not shown). No differences between manual and automated lengths were found. Statistical analysis (t-test) was used to compare methods and performed using Excel (2013).

Minitab 17 software (2010) was used for the statistical analyses of the cell compartment size. Mutant replicate from each image was compiled and organized by category (major axis [length], minor axis [diameter], area, and perimeter). Each category was entered and the data was compared with wild type using a t-test.

Results

Quantitative and qualitative phenotypic analyses of mutants lacking G protein signaling components

Previous research has shown that GNA-1, GNB-1, GNG-1 and RIC8 play important roles during growth and development in *N. crassa* (Yang *et al.*, 2002; Kays and Borkovich, 2004; Krystofova and Borkovich, 2005; Wright *et al.*, 2011). This study focused on the negative regulators of G protein signaling, the *rgs* genes. Additional phenotypic and molecular analyses for RGS single mutants and mutants lacking multiple RGS genes are included in Appendix A.

N. crassa was analyzed for basal vegetative growth, as well as aerial hyphae height under two different media conditions (Table 2.2). Statistical analyses were performed on the experimental results. Strains that were found to be statistically significantly different than wild type during vegetative growth were the Δ*gna-1*, Δ*gnb-1*, Δ*gng-1*, Δ*ric8*, and Δ*rgs-1* mutants. Therefore suggesting, that these genes are playing a role in hyphal growth and aerial hyphae formation.

Asexual development (aerial hyphae height) was measured on VM and VM supplemented with yeast extract. Mutants that showed a statistically significant result on VM alone when compared to wild type were Δ*gna-1*, Δ*gna-3*, Δ*gnb-1*, Δ*ric8* and Δ*rgs-2*. Yeast extract provides additional nutrients, including amino acids and nucleotides. Suggesting if the mutated gene plays a role in any of these nutritional biochemical

pathways, then yeast extract supplementation may restore the mutant back or close to wild type growth. Mutants that showed a statistically significant result on VM + 2% yeast extract when compared to wild type were Δ*gna-1*, Δ*gnb-1*, Δ*gng-1*, Δ*ric8* and Δ*rgs-2* (Table 2.2). Although supplementation with yeast extract increased the aerial hyphae height for Δ*rgs-2*, the increase was not enough to make it non-significant. Finally, assessment of conidiation in slants showed that Δ*rgs-2* and Δ*rgs-1* were the only two RGS mutants that had a reduced conidiation phenotype (Table 2.3).

Sexual development phenotypic assays were conducted as described in the Materials and Methods. The findings confirmed published results for Δ*gna-1*, Δ*gnb-1* and Δ*ric8* (Kays and Borkovich, 2004; Krystofova and Borkovich, 2005; Wright *et al.*, 2011). The female fertility of Δrg*s-3*, Δ*rgs-4*, and Δ*rgs-5* was similar to wild type. Δ*rgs-2* mutants produced very few protoperithecia and perithecia, but were able to shoot some ascospores (Table 2.3, Figure 2.2, Figure 2.3). Although Δ*rgs-1* produced a few protoperithecia, this strain never developed perithecia, thus causing it to be female-sterile (Table 2.3, Figure 2.2, Figure 2.3). Plate examinations of the *rgs* mutants are in found in Figure 2.2 and Figure 2.3. The results for the *rgs-1* and *rgs-2* mutants suggest that cycling of GDP and GTP on Gα subunit(s) is necessary for female fertility in *N. crassa*; constitutive occupancy with GTP does not favor fertility. This hypothesis was previously suggested to explain why introduction of a GTPase-deficient form of *gna-1* into a mutant lacking a pheromone receptor did not rescue its female sterility (Kim and Borkovich, 2004).

The first set of automated quantitative assays was focused on cell compartment size during vegetative growth. Figure 2.4 shows an example of an imaged being processed with the compartment size program GUI. This method allows the user to select the cell or cells of interest in a rapid, non-biased manner. The automated method detects the walls that separate the hyphal compartments, reducing the ROI into separate compartments. Once the cells have been selected, quantitative data for length, width (diameter), area, and perimeter are stored as a comma separated values (CSV) file, which can then be used for statistical analyses. Statistical analysis confirmed that there was no statistical difference between manual analysis and the automated method (Data not shown).

The program was used to analyze 12 strains, including wild type. Table 2.4 summarizes the results obtained for hyphal length, diameter, area, and perimeter. Figure 2.5 are the images representing the mutants. Both Δ*ric8* and Δ*gna-1* mutants have drastically narrower and smaller compartment size (Figure 2.3). The cell size program confirms these findings, by indicating that Δ*ric8* and Δ*gna-1* strains are statistically smaller than wild type using all three parameters (Table 2.4). In addition, Δ*rgs-1* is also smaller in all three analyzed parameters (Table 2.4). Δ*rgs-2* is not statistically smaller in compartment length, however it is smaller in diameter, area, and perimeter. Interestingly, the results from the program showed that Δ*rgs-3*, Δ*rgs*-4, and Δ*rgs-5* were statistically larger than wild type. Small hyphal compartment size might explain growth rate defects in these mutants. As seen in Table 2.2, Δ*ric8* and Δ*gna-1* both have statistically slower basal hyphae linear growth rate. These results for the *gna-1*, *rgs-3*, *rgs-4*, and *rgs-5*

suggests that the Gα and the RGS' are functioning in opposite roles in cell compartment size. The absence of *gna-1* is causing cell size to be narrower and smaller, whereas, maintaining the Gα constitutively active (Gα-GTP) causes the cells to be larger.

The second program quantified conidial spore size. Figure 2.6 shows an example of an image being processed via this program. Previously research noted that Δ*gna-1* conidia appeared smaller than wild type (Ivey *et al.*, 1996). Here, application of the conidial spore size program leads to the same finding, that Δ*gna-1* conidia spores are smaller than wild type (Table 2.5). Further directions will include testing the other G protein components mutants with this program.

Video microscopy was also performed for wild type and the Δ*gna-1* mutant strain. An example of the algorithm process is found in Figure 2.7. Both strains were processed as mentioned in the Materials and Methods. The results with wild type (Fig. 2.8A) suggest that overall hyphal growth rate is linear at a velocity of 0.207 μm/sec. As expected, the results for Δ*gna-1* also demonstrated linear growth. However, the velocity was slower than that of wild type, at 0.061 μm/sec (Fig. 2.8B). Previous published results involving manual calculations reported the growth rate for wild type vegetative hyphae as 0.201μm/s (Lopez-Franco *et al.*, 1994), which is very close to our finding of 0.207μm/s.

Discussion

In this study, we have analyzed *N. crassa* during growth and development using classical phenotypic assays, as well as using novel Video Bioinformatic imaging tools.

Classical phenotypic assays revealed 8 of the 11 G-protein signaling pathway mutants were defective at least one of these growth and developmental pathways. A Venn diagram summarizing phenotypes for these mutants is found in Figure 2.9. Given this information, we can draw a schematic diagram showing that RIC8 works with GNA-1, GNA-3 and the Gbeta-Ggamma heterodimer to regulate vegetative hyphae growth rate (Figure 2.10). RGS-1 may also be involved in hyphal growth, however further investigation is needed to prove this hypothesis.

The use of algorithm analysis on biological organisms has revolutionized the way scientists analyze their data. In this study, conventional analyses were conducted on G protein signaling mutants in addition to novel imaging techniques that revealed phenotypes never captured before. This study developed collaborations between Biologists and Engineers that enhanced the analysis process with video and image analysis algorithms. These methods have saved tremendous amounts of time and money. In addition, the data analysis was more unbiased by reducing human error, thus ensuring the authenticity of the results.

Quantifiable data was extracted using images, while growth rate was measured using Video Bioinformatics. The development of novel image processing tools has allowed for aspects in vegetative hyphae development never detected before. Our results from the cell size program may explain a possible mechanism, where GNA-1 and RIC8, RGS-3, -4 and -5 play a role in regulating cell size (Figure 2.11).

Future directions for use of these image processing tools may consists of the application to different *N. crassa* gene deletion strains, thus revealing defects not

captured by other phenotypic assays. In addition, other fungi or any organism with similar features can be analyzed using these programs. For example, there are other fungi that produce spores and quantifying the area of these spores is feasible, as long as phase contrast microscopy is used. Growth rate analysis on other polarized tip-growing organisms can also be quantified, thus expanding the use of these programs.

Table 2.1: ***N. crassa* strains used in Chapter 2.**

Strain	Relevant genotype	Comments	Source
74-OR23-IVA	Wild type, *mat A*	FGSC 2489[a]	FGSC
74- ORS-6a	Wild type, *mat a*		FGSC
3b10	Δ*gna-1::hph*$^+$, *mat a*		Kays and Borkovich, 2003
2562	Δ*gna-2::hph*$^+$, *mat A*		Won et, .2012
31c2	Δ*gna-3::hph*$^+$, *mat A*		Kays et al., 2000
R81a	Δ*ric8::hph*$^+$, *mat a*		Wright et al., 2011
1-2	Δ*rgs-1::hph*$^+$, *mat a*	FGSC 12372[a]	FGSC
7a	Δ*rgs-2::hph*$^+$, *mat a*	FGSC 21981[a]	FGSC
2a	Δ*rgs-3::hph*$^+$, *mat a*	FGSC 11421[a]	FGSC
7A	Δ*rgs-4::hph*$^+$, *mat A*	FGSC 12406[a]	FGSC
1996	Δ*rgs-5::hph*$^+$, *mat a*	FGSC 13651[a]	FGSC

[a]FGSC, Fungal Genetics Stock Center, Kansas City, MO.

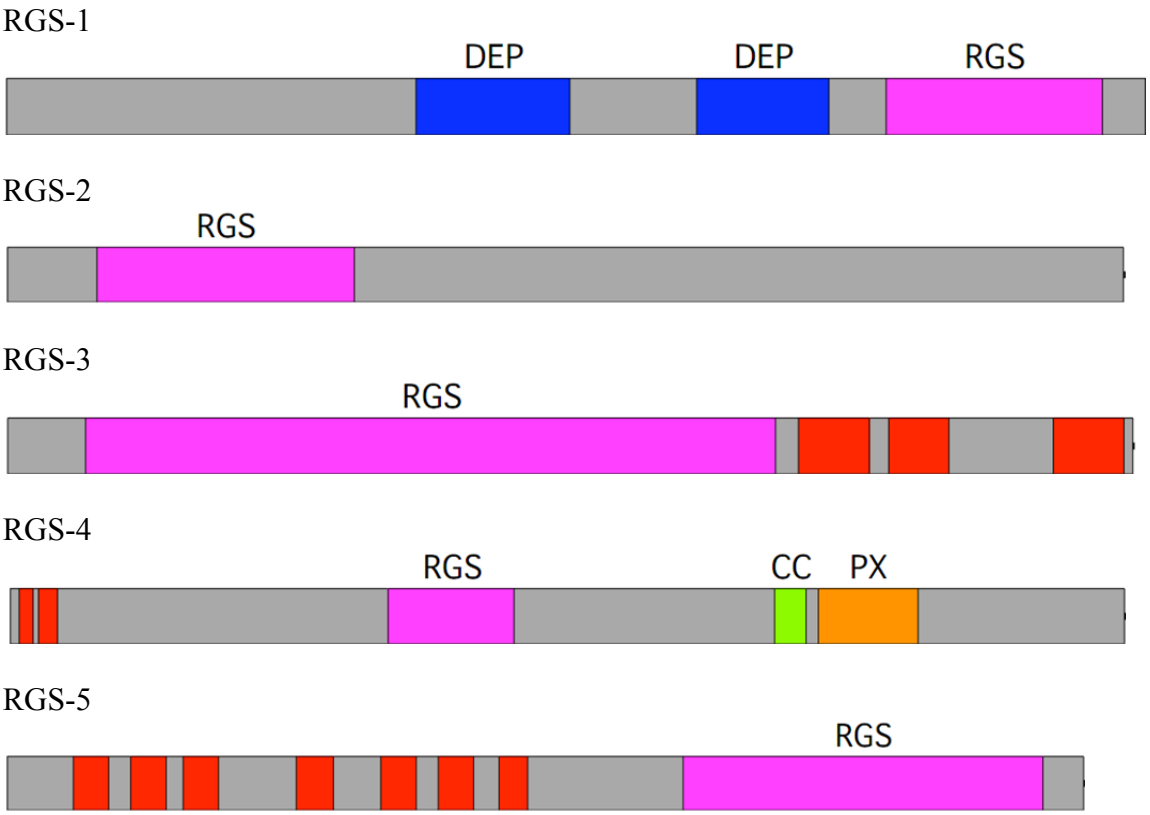

Figure 2.1: Predicted protein topology for RGS 1-5.

Protein domains were obtained using the bioinformatic tool; http://smart.embl-heidelberg.de/. RGS3-5 contains transmembrane domains. Transmembrane domain information was obtained from: http://www.cbs.dtu.dk/services/TMHMM/.

Table 2.2: Quantitative data for hyphal growth rate and aerial hyphae height

Deleted gene ID	Gene	Mating type	Basal hyphae linear growth rate (mm/day)	Aerial hyphal height on VM (mm/day)	Aerial hyphal height on VM+2% yeast extract (mm/day)
NCU06493	*gna-1*	*a*	44.8*	13.8*	19.0*
NCU06729	*gna-2*	*a*	82.1	41.8	37.0
NCU05206	*gna-3*	*A*	57.1	19.7*	34.8
NCU00041	*gnb-1*	*A*	53.1*	16.0*	25.8*
NCU00440	*gng-1*	*A*	46.8*	28.8	24.0*
NCU02788	*ric-8*	*a*	5.0*	6.7*	5.5*
NCU08319	*rgs-1*	*a*	54.1*	33.8	32.8
NCU05435	*rgs-2*	*a*	80.5	20.8*	25.3*
NCU08343	*rgs-3*	*A*	57.3	40.3	41.0
NCU16682	*rgs-4*	*A*	76.8	40.3	42.8
NCU09883	*rgs-5*	*a*	75.0	39.0	43.3
	Wild type	*a*	79.3	40.0	37.3
	Wild type	*a*		36.7	35.0

*The mean difference is significant at the 0.05 level

Shading indicates wild type control

Table 2.3: Conidiation and sexual development phenotypes

Deleted gene ID	gene	mating type	Conidia formation (slants)	Aerial hyphae formation (slants)	Protoperithecia formation	Perithecia formation	Ejected ascospores
NCU06493	*gna-1*	*a*	normal	normal	normal	none	none
NCU06729	*gna-2*	*a*	normal	normal	normal	normal	normal
NCU05206	*gna-3*	*A*	abundant	reduced	normal	normal	normal
NCU00041	*gnb-1*	*A*	normal	reduced	normal	none	none
NCU00440	*gng-1*	*A*	normal	normal	normal	normal	normal
NCU02788	*ric-8*	*a*	abundant	reduced	none	none	none
NCU08319	*rgs-1*	*a*	reduce	normal	few	none	none
NCU05435	*rgs-2*	*a*	reduce	reduced	few	few	few
NCU08343	*rgs-3*	*A*	normal	normal	normal	normal	normal
NCU16682	*rgs-4*	*A*	normal	normal	normal	normal	normal
NCU09883	*rgs-5*	*a*	normal	normal	normal	normal	normal
	Wild type	*a*	normal	normal	normal	normal	normal

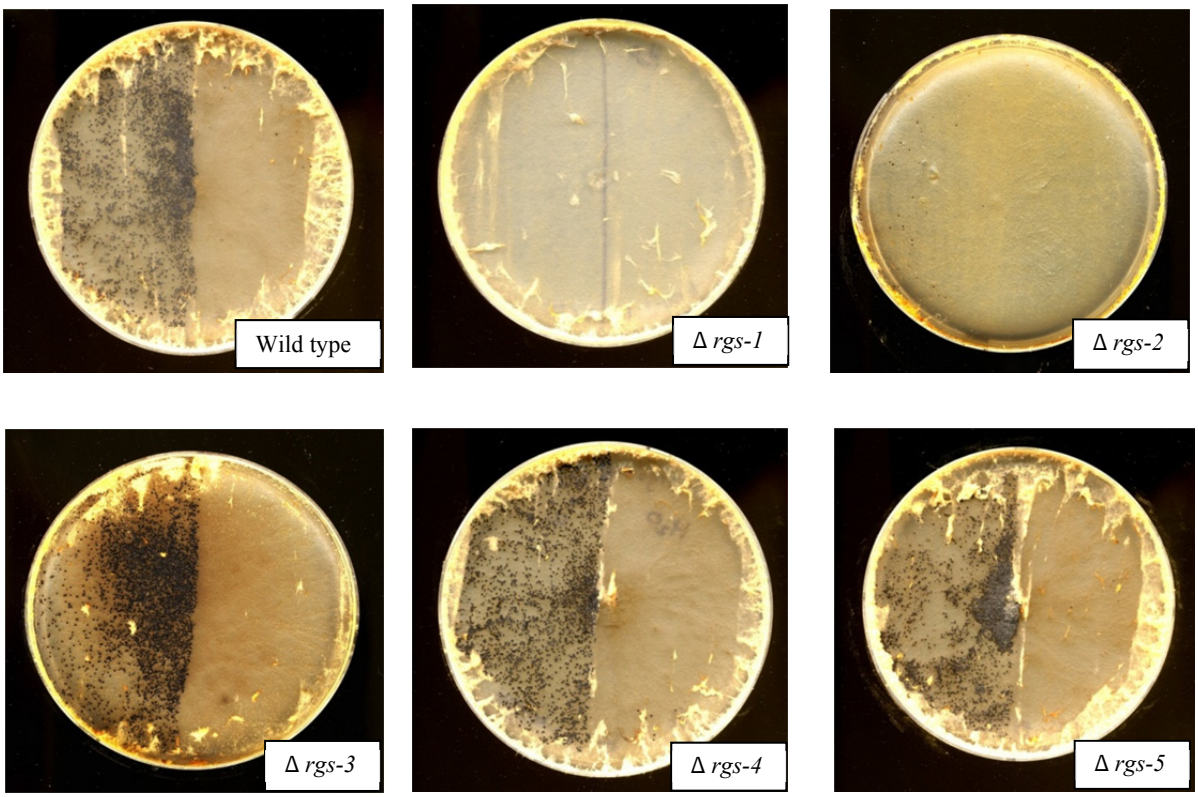

Figure 2.2: Female fertility assay/plates.

Strains were inoculated on an SCM agar plate and incubated at room temperature in constant light for 10 days. At this point, the left half of the pate was fertilized with conidia from an opposite mating type wild type strain, while the right side was treated with water (right side; controls). Plates were photographed 10 days later. Perithecia are the small black bodies evident on the left side of most plates. The Δ*rgs-1* mutant does not make protoperithecia, while Δ*rgs-2* shows reduced fertility by making very few female reproductive structures (see Figure 2.3). All other mutants exhibit normal fertility.

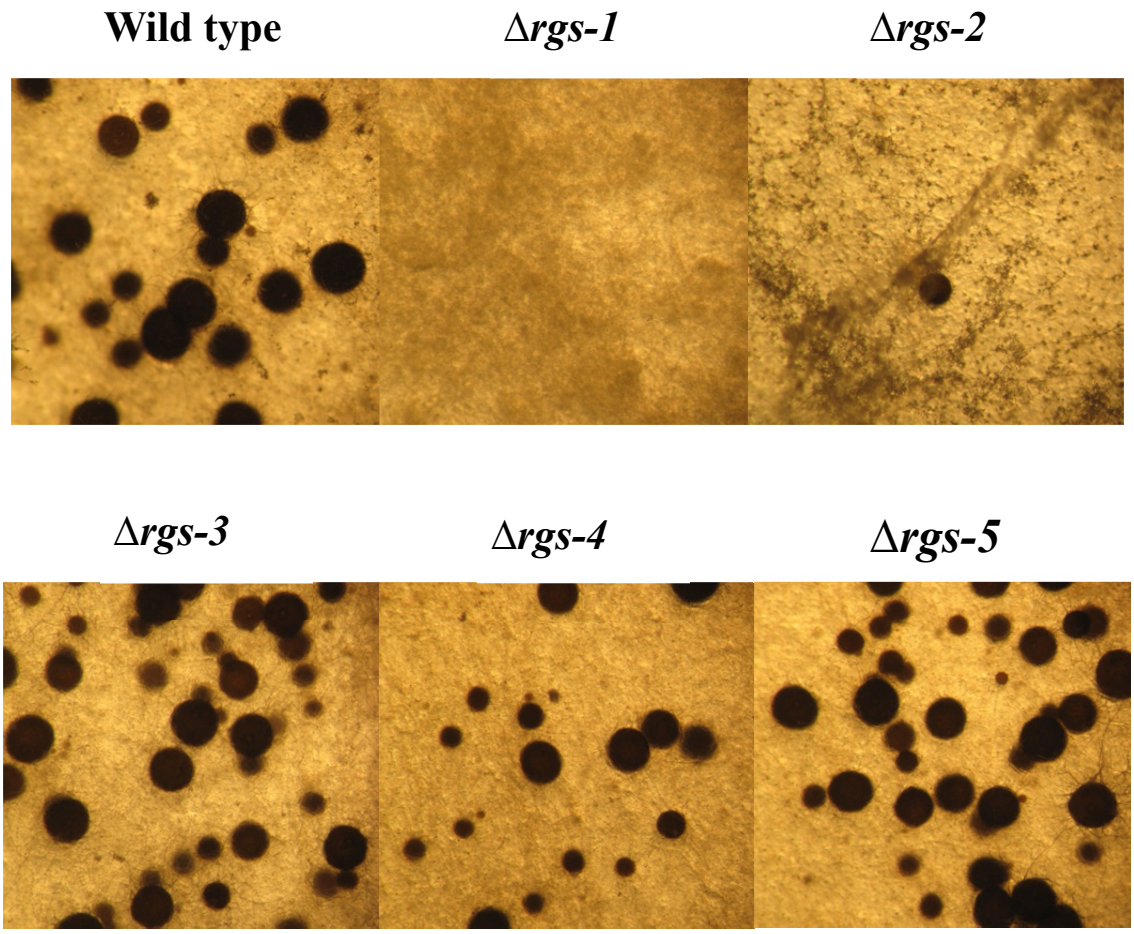

Figure 2.3: Female fertility assay/microscopic examination of perithecia.

Strains were inoculated as in Figure 2.2. Perithecia were photographed using an SZX9 stereomicroscope (Olympus) with a Powershot G10 Camera (Cannon USA, Lake Success, NY) at a magnification of 40x. Perithecia are the dark brown bodies.

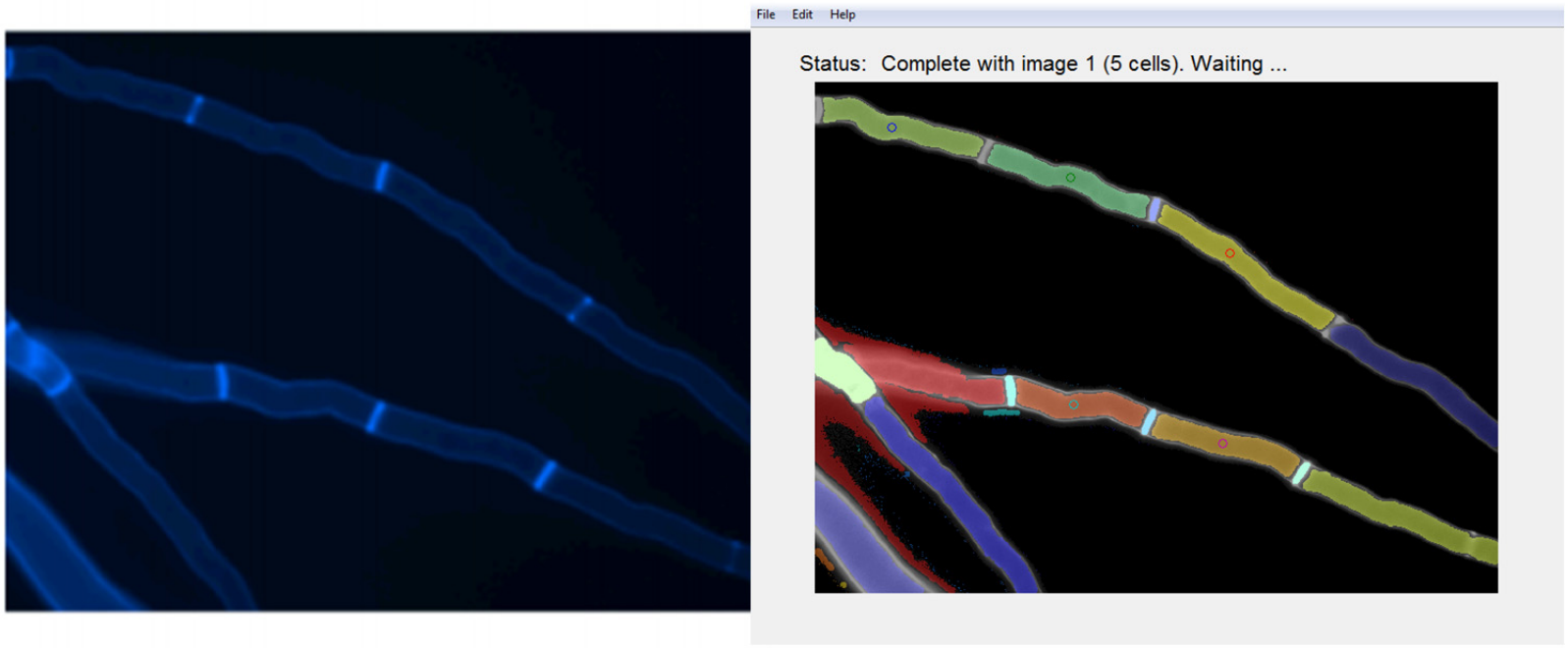

Figure 2.4: Automated analysis of hyphal cell compartments.

The primary image of hyphae stained with Calcoflour White on the left is converted to the digitized and colorized image on the right.

Table 2.4: **Results from hyphal cell compartment size video bioinformatics program**

Deleted gene ID	gene	mating type	Hyphal compartment Length (microns)	Hyphal compartment Diameter (microns)	Hyphal compartment Area (microns)	Hyphal compartment Perimeter (microns)
NCU06493	*gna-1*	*a*	46.9*	6.9*	225.3*	99.5*
NCU06729	*gna-2*	*a*	68.3	9.0	418.2*	144.7
NCU05206	*gna-3*	*A*	78.2	9.2	478.4	163.5
NCU00041	*gnb-1*	*A*	71.2	12.1	559.6	156.9
NCU00440	*gng-1*	*A*	78.9	11.2	628.3	172.9
NCU02788	*ric-8*	*a*	42.6*	4.1*	119.3*	85.9*
NCU08319	*rgs-1*	*a*	60.6*	8.3*	332.9*	126.6*
NCU05435	*rgs-2*	*a*	73.0	7.2*	286.9*	147.7
NCU08343	*rgs-3*	*A*	130.4*	16.0*	1386.9*	266.9*
NCU16682	*rgs-4*	*A*	175.2*	21.9*	2803.9*	373.8*
NCU09883	*rgs-5*	*a*	157.1*	21.8*	2350.7*	331.9*
	Wild type	*a*	79.2	10.6	619.2	173.2

*The mean difference is significant at the 0.05 level

Wild-type

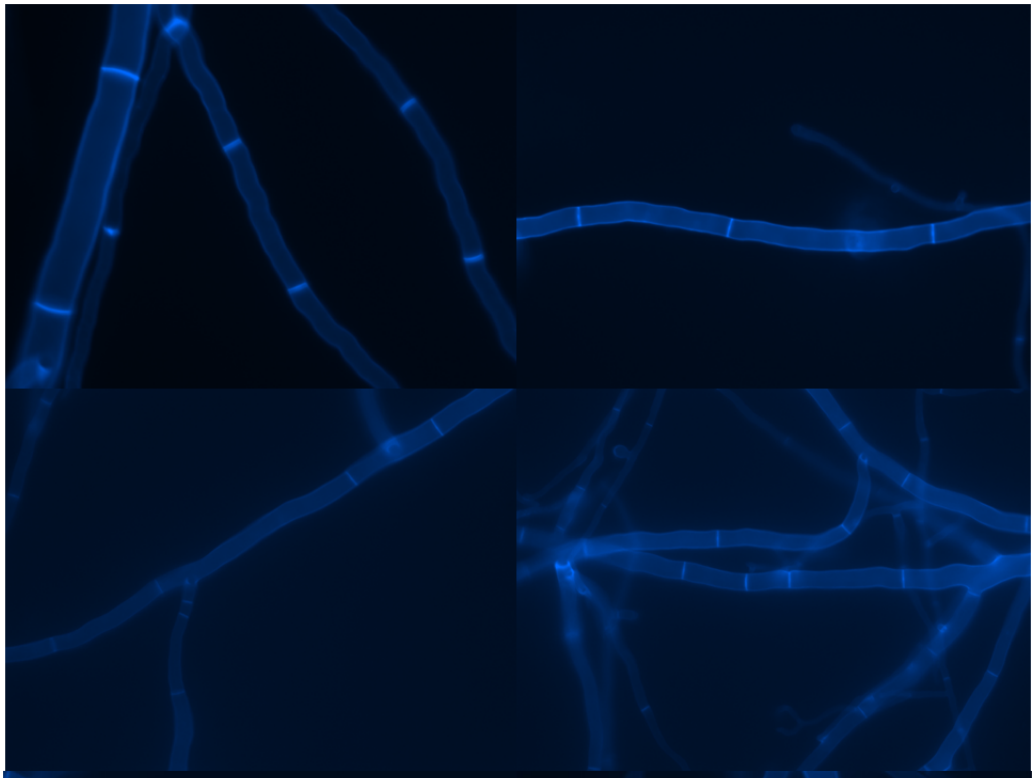

Δgna-1

Δgna-2

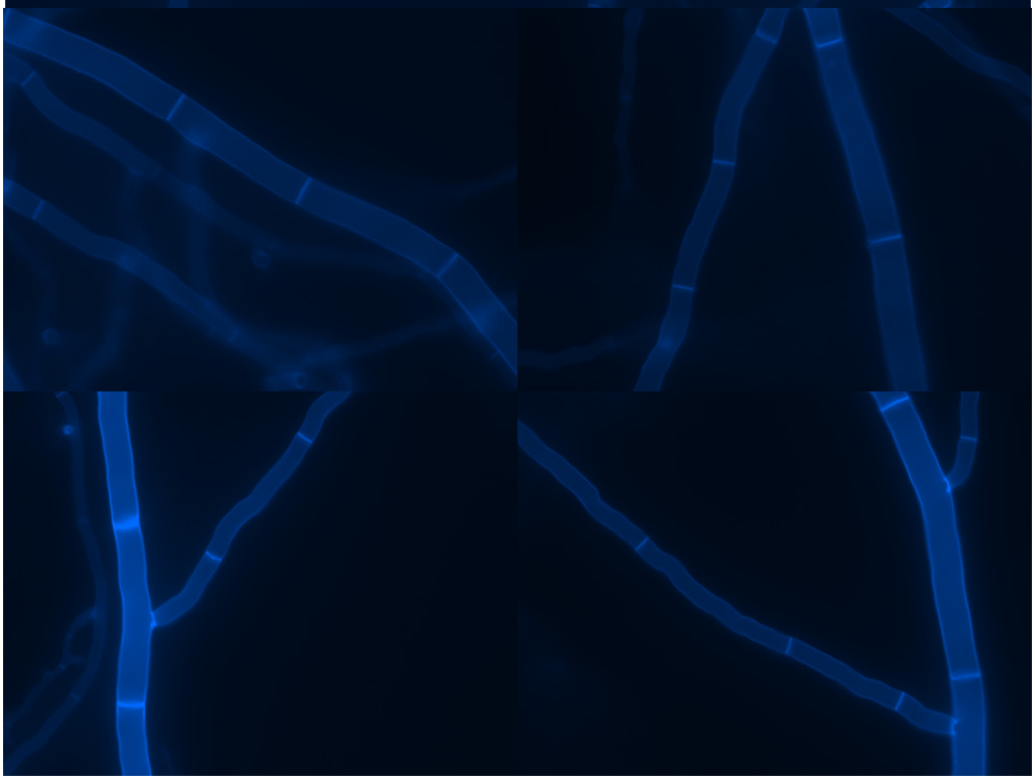

Δgna-3

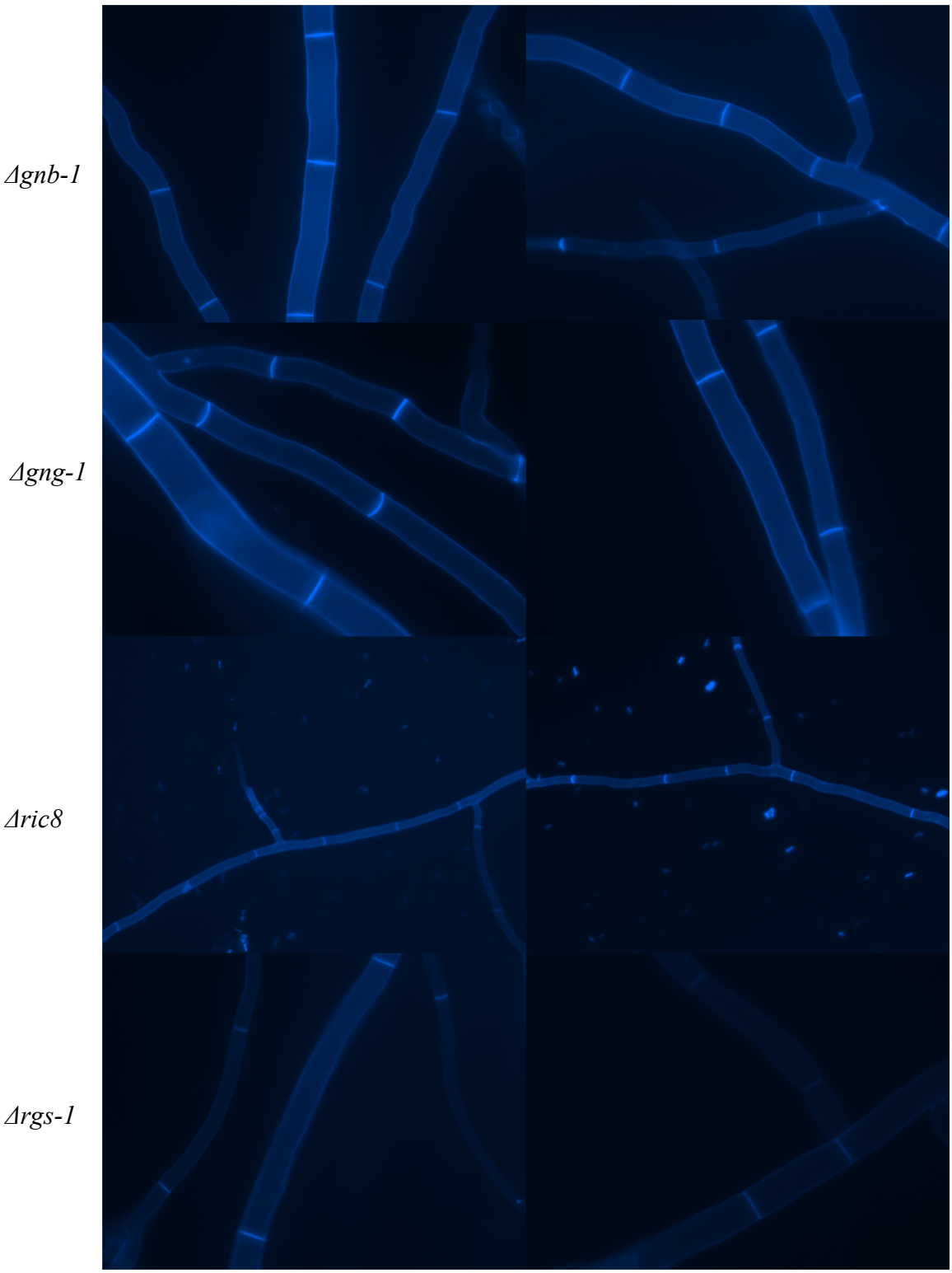
Δgnb-1
Δgng-1
Δric8
Δrgs-1

Δrgs-2

Δrgs-3

Δrgs-4

Δrgs-5

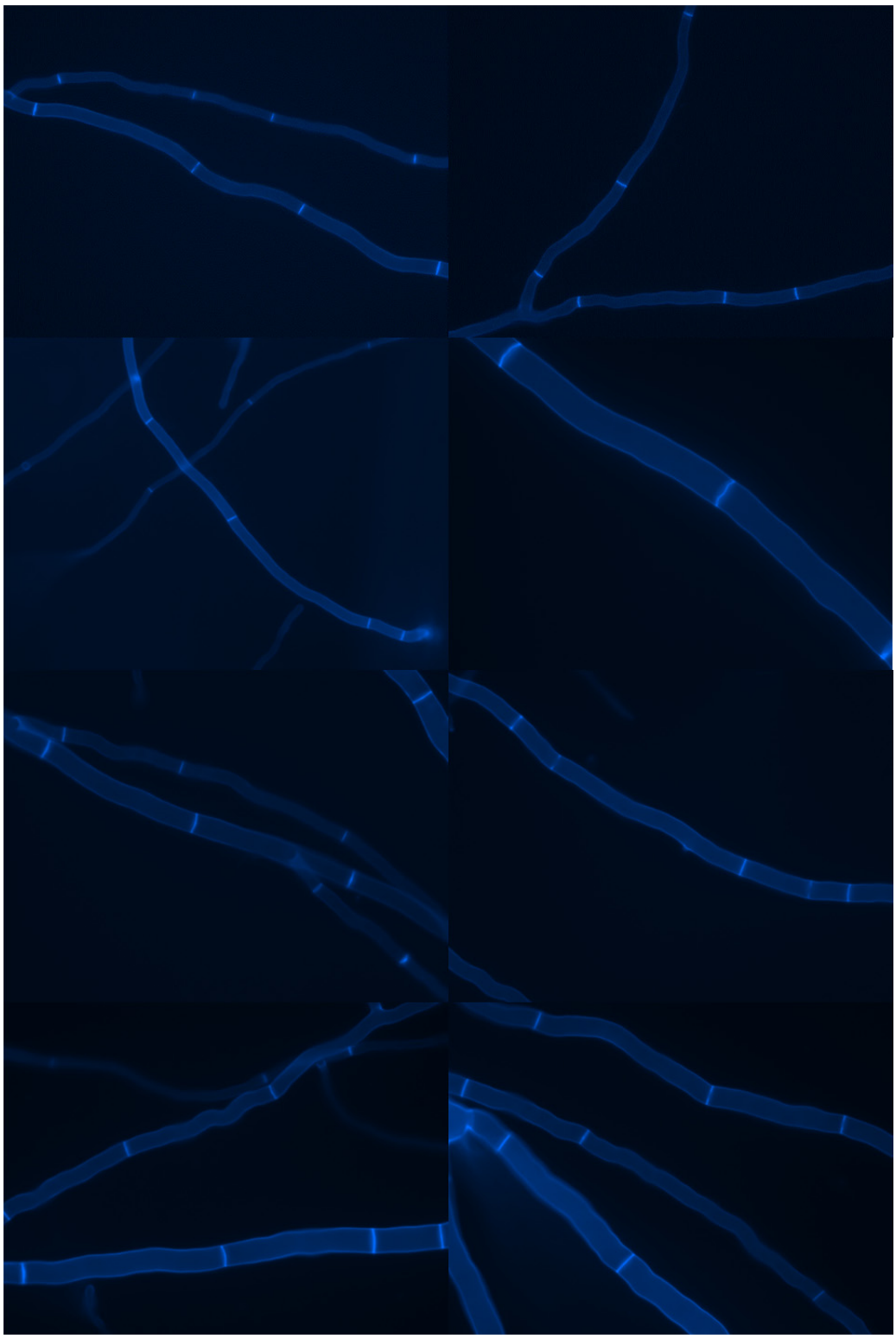

Figure 2.5: Colony edge hyphae stained with calcoflour white.

Cultures were incubated for 20-22 hour at 30°C in the dark. Vegetative hyphae were stained using a 1:1 ratio of Calcoflour White in VM liquid media. Samples were imaged immediately after staining using an Olympus IX71 inverted microscope (Olympus America, Center Valley, PA) with a 40x phase objective with the DAPI filter in place.

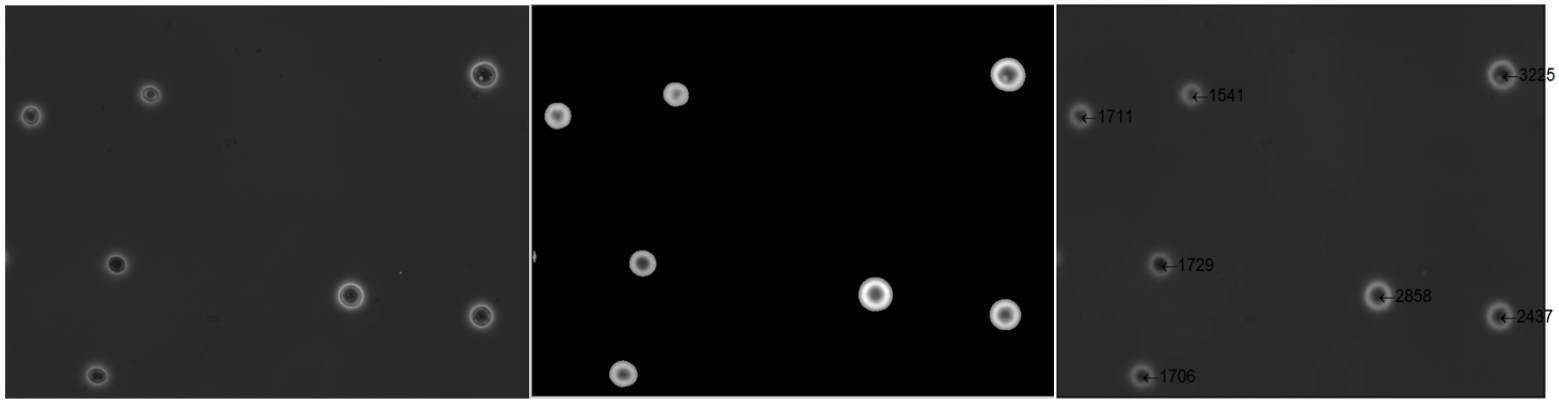

Figure 2.6: **Conidial spore image processing example**.

Original image (left), after being subjected to Gabor filtering (middle), and the results image (right).

Table 2.5: Results of *Δgna-1* and wild type conidial spore size

Sample	N	Mean	SE Mean
Wild type	**41**	**779**‡	**180**
Δgna-1	**43**	**398**‡	**39**

*P-Value = 0.037

‡Values are given in pixels

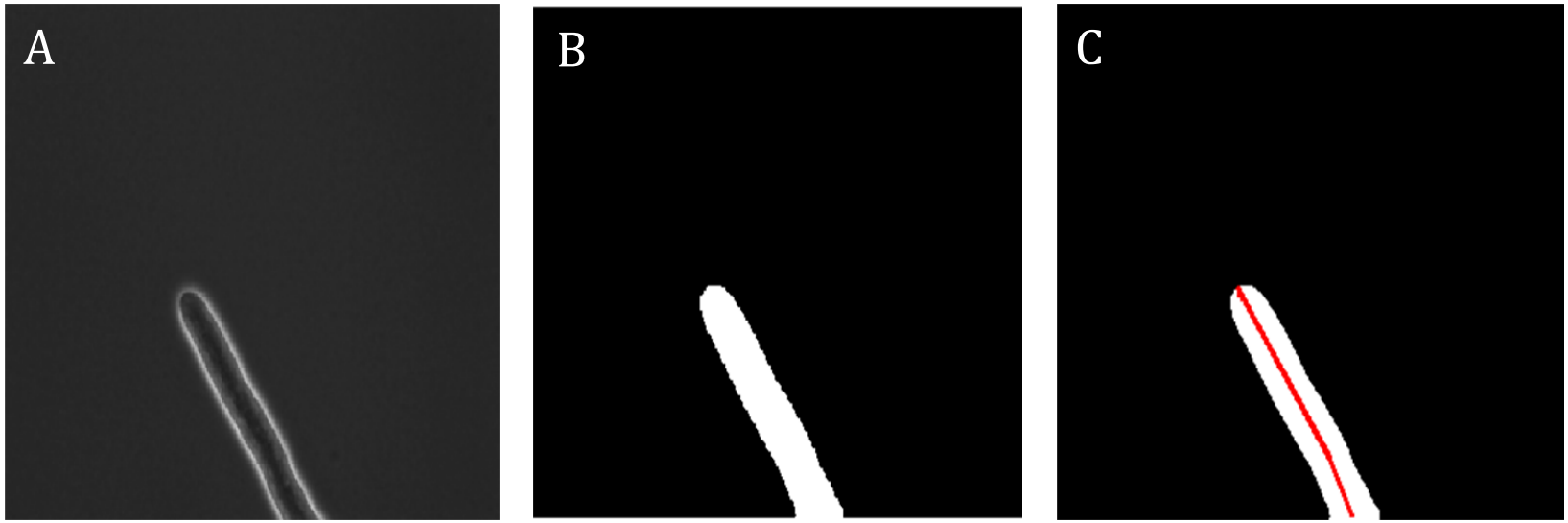

Figure 2.7: Hyphal growth rate video extraction.

Initial image (A), is subjected to segmentation using active contours method (B). Performing gradient descend on the hyphae to find the line of symmetry (C).

A

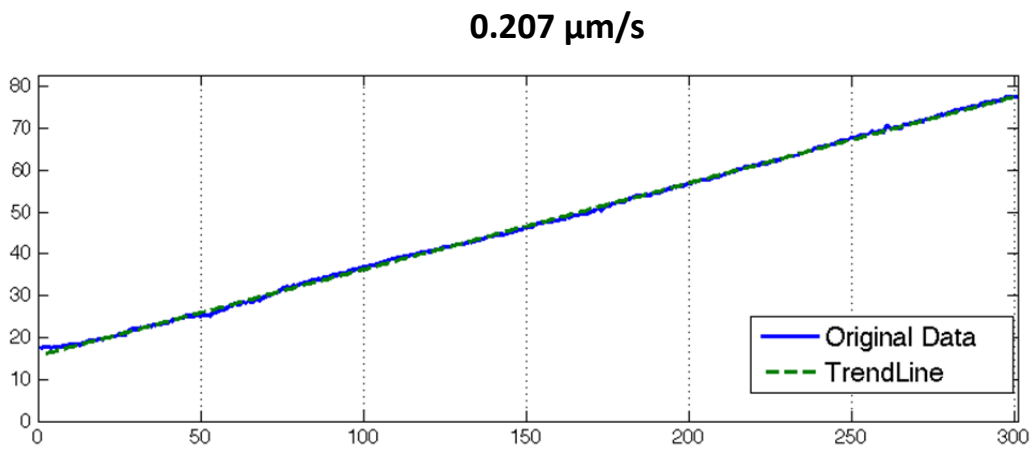
0.207 µm/s
Original Data
TrendLine
0
10
20
30
40
50
60
70
80
0
50
100
150
200
250
300

B

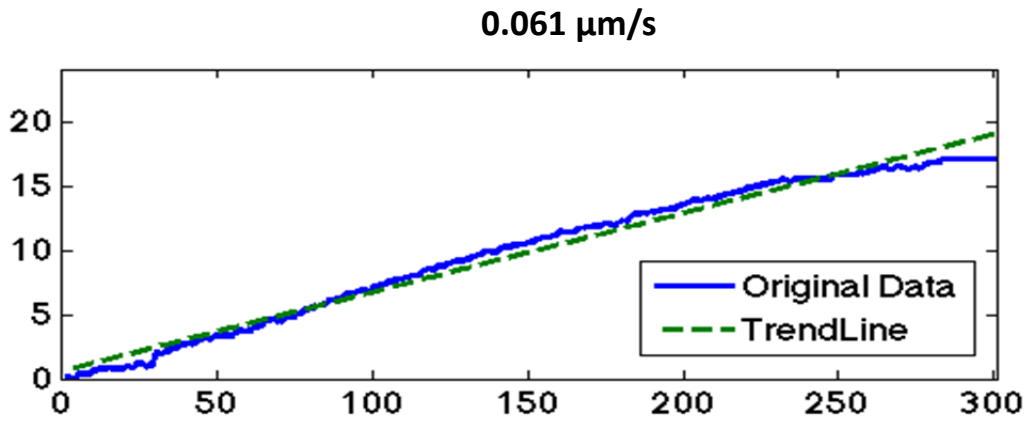
0.061 µm/s
Original Data
TrendLine
0
5
10
15
20
0
50
100
150
200
250
300

Figure 2.8: Determination of hyphal growth rate.

(A) Length of the midline of the wild type hypha over time. The green dashed line is the smoothed measurements from the solid blue line. The smoothed measurements were obtained with a moving average. (B) Length of the midline of the *gna-1* mutant strain hypha over time.

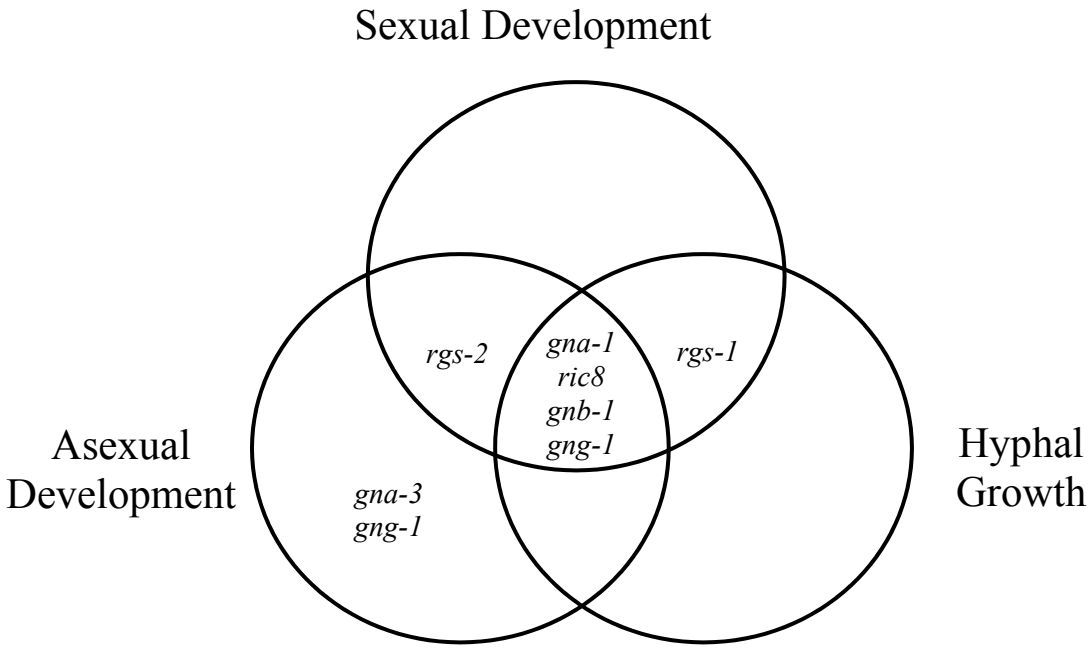

Figure 2.9: Venn diagram displaying G protein component mutants with phenotypes in growth and development.

From the 11 mutants, 8 (73%) exhibited a defect in at least one assay for hyphal growth or asexual or sexual development, as shown. Mutants with defects are indicated as gene names for the deleted genes.

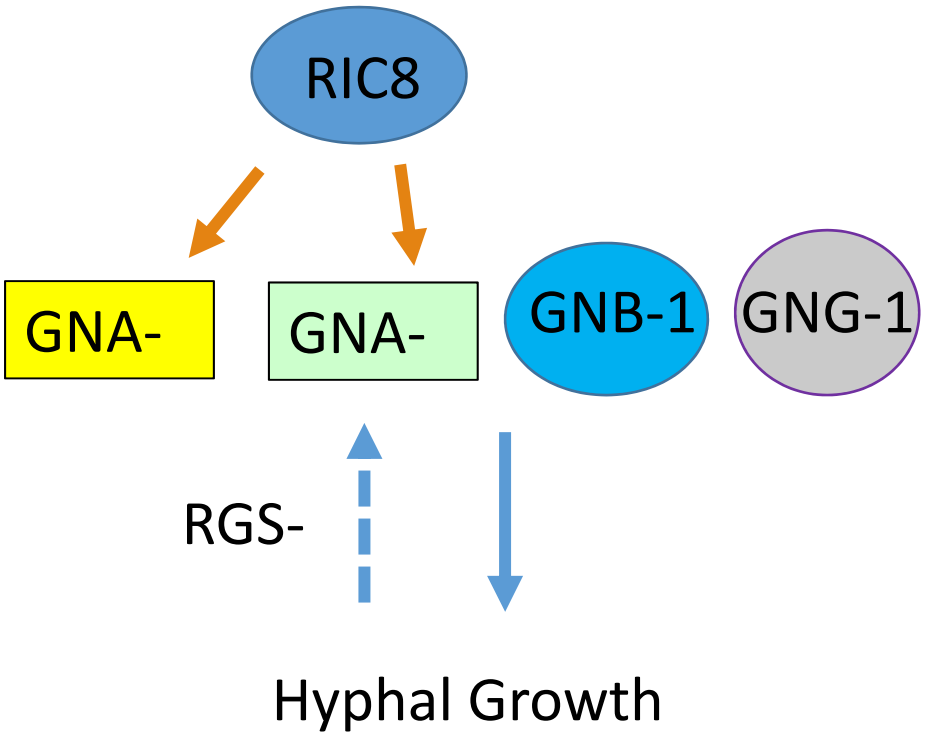

Figure 2.10: **Proposed pathway in regulating hyphal growth.**

RIC8 is positively regulating GNA-1 and GNA-3 to affect hyphal growth. GNB-1 and GNG-1 heterodimer is also positive regulators for hyphal growth. RGS-1 may also be involved in regulating hyphal growth (dashed arrow).

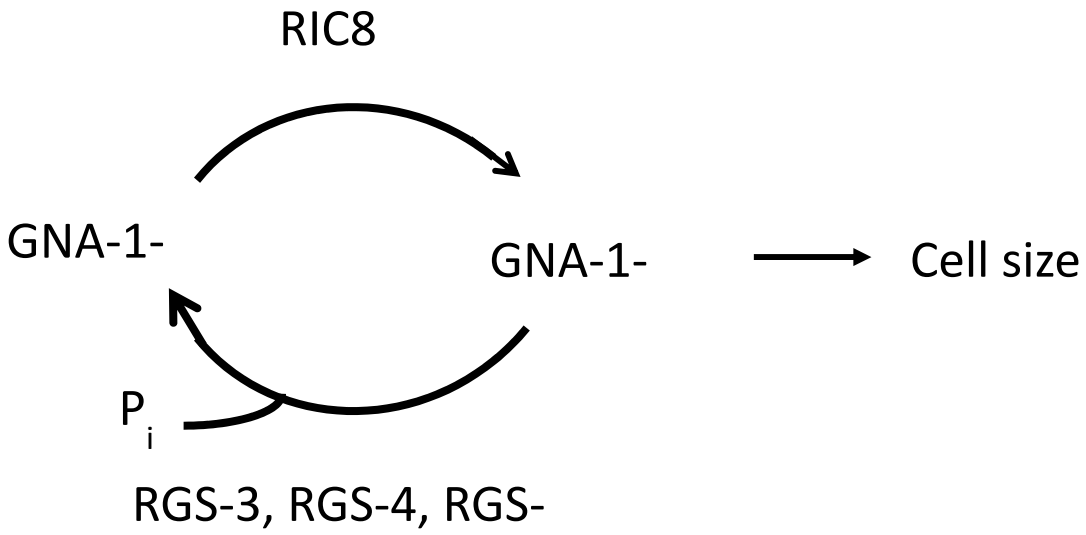

Figure 2.11: **Proposed pathway in regulating cell size.**

RIC8 is activating GNA-1, in order to regulate cell size. RGS-3, -4, and -5 appear to negative regulators in the mechanism.

References

(2010). MATLAB software .7.10.0.584 Natick, MA.

(2010) Minitab 17 Software. State College, PA: Minitab, Inc. (www.minitab.com)

(2013). Excel, Redmond, Washington: Microsoft.

Barratt, R.W., and Garnjobst, L. (1949). Genetics of a colonial microconidiating mutant strain of *Neurospora crassa*. Genetics *34*, 351-369.

Elorza, M.V., Rico, H., and Sentandreu, R. (1983). Calcofluor white alters the assembly of chitin fibrils in *Saccharomyces cerevisiae* and *Candida albicans* cells. Journal of general microbiology *129*, 1577-1582.

Ghosh, A., Servin, J.A., Park, G., and Borkovich, K.A. (2014). Global Analysis of Serine/Threonine and Tyrosine Protein Phosphatase Catalytic Subunit Genes in *Neurospora crassa* Reveals Interplay Between Phosphatases and the p38 Mitogen-

Activated Protein Kinase. G3 *4*, 349-365.

Gopinath, S., Wen, Q., Thakoor, N., Luby-Phelps, K., and Gao, J.X. (2008). A statistical approach for intensity loss compensation of confocal microscopy images. Journal of microscopy *230*, 143-159.

Hickey, P.C., Swift, S.R., Roca, M.G., and Read, N.D. (2004). Live-cell Imaging of filamentous fungi using vital fluorescent dyes and confocal microscopy. Meth Microbiol *34*, 63-87.

Ivey, F.D., Hodge, P.N., Turner, G.E., and Borkovich, K.A. (1996). The G alpha i homologue gna-1 controls multiple differentiation pathways in *Neurospora crassa*. Mol Biol Cell *7*, 1283-1297.

Kays, A.M., and Borkovich, K.A. (2004). Severe impairment of growth and differentiation in a *Neurospora crassa* mutant lacking all heterotrimeric G alpha proteins. Genetics *166*, 1229-1240.

Kim, H., and Borkovich, K.A. (2004). A pheromone receptor gene, pre-1, is essential for mating type-specific directional growth and fusion of trichogynes and female fertility in *Neurospora crassa*. Mol Microbiol *52*, 1781-1798.

Kolmark, G., and Westergaard, M. (1949). Induced back-mutations in a specific gene of *Neurospora crassa*. Hereditas *35*, 490-506.

Krystofova, S., and Borkovich, K.A. (2005). The heterotrimeric G-protein subunits GNG-1 and GNB-1 form a Gbetagamma dimer required for normal female fertility, asexual development, and galpha protein levels in *Neurospora crassa*. Eukaryot Cell *4*, 365-378.

Li, C., Xu, C., Gui, C., and Fox, M.D. (2010). Distance regularized level set evolution and its application to image segmentation. IEEE transactions on image processing : a publication of the IEEE Signal Processing Society *19*, 3243-3254.

Lindegren, C.C. (1932). The genetics of *Neurospora* I. The inheritance of response to heat-treatment. Bull Torrey Botanicals Club, 85-102.

Lopez-Franco, R., Bartnicki-Garcia, S., and Bracker, C.E. (1994). Pulsed growth of fungal hyphal tips. Proc Natl Acad Sci U S A *91*, 12228-12232.

Mclean, K.M., and Prosser J.I. (1987). Development of vegetative mycelium during growth of *Neurospora crassa*. Trans. Br. Mycol. Soc., 489-495.

Mehrotra, K.N., Namuduri, K.R., and Ranganathan, N. (1992). Gabor filter-based edge detection. Pattern Recognit. *25*, 1479-1492.

Otsu, N. (1979). A threshold selection method from gray-level histograms. IEEE Transactions on Systems, Man, and Cybernetics *SMC-9*, 62-66.

Park, G., Servin, J.A., Turner, G.E., Altamirano, L., Colot, H.V., Collopy, P., Litvinkova, L., Li, L., Jones, C.A., Diala, F.G., Dunlap, J.C., and Borkovich, K.A. (2011). Global analysis of serine-threonine protein kinase genes in Neurospora crassa. Eukaryot Cell *10*, 1553-1564.

Ross, E.M., and Wilkie, T.M. (2000). GTPase-Activating Proteins for heterotrimeric G proteins: Regulators of G protein signaling (RGS) and RGS-like proteins. Annu Rev Biochem, 795-827.

Su, H., Yin, Z., Huh, S., and Kanade, T. (2013). Cell segmentation in phase contrast microscopy images via semi-supervised classification over optics-related features. Medical image analysis *17*, 746-765.

Turner, G.E. (2011). Phenotypic analysis of *Neurospora crassa* gene deletion strains. Methods Mol Biol *722*, 191-198.

Vogel, H.J. (1964). Distribution of lysine pathways among fungi - Evolutionary implications. Am Nat *98*, 435-446.

Westergaard, M., and Mitchell, H.K. (1947). *Neurospora* V. A synthetic medium favoring sexual reproduction. Amer. J. Bot. *34*, 573-577.

White, B., and Woodward, D. (1995). A simple method for making disposable race tubes. Fungal Genetics Newsletter *42*, 79.

Wright, S.J., Inchausti, R., Eaton, C.J., Krystofova, S., and Borkovich, K.A. (2011). RIC8 is a guanine-nucleotide exchange factor for Galpha subunits that regulates growth and development in *Neurospora crassa*. Genetics *189*, 165-176.

Yang, Q., Poole, S.I., and Borkovich, K.A. (2002). A G-protein beta subunit required for sexual and vegetative development and maintenance of normal G alpha protein levels in *Neurospora crassa*. Eukaryot Cell *1*, 378-390.

Chapter 3

Global analysis of predicted G protein coupled receptor genes in the filamentous fungus, *Neurospora crassa*

Abstract

G protein coupled receptors (GPCRs) regulate facets of growth, development and environmental sensing in eukaryotes. The genome of the filamentous fungus *Neurospora crassa* predicts 43 GPCR genes, but only five have been functionally characterized. Here, we analyzed 36 available GPCR mutants for phenotypes and patterns of gene expression. Five mutants had defects in extension of basal hyphae, 14 in asexual sporulation and six in sexual development, resulting to a total of 17 mutants (47%) having at least one growth or developmental phenotype. We identified 18 mutants (56%) with chemical sensitivity or nutritional phenotypes (11 uniquely), bringing the total number of mutants with at least one phenotype to 28 (78%). Publically available transcriptomic data for GPCR genes correlated with the phenotypes observed for many mutants and also suggested overlapping functions for several groups of co-transcribed genes. This study is the first systematic analysis of the large group of Pth11-related GPCRs. Out of 20 available mutants, five are impaired in hyphal growth, eight in asexual sporulation, one in sexual development, and five have unique chemical sensitivity or nutritional defects, for a total of 15 (75%) of Pth11-related GPCR mutants with at least one phenotype. Gene expression trends for GPCR genes correlated with the phenotypes observed for many

mutants and also suggested overlapping functions for several groups of co-transcribed genes. Several members of the Pth11-related class have phenotypes and/or are differentially expressed on cellulose, suggesting a possible role for this gene family in plant cell wall sensing or utilization.

Introduction

G protein coupled receptors (GPCRs) are responsible for a diversity of cell functions, including environmental sensing, metabolism, immunity, growth, and development in eukaryotic cells (Chini *et al.*, 2013; Bock *et al.*, 2014). GPCRs are seven alpha-helical transmembrane (TM) proteins anchored in the plasma membrane, with an intracellular carboxyl- and extracellular amino-terminus (Chini *et al.*, 2013; Shukla *et al.*, 2014). The heterotrimeric G protein signaling cascade initiates with the GPCR sensing the stimulus (ligand) and then transducing this signal to the inside of the cell via heterotrimeric G proteins (Tesmer, 2010). Heterotrimeric G proteins are composed of three subunits (α, β and γ) that are associated with the GPCR in the inactive state. Ligand binding to the GPCR causes a conformational change within the receptor that leads to exchange of GDP for GTP on the Gα subunit and dissociation of the Gα from the Gβγ heterodimer and the GPCR (Tesmer, 2010; Jastrzebska, 2013). Both the Gα-GTP and Gβγ can then regulate downstream effectors, which include mitogen activated protein kinase (MAPK) cascades, ion channels, adenylyl cyclases, phosphodiesterases, and phopholipases (Mende *et al.*, 1998; Neves *et al.*, 2002; Chini *et al.*, 2013).

Heterotrimeric G proteins and GPCRs have been demonstrated to regulate growth and development in *N. crassa* (Ivey *et al.*, 1996; Baasiri *et al.*, 1997; Kays *et al.*, 2000; Kays and Borkovich, 2004; Kim and Borkovich, 2004; Krystofova and Borkovich, 2005, 2006; Li and Borkovich, 2006; Li *et al.*, 2007; Kim *et al.*, 2012; Won *et al.*, 2012). *N. crassa* possesses three Gα, one Gβ and one Gγ subunit(s), and 10 putative GPCRs were originally annotated in the *N. crassa* genome sequence (Galagan *et al.*, 2003; Borkovich *et al.*, 2004). Following the annotation of GPCR genes in the filamentous fungal pathogen *Magnaporthe oryzae*, it provided evidence for additional GPCR classes in filamentous fungi, thus increasing the number to 43 GPCRs (Kulkarni *et al.*, 2005).

A recent study reported functional information for 15 GPCRs corresponding to Classes I-IX in the filamentous fungus *Aspergillus flavus* (Affeldt *et al.*, 2014). However 38 of the 43 identified putative GPCRs have not been functionally characterized in *N. crassa*. Our study is the first to probe functions for the large family of Pth11-related GPCRs in fungi, an implicated pathogenic receptor. In this study, we systematically analyze available *N. crassa* knockout mutants lacking annotated GPCR genes to determine their growth, developmental and chemical sensitivity phenotypes (Table 3.1). We take advantage of existing mRNA profiling datasets to mine expression trends for several GPCR genes during growth and development. We demonstrate phenotypes for many of the uncharacterized mutants, as well as novel chemical phenotypes for some previously studied mutants.

The text in Chapter 3 of this dissertation included in a paper under review in the journal *Genes, Genomes, Genetics* (G3) entitled “Global analysis of predicted G protein

coupled receptor genes in the filamentous fungus, *Neurospora crassa*." I would like to acknowledge all of my students who contributed enormous amount of work collecting phenotypic information for the GPCR mutants during the Spring quarter 2014 *Experimental Microbiology* (MCBL 125) course at UCR (I was the teaching assistant). Chemical data collection for the GPCR mutants was performed by undergraduate students Itallia V. Pacentine, Andrew Lim, and Nayeli Guerrero. Heatmap construction was performed by graduate student Steven Ahrendt using data I obtained and organized from publically available sources. Steven Ahrendt also constructed the phylogenetic tree containing the Pth11-related GPCRs. I worked very closely with Dr. Katherine Borkovich during the statistical analysis of the chemical sensitivity data and the writing of this manuscript.

Materials and Methods

Media and strains:

Vogel's minimal medium ,VM, (Vogel, 1964) was used to support vegetative growth and development. Sexual differentiation was promoted by culturing on synthetic crossing medium (SCM) plates (Westergaard and Mitchell, 1947). Colony formation was facilitated by growth on sorbose-containing medium (FGS) plates (Davis and deSerres, 1970). Where indicated, hygromycin B (Calbiochem, San Diego, CA) was used at a concentration of 200 μg/ml in media. Media were inoculated using conidia propagated on VM agar slants.

Wild-type strains ORS-SL6a (FGSC 4200; *mat a*) and 74-OR23-IVA (FGSC 2489; *mat A*) were obtained from the Fungal Genetics Stock Center (FGSC; Kansas City, MO). Available G protein coupled receptor (GPCR) homokaryotic mutants were obtained from the FGSC or created in our laboratory. A total of seven mutants were not available at the time of this study. Knockouts of NCU03253 (*gpr-8*), NCU05101 (*gpr-19*) and NCU05187 (*gpr-20*) were attempted, but failed, either due to an inability to obtain knockout constructs or *N. crassa* primary transformants. The gene structures for NCU17171 (*gpr-26*) and NCU16721 (*gpr-28*) were re-annotated after mutant construction, and the available knockout mutants (former NCU06891 and NCU07591, respectively) are incorrect.

Knockout mutants that were deposited at the FGSC as heterokaryons (NCU09796, NCU00700 and NCU08429) were purified to homokaryons using a genetic cross to wild type strain FGSC2489, as previously described (Colot *et al.*, 2006). All putative homokaryons were checked for the presence of the knockout cassette using gene-specific and *hph* primers in diagnostic PCRs as previously described (Ghosh *et al.*, 2014).

Growth, developmental, chemical sensitivity and nutritional phenotypes:

Phenotypic assays were conducted essentially as previously described (Park *et al.*, 2011b; Turner, 2011; Ghosh *et al.*, 2014), except that race tubes were prepared using 25 ml plastic disposable pipets (White and Woodward, 1995). Some phenotypic tests used in earlier studies were omitted, including assessment of pigmentation and aerial hyphae

formation on yeast extract-containing medium. For quantitative growth and developmental assays (apical extension rate and aerial hyphae height), mutants that exhibited a ± 5 mm/day difference relative to wild type were considered significant (Colot *et al.*, 2006; Park *et al.*, 2011b). For detailed analysis of beak formation in the CRL mutant class of GPCR mutants, strains were inoculated on synthetic crossing medium, SCM, (Westergaard and Mitchell, 1947) plates and incubated under constant light for one week at 25°C. Cultures were fertilized using conidia from a wild type strain of opposite mating type at 7 days post-inoculation. Formation of perithecia was scored one week after fertilization and beak morphology and ascospore ejection two weeks after fertilization. Images of perithecia were captured using a SZX9 stereomicroscope (Olympus) and a digital camera. Delayed ascospore ejection and beak formation was checked after an additional week. Wild-type strain (FGSC 4200; *mat a*) was used as a control.

For chemical sensitivity screens, mutants were inoculated at the edge of 60x15mm VM plates with and without chemical. The following chemicals and concentrations were assayed: sodium chloride (0.35 M), sorbitol (0.8 M), cytochalasin A (40 ng/ml; Sigma, St. Louis, MO), benomyl (92 ng/ml; Fluka, St. Louis, MO), tert-butyl hydroperoxide (0.13 mM; Sigma), Menadione (100 mM; Sigma), FK-506 (50 ng/ml; LC Laboratories, Woburn, MA) and fludioxonil (2.75 ng/ml; a gift from Frank Wong and Allison Tally). Sorbitol and sodium chloride were added to VM agar medium prior to autoclaving, while all other chemicals were added to cooled autoclaved VM agar medium using filter-sterilized concentrated stock solutions. Plates were incubated in the dark for

20-22 h at 30°C. VM plates lacking chemical were used as controls. The percent growth on the chemical was determined by dividing the colony radius for the plate containing the chemical by that of a VM plate. Four biological replicates were used in each of three independent experiments. Student's t-test (paired, two-tailed) was used to identify mutants with significantly different sensitivity relative to wild type. A mutant was considered different from wild type if $p \leq 0.05$ in at least two experiments and ≤ 0.20 in all three experiments. Mutants with better growth on a chemical relative to wild type were scored as resistant (R; Table 3.2), while slower-growing mutants were scored as sensitive (S; Table 3.2).

The GPCR mutants were also tested for nutritional phenotypes using 60x15 mm VM agar plates. Avicel (crystalline agarose; Sigma) was substituted for sucrose in VM medium at a concentration of 2 %. Yeast extract was added to VM medium to a concentration of 2% w/v. Incubation and measurement of plates and identification of mutants that were significantly different than wild type was determined as described for chemical sensitivity screening, above.

Clustering of *N. crassa* GPCR expression data and heatmap generation:

Expression data was mined for GPCR genes from four different datasets. Each dataset pertained to a specialized tissue type during development or an environmental condition. RNA-sequencing data was obtained for sexual development (Wang *et al.*, 2014), while microarray data was utilized for colony development (Kasuga and Glass, 2008) and a time course of conidiation (Greenwald *et al.*, 2010). Lastly, RNA sequencing

data for expression using 4 h liquid cultures grown on either sucrose or the alternative carbon source avicel (Coradetti *et al.*, 2012) were downloaded from (http://www.ncbi.nlm.nih.gov/geo; Accession number GSE35227). In order to visualize the expression data, heatmaps were generated with the pheatmap package (V1.0.2); (Kolde, 2015) using R (v3.1.1);(Team_RC, 2014). Expression data for each gene was standardized using the included scaling function in pheatmap.

Phylogenetic analysis of putative Pth11-related proteins:

The Pth11 protein sequence from *Magnaporthe grisea* and the 25 Pth11-like *N. crassa* GPCR protein sequences were aligned with T-coffee using default parameters and trimmed using TrimAl with a threshold of 0.7 (Notredame *et al.*, 2000; Capella-Gutierrez *et al.*, 2009). The programs seqboot, protpars, and consense, belonging to the Phylip package were used to generate a consensus parsimony tree using 100 bootstrap replicates (Felsenstein, 1989).

Results

***Neurospora crassa* GPCR families shared with other eukaryotes:**

Mammalian GPCRs have been classified using the A-F classification scheme (Attwood and Findlay, 1994) and more recently, the GRAFS method (Fredriksson *et al.*, 2003; Schioth and Fredriksson, 2005). The A-F classification contains six major superfamilies of GPCRs: Class A (rhodopsin like), Class B (secretin like), Class C

(metabotropic glutamate/pheromone), Class D (fungal pheromone), Class E (cAMP receptors), and Class F (Frizzled/Smoothened family). The GRAFS classification grouped the human GPCRs into five families: Glutamate (Class C), Rhodopsin (Class A), Adhesion (Class B), Frizzled/Taste2 (Class F), and Secretin (Class B). Of the 367 predicted human GPCRs, 284 belong to Class A, 50 to Class B, 17 to Class C, and 11 to Class F/S (Vassilatis *et al.*, 2003).

The presence of GPCRs in the model plant *Arabidopsis thaliana* is controversial, with one group predicting up to seven genes (Taddese *et al.*, 2014) and others predicting one [GCR1; (Pandey and Assmann, 2004)] or none (Urano and Jones 2013). GCR1 has several characteristics of GPCRs and exhibits homology to GRAFS classes A, B (Taddese *et al.*, 2014) and E (Pandey and Assmann, 2004). It has been proposed that *A. thaliana* does not need GPCRs, as the sole Gα protein, GPA1, has an extremely high nucleotide exchange rate and low GTPase activity (Johnston *et al.*, 2007), which should lead to a preponderance of the GTP-bound form *in vivo* (Johnston *et al.*, 2007; Urano and Jones, 2014).

A recent analysis provided evidence for four of the five GRAFS families (secretin is absent) in fungi (Krishnan *et al.*, 2012). This work also provided evidence that the fungal cAMP and rhodopsin families share a common ancestor. Other studies have proposed up to 14 classes of GPCRs in fungi (Kulkarni *et al.*, 2005; Zheng *et al.*, 2010; Gruber *et al.*, 2013). Using the GRAFS and fungal classification schemes, the yeast *S. cerevisiae* has 13 predicted GPCRs, with two members in one GRAFS/fungal class (D;

pheromone receptors) and the remaining 11 proteins in 7 different fungal groupings (Table 3.1; data not shown).

Previous studies have identified 43 putative GPCR genes in the *N. crassa* genome (Galagan *et al.*, 2003; Borkovich *et al.*, 2004; Li *et al.*, 2007) (Table 3.1). Of the GPCR families found in mammals, *N. crassa* possesses one Adhesion family GPCR (GPR-1; (Krystofova and Borkovich, 2006) and two cAMP family GPCRs (GPR-2, GPR-3; (Galagan *et al.*, 2003; Borkovich *et al.*, 2004). *N. crassa* also possesses a mPR class (Class VIII), with homology to seven-helix progestin receptors in mammals (Thomas *et al.*, 2007). These proteins are members of the progesterone and AdipoO receptor (PAQR) group of proteins found in many eukaryotes. Evidence that these proteins can function as bona-fide GPCRs in filamentous fungi is suggested by studies in *Sporothrix schenckii*, showing that progesterone is a ligand for a PAQR that also interacts with a Gα protein (Gonzalez-Velazquez *et al.*, 2012). The *N. crassa* genome also predicts one seven-helix protein containing a Lung_7-TM_R domain (Liu *et al.*, 2004) with homology to *S. cerevisiae* PTM1, a protein of unknown function (Inadome *et al.*, 2005). Finally, *N. crassa* possesses one protein with weak similarity to Family C-like (metabotropic glutamate/pheromone) GPCRs in chicken (Zheng *et al.*, 2010).

We identified proteins homologous to the *N. crassa* predicted GPCRs in the yeast *S. cerevisiae* using BLAST searches (Altschul *et al.*, 1990). We and others have previously identified proteins similar to predicted *N. crassa* GPCRs in the filamentous fungus *Aspergillus nidulans* (Lafon *et al.*, 2006; Li *et al.*, 2007) (Table 3.1). The results show that *S. cerevisiae* possesses proteins similar to 12 of the *N. crassa* predicted

GPCRs, with members in classes I-IV, VIII-XI and XIII, and an additional member (total of three proteins) in the microbial opsin class (Table 3.1). *A nidulans* and *N. crassa* share homologs for most predicted *N. crassa* genes, with the exception of the Class XI GPCR89/ABA related gene *gpr-12* and one Pth11-related GPCR, *gpr- 31* (Table 3.1).

Pth11 is a seven-helix transmembrane protein required for development of the infectious appressorium structure and pathogenesis in *M. oryzae* (DeZwaan *et al.*, 1999). It has recently been demonstrated that Pth11, the Gα protein MagA, the RGS Rgs1 and the adenylyl cyclase Mac1 are co-localized on late endosomes during the early stages of pathogenesis, which would enable effective signal transmission (Ramanujam *et al.*, 2013). Sequencing of numerous fungal genomes revealed that filamentous fungi contain a large number of proteins with homology to Pth11 (Kulkarni *et al.*, 2005; Li *et al.*, 2007; Zheng *et al.*, 2010; Gruber *et al.*, 2013), including 25 in *N. crassa* (Kulkarni *et al.*, 2005; Li *et al.*, 2007). This was particularly surprising in the case of *N. crassa*, since the wide array of genome defense mechanisms in this species is thought to have limited the number of gene families (Galagan *et al.*, 2003). The presence of a large number of Pth11-related proteins suggests that members of this class serve important functions in *N. crassa*.

Mutants with phenotypes during asexual growth and development:

We had previously produced knockout mutants for 10 predicted GPCR genes in our laboratory [(Bieszke *et al.*, 1999; Kim and Borkovich, 2004; Krystofova and Borkovich, 2006; Li and Borkovich, 2006; Kim *et al.*, 2012); unpublished]. Mutation of

all predicted GPCR genes was attempted by the Neurospora Genome Project (Colot *et al.*, 2006; Dunlap *et al.*, 2007; Park *et al.*, 2011a). Mutants for seven genes were not available (see Methods), leaving us with 36 viable mutants to analyze.

We analyzed the 36 available GPCR knockout mutants for a variety of growth and developmental phenotypes (Table 3.1; Figure 3.1), first focusing on hyphal growth and asexual sporulation (macroconidiation). The macroconidiation (conidiation) pathway is induced when *N. crassa* is exposed to oxygen (plate cultures) or to a variety of environmental stresses during growth in submerged culture [rev. in (Springer, 1993; Davis and Perkins, 2002; Borkovich *et al.*, 2004)]. The pathway begins with formation of aerial hyphae, tube-like structures that rise up roughly perpendicular to the substratum. Aerial hyphae form constrictions between cell compartments at their tips that eventually lead to formation of mature conidia that can be dispersed by mechanical perturbation or wind currents (Springer, 1993).

We obtained quantitative data for hyphal growth rate and aerial hyphae height and qualitative data for conidia production (Table 3.1). We identified a total of five knockout mutants (14%) with defects in extension of basal hyphae (Figure 3.1; Table 3.1). Of interest, all five belong to Class XIV (Pth11-like). Δ*gpr-31* was the only mutant among the group that had an increased growth rate relative to wild type; all others (Δ*gpr-15*, Δ*gpr-23*, Δ*gpr-29*, and Δ*gpr-38*) grew more slowly than wild type. We previously analyzed 77 protein kinase and 24 protein phosphatase viable mutants in *N. crassa*, with the results demonstrating that 42% of kinase and 50% of phosphatase mutants have a growth rate phenotype (Park *et al.*, 2011b; Ghosh *et al.*, 2014). Thus, the findings for

GPCR mutants suggest either that GPCRs are not critical for growth rate regulation or the presence of gene redundancy.

A total of 14 GPCR mutants (39%) had defects in asexual development, specifically in formation of aerial hyphae (Figure 3.1; Table 3.1). There were no GPCR mutants with obvious defects in conidia production. Of the mutants with aerial hyphae defects, 57% (8/14) are characterized as Class XIV (Pth11-like). Amongst the 14 mutants with aerial hyphae defects, half had a reduced phenotype, while the other half an increased aerial hyphae phenotype. Finally, of the five mutants with defects in basal hyphal growth, three also exhibited reduced formation of aerial hyphae (Δ*gpr-23*, Δ*gpr-29* and Δ*gpr-31*). The proportion of predicted GPCR mutants with defects in asexual development (39%) is similar to that observed for protein kinase mutants (40%), but less than that for protein phosphatase (58%) mutants (Park *et al.*, 2011b; Ghosh *et al.*, 2014).

Mutants with defects in sexual development:

Low nitrogen, as found in synthetic crossing medium (SCM), induces development of female reproductive structures (protoperithecia) (Westergaard and Mitchell, 1947; Raju, 1992) approximately seven days post-inoculation. Fertilization occurs when a specialized hyphae (trichogyne) from the protoperithecium fuses with a cell from an opposite mating type cell (male). After nuclear fusion, meiosis is followed by a round of mitosis and sexual spores (ascospores) that formed within the mature perithecium.

This study analyzed three phases in the sexual cycle: protoperithecia, perithecia, and ascospore formation. A total of six GPCR mutants (17%) showed a defect in sexual development (Figure 3.1, Table 3.1). As previously reported by our group (Kim and Borkovich, 2004, 2006; Kim *et al.*, 2012), the two pheromone receptor mutants displayed defects in sexual development, with *pre-2* affecting all three phases (protoperithecia, perithecia, and ascospore formation), and *pre-1* affecting perithecia and ascospore formation. However, it is should be noted that the sexual defects of these mutants are mating-type dependent; Δ*pre-2* is only female-sterile in *mat a*, and Δ*pre-1* in *mat A* (Kim and Borkovich, 2004; Kim *et al.*, 2012) (Table 3.1). The other four GPCR mutants with sexual defects (Δ*gpr-1*, Δ*gpr-2*, Δ*gpr-3*, and Δ*gpr-15*) all exhibited phenotypes in the perithecial phase, with Δ*gpr-15* having both a protoperithecial and perithecial defect. In spite of their perithecial phenotypes, these four mutants still produced ascospores and thus are technically female-fertile (Table 3.1). Thus, allowing for the mating type specificity of the pheromone receptor mutations, the results showed that no single GPCR gene was essential for female fertility in *N. crassa*. This contrasts with the role of protein kinases and phosphatases in female fertility in *N. crassa*, with 42% of kinase and 63% of phosphatase viable mutants exhibiting a sexual cycle phenotype, and complete female sterility observed for 39 of the kinase and four of the phosphatase mutants (Park *et al.*, 2011b; Ghosh *et al.*, 2014).

Mutants with defects in multiple phases of the lifecycle:

The results described above revealed that 17 of the 36 predicted GPCR mutants (47%) exhibited at least one growth or developmental phenotype (Table 3.1). This number is slightly reduced relative to the kinases [57%; (Park *et al.*, 2011b)], but is two-fold lower than observed for the phosphatase mutants [91%; (Ghosh *et al.*, 2014)]. There were no GPCR mutants with defects in all three phenotypic categories, but eight mutants possessed phenotypes in two categories (Figure 3.1; Table 3.1). The four mutants with defects in both asexual and sexual development included the Δ*pre-2* pheromone receptor mutant and those lacking any one of the three CRL receptor genes (*gpr-1*, *gpr-2* and *gpr-3*). The remaining four mutants with defects in two categories (hyphal growth and either asexual or sexual development) were all in the Pth11-related Group (Figure 3.1; Table 3.1). The relatively low number of GPCR mutants with defects in more than one of the analyzed stages contrasts with that observed for protein kinases (31; 40%) and phosphatases (12; 50%), again suggesting either specialization, participation in pathways not uncovered during our study, or gene redundancy in the predicted GPCRs.

The CRL class of predicted GPCRs is required for normal formation of perithecial beaks and ascospore ejection:

We were interested to find that all three CRL (Class V) mutants possessed defects in both asexual and sexual development (Table 3.1). Notably, *gpr-1* was previously reported to have an important role in proper formation of perithecial beaks (Krystofova and Borkovich, 2006). Beaks are structures formed at the tip of perithecia that are

positively phototrophic to blue light and which normally contain an opening (ostiole) from which the mature ascospores are ejected (Harris *et al.*, 1975; Harding and Melles, 1983). Δ*gpr-1* beaks are deformed and lack ostioles, leading to rupture of the perithecium during discharge of ascospores (Krystofova and Borkovich, 2006). Based on the phenotype of Δ*gpr-1* mutants, we decided to explore beak formation in Δ*gpr-2* and Δ*gpr-3* single mutants, as well as mutants lacking *gpr-1* and various combinations of the other two CRL genes (Figure 3.2).

As shown previously, Δ*gpr-1* beaks do not form ostioles and therefore cannot eject ascospores (Figure 3.2; data not shown). Loss of *gpr-2* or *gpr-3* leads to formation of beaks that bend downwards and/or are torn during ascospore ejection (Figure 3.2). Similarly, mutants lacking *gpr-1* in combination with *gpr-2* and/or *gpr-3* form beaks that are not positively phototrophic and do not contain ostioles (Figure 3.2). Thus, all three CRL genes influence beak morphology and ascospore discharge in *N. crassa*.

Chemical sensitivity and nutritional screens reveal additional GPCR mutants with phenotypes:

As shown in our previous studies with *N. crassa* protein kinase and phosphatase mutants (Park *et al.*, 2011b; Ghosh *et al.*, 2014) and in work with the yeast *S. cerevisiae* (Hillenmeyer *et al.*, 2008), chemical sensitivity and nutritional screening is a useful tool to uncover functions for mutants that lack observable growth or developmental defects. With this in mind, we conducted chemical/nutritional screens on the 36 GPCR mutants, using a total of 10 chemicals. Mutants were grown on agar medium with and without the

added chemical, the percent growth determined and compared to wild type (see Materials and Methods). Mutants with relative growth rates statistically greater than or less than wild type were categorized as resistant or sensitive, respectively (Table 3.2). The chemicals used induced osmotic stress [sorbitol and NaCl; (Ivey *et al.*, 1996)], oxidative stress [menadione and tert-butyl hydrogen peroxide; (Kato *et al.*, 2004; Belden *et al.*, 2007)], cytoskeletal disruption [cytochalasin A and benomyl; (Willhite, 1983; Cooper, 1987)], inhibition of the Ca^{2+}-calmodulin dependent phosphatase calcineurin [FK506; (Prokisch *et al.*, 1997)], fungicidal activity [fludioxonil; (Ochiai *et al.*, 2001)] and nutritional substitution or supplementation (Avicel and yeast extract).

No mutants were significantly different than wild type during growth on NaCl or benomyl, and therefore these two agents are not shown in Table 3.2. A total of 18 GPCR mutants exhibited at least one phenotype using the other eight chemicals in the screen and 11 of these mutants did not exhibit a growth or developmental phenotype. More than half (10/18; 56%) of the 18 mutants with chemical phenotypes are classified as Pth11-like receptors.

The chemical that yielded the largest number of mutants with phenotypes was cytochalasin A, with six affected strains (Table 3.2). Cytochalasin A interferes with actin function by inhibiting polymerization of monomers (Cooper, 1987). Three mutants (Δ*gpr-5*, Δ*gpr-6* and Δ*gpr-25*) were found to be resistant to cytochalasin A, while Δ*gpr-1*, Δ*gpr-23* and Δ*gpr-29* strains were sensitive. GPR-5 and GPR-6 are similar to Stm1p, a PQ-loop family protein originally implicated in nitrogen sensing upstream of the Gα protein Gpa2 in *S. pombe* (Chung *et al.*, 2001), with more recent evidence suggesting that

the *S. cerevisiae* homolog YPQ1 may function as a vacuolar amino acid transporter (Sekito *et al.*, 2014). The finding that two Stm1p-related proteins confer resistance to cytochalasin A in *N. crassa* suggests a connection between actin polymerization and G protein signaling or vacuolar amino acid transport. GPR-1 is a CRL, while *gpr-23*, *gpr-25* and *gpr-29* encode Pth11-related proteins. Of these, GPR-25 is the closest *N. crassa* homolog to *M. oryzae* Pth11 (Figure 3.6). The cytochalasin A phenotype for Δ*gpr-25* mutants may point to a role for GPR-25 in actin dynamics.

FK506 inhibits the phosphatase calcineurin, which is regulated by Ca^{2+}-calmodulin. Five GPCR mutants, Δ*gpr-7*, Δ*gpr-10*, Δ*gpr-16*, Δ*gpr-27*, and Δ*gpr-31,* were all resistant to FK506, suggesting a possible role in regulation of the phosphatase or modulating calcium signaling. Of interest, the closest yeast homolog for *N. crassa* GPR-10 is Izh2p (Table 3.1). Izh2p and three other proteins in yeast each have four metal ion binding sites and have been variously implicated in zinc homeostasis, regulation of membrane sterol content and a signaling pathway upstream of the Zap1 transcription factor (Lyons *et al.*, 2004). Izh2p is of particular interest, since it has recently been shown to function as a receptor for plant PR-5 proteins and is required for the response to polyene antifungal drugs (Narasimhan *et al.*, 2005; Villa *et al.*, 2011). Our finding that these *N. crassa* mutants are resistant to FK506 suggests that the calcineurin phosphatase may be a component of the downstream pathway.

Two GPCR mutants, *Δgpr-9* and *Δgpr-29*, showed increased resistance to osmotic stress induced by sorbitol. GPR-9 is most homologous to the *S. cerevisiae* protein Izh3p, a mPR-like PAQR class protein similar to Izh2p, while GPR-29 is a Pth11-related

receptor. Izh3p dosage affects resistance to polyene drugs in yeast, similar to Izh2p (Villa *et al.*, 2011).

Peroxide, menadione and fludioxonil testing each yielded one GPCR with a phenotype (Δ*gpr-23*, Δ*nop-1* and Δ*gpr-24*). We observed that Δ*nop-1* mutants are resistant to the reactive oxygen species (ROS) generating compound menadione. The only phenotypes that had previously been noted for Δ*nop-1* mutants were effects on colony morphology (Bieszke *et al.*, 1999) and conidiation-regulated gene expression (Bieszke *et al.*, 2007). The menadione phenotype is of particular interest since a link between conidiation and ROS has been determined for *N. crassa*, with elevated ROS correlating with aerial hyphae and conidia development (Hansberg *et al.*, 1993). Our demonstration that Δ*nop-1* mutants are more resistant to menadione correlates with the slightly increased formation of aerial hyphae in these mutants in plate cultures and with elevated expression of certain conidiation specific genes at specific times during asexual development (Bieszke *et al.*, 2007).

We also explored growth of the mutants in medium supplemented with yeast extract or with crystalline cellulose (Avicel) as an alternative carbon source. Δ*gpr-11* mutants grew better than wild type in medium containing yeast extract (Table 3.2). This was the only phenotype noted for this Lung 7-TM superfamily protein during our study. Three Pth11 class mutants, Δ*gpr-32*, Δ*gpr-36*, and Δ*gpr*-39, grew better than wild type on medium containing 2% Avicel as an alternative to sucrose (Table 3.2). This finding suggests that these Pth11 class proteins may participate in sensing plant-related carbohydrates.

The total number of GPCR mutants with at least one growth/morphological or chemical sensitivity phenotype was 29 (81%). This fraction is greater than that observed for protein kinase mutants (71%), but less than the protein phosphatases (100%).

Predicted GPCR genes are differentially expressed during growth and development:

RNA expression data for GPCRs was mined from publically available datasets. Experiments included those performed under different environmental conditions and time-courses for specialized tissue types (Kasuga and Glass, 2008; Greenwald *et al.*, 2010; Coradetti *et al.*, 2012; Nordberg *et al.*, 2014; Wang *et al.*, 2014). In all instances, data was analyzed and visualized using pheatmap (V1.0.2); (Kolde, 2015); (Figure 3.3-3.5).

We first analyzed an RNAseq dataset for sexually differentiating cultures that included eight time-points (0, 2, 24, 48, 72, 98, 120, and 144 h after fertilization) (Wang *et al.*, 2014). At time 0 h, cultures contain vegetative hyphae and unfertilized female structures (protoperithecia). Within 24 h after fertilization, perithecia can be observed. Croziers, structures that will develop into asci containing the meiotic progeny (ascospores) become apparent between 48-72 h after fertilization (Raju, 1992; Read and Beckett, 1996). After 96 h, asci become detectable and at 120-144 h perithecia produce beaks, a structure required to eject ascospores into the environment.

The dataset for sexual development contained expression data for 37 of the 43 predicted GPCR genes, with the genes falling into five major groups (Figure 3.3). Group 1 genes are all down-regulated after 72 h, at the time when the synchronization of nuclei

is occurring in the croziers. Group 1 can be subdivided into subgroups 1A and 1B, which differ in their patterns of expression prior to 72 h. The three genes in Subgroup 1A (*gpr-6* and two Pth11-related genes) are upregulated at 2 h after fertilization, with expression diminishing at 24 h, rising again at 48 h. Cluster 1B genes (*gpr-10* and three Pth11-related GPCRs) are highly expressed at 0 and 2h after fertilization, but then resemble Subgroup 1A for the rest of the time course.

Group 2 genes (*gpr-8* and four Pth11-related GPCRs) exhibited highest levels of expression at 24 or 48 h after fertilization (the time when perithecia first become visible), with relatively lower levels at 72-144 h. Group 3 genes (seven total) have relatively low levels of expression until 48-72 h, corresponding to the emergence of croziers. In general, Group 3 gene expression remains high throughout the rest of perithecial development. Three Group 3 genes have been previously examined for expression during at least one phase of sexual development using northern analysis: *pre-2*, *gpr-1* and *nop-1*. In congruence with the RNAseq data, expression of the pheromone receptor *pre-2* is low in *mat A* protoperithecia (0 h), but increases after fertilization with *mat a* conidia (Kim *et al.*, 2012). Northern analysis demonstrated that The CRL GPCR *gpr-1* is highly expressed in protoperithecia, with even greater levels in perithecia (Krystofova and Borkovich, 2006) and the RNAseq results showed that mRNA levels are greater during the time of perithecial development than in protoperithecia (Figure 3.3). Finally, although the microbial opsin *nop-1* is highly expressed in protoperithecia, levels in perithecia have not been investigated using northern analysis (Bieszke *et al.*, 1999), precluding direct comparison to the RNAseq results.

Group 4 (nine genes) is divided into Subgroups 4A and 4B (Figure 3.3). In general, genes in both subgroups exhibit their highest levels of expression at 0 h, prior to fertilization. Group 4A genes have dropped to their lowest levels of expression by 120-144 h, while expression of most Group 4B genes rises again later during perithecial development. The authors of the RNAseq study noted that due to the difficulty in obtaining pure reproductive structures, vegetative hyphae is likely present in the samples prior to 48 h post-fertilization (Wang *et al.*, 2014). With this in mind, it is important to note that mutants lacking three of the genes in Group 4 had a phenotype during growth or sexual or asexual development. Δ*gpr-3* has defects in asexual and sexual development; Δ*gpr-31* in asexual development and linear growth; and Δ*gpr-17* only in asexual development (Table 3.1, Figure 3.1).

Group 5 is the largest, with 12 genes (Figure 3.3). Most of the genes in this group are up-regulated 120-144 h after fertilization, when mature perithecia are present. However, only the CRL *gpr-2* and the pheromone receptor *pre-1* play obvious roles during sexual development (Table 3.1). The finding that the other 10 genes have no obvious sexual cycle phenotype suggests at least some of them may be functionally redundant. Finally, the expression trend for *pre-1* is supported by previous northern analysis revealing increased expression of *pre-1* in *mat A* protoperithecia after fertilization with *mat a* conidia (Kim and Borkovich, 2004).

We next mined microarray expression data from six time points during vegetative colony development (1, 3, 9, 15, 21, and 27 h) (Kasuga and Glass, 2008). Colony establishment consists of multiple events: hyphal extension, branching, anastomosis, and

asexual sporulation (Kasuga and Glass, 2008). Early features of colony establishment can be seen in the 1 h time point at the leading hyphal edge. This "periphery growth zone" is rich with organelles, such as endoplasmic reticulum, Golgi apparatus, polysomes and mitochondria. Asexual development involves aerial hyphae growing upward from the colony, followed by production of conidiophores and mature conidia from the tips of aerial hyphae. Asexual development structures were first seen at 15 h and mature conidia at 27 h (Kasuga and Glass, 2008).

We mapped expression for 20 GPCRs, present in four groups (Figure 3.4A). Group 1 genes are highly expressed in leading basal hyphae, and tend to decrease in expression in older parts of the colony (Figure 3.4A). The only exceptions are *gpr-2* and *gpr-37*, which exhibit elevated expression at 27 h. Δ*gpr-2* mutants have defects in aerial hyphae development (Table 3.1), consistent with increased expression of *gpr-2* later during colony development. Group 2 (4 genes) has a pattern of high expression early and late during colony development (Figure 3.4A). This group includes two genes (*gpr-3* and *gpr-30*) that are required for normal aerial hyphae development. The expression of Group 3 genes peaked late during asexual sporulation (27h) at the time when conidia are mature. Of these four genes, mutants lacking *gpr-23* have defects in aerial hyphae development (Table 3.1; also see below). Lastly, Group 4 genes have low levels of expression early during colony development, with most increasing from 3-21 h and then falling again at 27 h (Figure 3.4A). This group includes two genes (*gpr-16* and *gpr-39*) that are required for normal aerial hyphae development (Table 3.1).

Expression data for a time course of asexual development was mined from microarray data (Greenwald *et al.*, 2010) (Figure 3.4B). RNA was extracted from the entire colony at 0, 2, 4, 8, 10 and 24 h. At 12 h, the basal hyphae (bottom) was collected separately from the upper portion of the colony containing aerial hyphae and conidia. This was done to detect expression of genes in the cell types that give rise to aerial hyphae and mature conidia. Only the top of the colony was analyzed at 14 and 18 h, to focus on genes expressed in aerial hyphae and conidia. We were able to detect expression of four GPCR genes (*gpr-8*, *gpr-23*, *gpr-17* and *nop-1*) in this dataset (Figure 3.4B).

Mutants lacking *gpr-23* have a defect in both hyphal growth and asexual development (Table 3.1). Therefore, it is of interest that *gpr-23* expression is highest during the early stages of colony establishment from 0-4 h, the time during which aerial hyphae production is initiated. As supported by previous work (Bieszke *et al.*, 2007), *nop-1* is a late-stage conidiation gene with high transcript levels from 12-24 h in aerial hyphae tissue (Greenwald *et al.*, 2010). Δ*nop-1* mutants have defects in aerial hyphae development (Table 3.1).

We next analyzed RNAseq expression data for strains grown in two different carbon sources: sucrose and crystalline cellulose (Avicel) (Figure 3.5) (Coradetti *et al.*, 2012). Sucrose is the carbon source used for VM medium and, with the exception of testing growth on Avicel (see below), was present in all media used for phenotypic analysis in our study. We detected expression for 40 GPCR genes in the dataset (Figure 3.5). Since we had tested available mutants for increased or decreased growth relative to

wild type on Avicel (Table 3.2), we were able to compare growth phenotypes and gene expression for numerous GPCR genes.

The majority of GPCR genes (24) were expressed to higher levels on Avicel relative to sucrose (Figure 3.5). Among these, 10 genes (*nop-1*, *gpr-3*, *gpr-8*, *gpr-11*, *gpr-18*, *gpr-24*, *gpr-30*, *gpr-31*, *gpr-34* and *gpr-39*) had mean expression levels greater than 200 reads per kilobase per million mapped reads (RPKM) on Avicel (Figure 3.5). From this highly expressed group, *nop*-1 had the greatest fold difference of 166, while *gpr-34* was second, with a 32-fold difference comparing Avicel vs. sucrose. Of interest, 60% of the genes with the highest expression levels on Avicel are annotated as Pth11-related. As described above, our analysis revealed that three GPCR mutants (Δ*gpr-32*, Δ*gpr-36* and Δ*gpr-39*; all Pth11-related class) had a phenotype during growth on Avicel (Table 3.2). mRNA levels for all three of these genes are greater on Avicel than sucrose (Figure 3.5), with *gpr-39* levels increased 6-fold on Avicel vs. sucrose). These observations suggest that the other GPCRs that are highly expressed on Avicel may be required for growth on this carbon source, but that gene redundancy is masking phenotypes in single mutants. This is of particular interest for the Pth11-related group, as 14 out of the 22 detected genes are expressed to higher levels on Avicel than sucrose (Figure 3.5) and this class of GPCRs has the most members that are required for normal growth on Avicel.

There are nine genes (*gpr-9*, *gpr-10*, *orp-1*, *gpr-17*, *gpr-22*, *gpr-23*, *gpr-29*, *gpr-35* and *gpr-37*) for which the mRNA amount is at least two-fold greater during growth on sucrose vs. Avicel (Figure 3.5). This set includes the two mPR-like GPCRs in *N. crassa* (*gpr-9* and *gpr-10*; Table 3.1). In particular, when cultured on sucrose, *gpr-10* is the most

highly expressed GPCR in the dataset. Δ*gpr-10* (and Δ*gpr-9*) mutants had no growth or developmental phenotypes on VM medium, perhaps reflecting gene redundancy between these two mPR-like GPCRs in *N. crassa*.

Phylogenetic analysis of *N. crassa* Pth11-related GPCRs:

The 25 *N. crassa* Pth11-related GPCR protein sequences were aligned with the *M. grisea* Pth11 protein sequence (MG05871) (see Materials and Methods). The alignment was adjusted manually to account for conservation of the CFEM domains present in *N. crassa* GPR-25 and *M. oryzae* Pth11. The CFEM domain consists of a conserved sequence containing eight cysteines that is proposed to play an important role in fungal pathogenesis (95). GPR-25 is the only *N. crassa* GPCR with a CFEM domain and is the protein most similar to *M. oryzae* Pth11 in *N. crassa* (Figure 3.6).

A phylogenetic tree was generated from the alignment data (Figure 3.6). The tree revealed seven distinct groups among the *N. crassa* Pth11-related proteins. In Group 1, three Pth11-related genes were highly expressed on Avicel (expression greater than 200 FPKM; *gpr-18*, *gpr-30* and *gpr-34*; Figure 3.5). A mutant was not available for *gpr-18*, but the Δ*gpr*-32 strain had a phenotype when grown on Avicel (Δ*gpr-30* was normal). Therefore, not only does Group 1 have protein-based homology, but its members may function in processing Avicel.

The tree revealed eight clusters, each containing two closely related proteins. Inspection of the characteristics of several of these pairs revealed shared patterns of gene expression and/or phenotypes that suggest overlapping functions. For example, *gpr-18*

and *gpr-32* cluster together in Group 1. Both genes are more highly expressed on Avicel relative to sucrose (Figure 3.5); are similarly expressed during sexual development (Group 5; Figure 3.3); and are in neighboring expression clusters for colony development (Groups 3 and 4; Figure 3.4A). Although the mutant for *gpr-18* was not available, Δ*gpr-32* mutants have a phenotype on Avicel (Table 3.2).

gpr-36 and *gpr-24* are related proteins in Group 3. Both genes are more highly expressed on Avicel than sucrose (Figure 3.5), but have differing patterns of expression during sexual development (Figure 3.3). Δ*gpr-36* has a phenotype on Avicel, while Δ*gpr-24* has a chemical phenotype on fludioxonil (Table 3.1). *gpr-15* and *gpr-29* branch together in Group 3. These two genes have similar patterns of expression during sexual development (Figure 3.3), but exhibit opposite trends during growth on sucrose vs. Avicel (Figure 3.5). Importantly, while Δ*gpr-15* and Δ*gpr-29* mutants both have reduced linear growth rates, Δ*gpr-15* uniquely possesses defects in sexual development and Δ*gpr-29* in aerial hyphae extension (Table 3.1). These results may indicate that these two genes have overlapping functions not only during linear hyphal growth, but also possibly asexual and sexual development.

gpr-22 and *gpr-23* are another closely related pair in Group 3. Both genes are more highly expressed on sucrose than Avicel (Figure 3.5), are in the same expression group during sexual development (Group 2; Figure 3.3), and share phenotypic defects in aerial hyphae development (Table 3.1). Expression of *gpr-23*, but not *gpr-22*, was detected during the time course of asexual development in two microarray experiments

(Figure 3.4A, B). These results strongly suggest a role for these two genes in asexual development and Avicel utilization.

gpr-16 and *gpr-39* comprise Group 6. These genes are co-expressed during the time courses for sexual development and colony growth (Figure 3.3, Figure 3.4A). Both mutants have defects in aerial hyphae development, coinciding with their expression later during colony development (Table 3.1; Figure 3.4A). Of interest, these two proteins are the most closely related to GPR-25, the Pth11 homolog in *N. crassa*. As mentioned above, Δ*gpr-25* mutants are resistant to the actin depolymerizing agent cytochalasin A. The observation of functions for *gpr-16* and *gpr-39* in aerial hyphae development may indicate similarities in regulation of this process and the infectious appressorium in *M. oryzae* by G protein signaling. Furthermore, the phenotype of Δ*gpr-25* mutants may indicate a role for actin polymerization in this process.

Our phylogenetic results have some similarities but also differ from those of Kulkarni *et al.* who performed analysis using all *M. oryzae* and *N. crassa* Pth11-related proteins. As mentioned above, GPR-25 is the closest *N. crassa* homolog to *M. oryzae* Pth11 in both studies (Kulkarni *et al.*, 2005) (Figure 3.6). In addition, GPR-16 (NCU02903) and GPR-39 (NCU09823) are the nearest *N. crassa* relatives to *N. crassa* GPR-25 (Figure 3.6). However, there are several instances of closely related pairs of *N. crassa* proteins that did not cluster together in the Kulkarni study (e.g., GPR-18 and GPR-32; GPR-24 and GPR-36), possibly due to the absence of the *M. oryzae* proteins in our analysis or the different method used to produce the tree.

Discussion

We have analyzed available mutants for annotated GPCR genes in *N. crassa*. Of the 36 available mutants, 29 (81%) exhibited at least one phenotypic defect, and 15 of these are members of the Pth11-related class. In addition, 59% (10/17) of the GPCR genes with a phenotype in one the three major growth/developmental pathways analyzed were Pth11-like. Specifically, 17% (1/6) of sexual development, 57% (8/14) of aerial hyphae and 100% (5/5) of hyphal growth mutants lacked Pth11-related genes, revealing the functional importance of this group, particularly for hyphal growth and aerial hyphae development.

A recent study of GPCR knockout mutants in the filamentous fungal pathogen *Aspergillus flavus* analyzed 15 mutants in Groups I-IX (Affeldt *et al.*, 2014). *N. crassa* has 14 genes in these groups. The *A. flavus* study did not include Groups X-XIII or the Pth11-related class (named class XIV in our study), corresponding to 31 genes in *N. crassa* and the majority of predicted GPCRs in filamentous fungi. Although *N. crassa* mutants for groups VII and XIII were not available for our study, we are the first to systematically analyze mutants in the Pth11-related class of predicted GPCR genes in a filamentous fungus. Only a small subset of the phenotypic analyses addressed in the *A. flavus* study overlapped with those in our experiments, including hyphal extension on sucrose-containing medium and sensitivity to hydrogen peroxide and sodium chloride (Affeldt *et al.*, 2014). Inspection of the data showed there was no overlap in the three phenotypes for the corresponding *A. flavus* and *N. crassa* mutants. It is difficult to draw strong conclusions from such a small set of phenotypes, and further experimentation is

necessary to investigate evolutionarily conserved functions for predicted GPCRs in the two species.

Our results with GPCR genes contrast with those obtained for analysis of other *N. crassa* gene groups implicated in early steps in signal transduction in eukaryotes: serine-threonine protein kinases and serine-threonine and tyrosine protein phosphatases (Park *et al.*, 2011b; Ghosh *et al.*, 2014). The number of predicted GPCRs (Chung *et al.*, 2001) is intermediate between serine-threonine protein kinases (Park *et al.*, 2011a) and protein phosphatases (Ghosh *et al.*, 2014). In terms of the number of mutants with growth, developmental or chemical/nutritional phenotypes, GPCRs are also intermediate with 81%, as 100% of the viable phosphatase mutants had at least one phenotype, while 71% of the viable serine/threonine protein kinase mutants had at least one phenotype. Closer inspection of phenotype classes indicates that in comparison to GPCRs, a larger proportion of kinase and phosphatase mutants have defects in sexual development or are multiply defective in the three major growth/developmental pathways. This result may reflect greater gene redundancy in the GPCRs and/or their involvement in functions that were not assayed during our investigations.

We used existing RNA profiling data from three datasets to mine expression trends for GPCR genes during perithecial development, colony growth, conidiation and growth on Avicel. We were able to analyze 37/43 genes (86%) from the sexual development time course, 20/43 (47%) in the colony establishment dataset, 4/43 (9%) during the conidiation time course and 40/43 genes during expression on Avicel vs. sucrose (93%). We observed several instances where the expression and phenotypic data

appeared to overlap. From the colony development time course data, we noted that the CRL GPCR *gpr-2* is expressed in the older parts of the colony (Figure 3.4A). Consistent with this observation, Δ*gpr-2* mutants have defects in aerial hyphae development (Table 3.1). During the conidiation time course, we saw that mRNA levels for the Pth11-like GPCR gene *gpr-23* are greatest during the time aerial hyphae production is initiated (Figure 3.4B), and mutants lacking this gene have defects in basal hyphae extension and aerial hyphae development (Table 3.1).

We also noted instances where only one gene in a larger group of co-expressed genes yielded a phenotype for that process. For example, during the sexual development time course, although the majority of Group 5 genes are highly expressed at the time of perithecial maturation (Figure 3.3), only two genes in this group, the CRL *gpr-2* and the pheromone receptor *pre-1*, have sexual development defects (Table 3.1). The finding that the other 10 genes have no obvious sexual cycle phenotype suggests that at least some of them may be functionally redundant.

As previously mentioned, 20 genes were available for expression analysis on Avicel and sucrose. Of interest, 14 out of the 20 available (70%) were Pth11-class genes that were expressed to higher levels on Avicel than sucrose. This observation, along with the fact that all three of the mutants (*Δgpr-32, Δgpr-36*, and *Δgpr-39*) with defects during growth on Avicel were Pth11-related genes, suggests that this group of predicted GPCRs may function in sensing or utilization of plant-derived biomass. In the phylogenetic tree (Figure 3.6) Group 1 was particularly noteworthy, as three of the genes (*gpr-34, gpr-30*, and *gpr-18)* were highly expressed on Avicel and one member (not highly expressed) had

a resistance phenotype on Avicel. We hypothesize that construction and analysis of strains carrying multiple knockout mutations in Group 1 genes may reveal additional genes with phenotypes on Avicel.

In this study we examined the expression and functions of predicted GPCR genes during growth and development in *N. crassa*. Although none of the four transcriptomic data sets included data for every predicted GPCR, all contained data for the gene in at least one unavailable mutant. We obtained expression data for many GPCR genes that did not yield a phenotype when mutated. In several cases, closely related genes shared expression patterns, but only one mutant had a phenotype, suggesting overlapping functions for the two genes. These findings can be addressed in the future through construction of strains carrying multiple GPCR gene knockouts. Special interest was taken in the Pth11-related class due to its influence on asexual development and hyphal growth. This study has expanded knowledge of a gene family related to a pathogenicity locus in a fungal plant pathogen using an easily tractable non-pathogenic fungal species.

Table 3.1: *Neurospora crassa* G protein coupled receptor gene families and summary of growth/developmental and chemical sensitivity/nutrition phenotypes.

Fungal GPCR Class	Description GPCR Class	NCU[a]	*N. crassa* Gene(s)[b]	*Saccharomyces cerevisiae* Homolog[c]	*Aspergillus nidulans* Homolog[d]	Linear Growth[e]	Asexual Development[f]	Sexual Development[g]	Chemical Sensitivity[h]/ Nutrition[i]
I	Fungal Pheromone	05758	*pre-2*	*STE2*	*gprA*		AH	PP,P,A[j]	
II	Fungal Pheromone	00138	*pre-1*	*STE3*	*gprB*			P,A[j]	
III	Carbon Sensory	06312	*gpr-4*	*GPR1*	None				
IV	Stm1-like	00300	*gpr-5*	*YPQ1*	AN5720				C
IV	Stm1-like	09195	*gpr-6*	*RTC2*	AN5720				C
V	cAMP Receptor-Like	00786	*gpr-1*	None	AN8262		AH	P	C
V	cAMP Receptor-like	04626	*gpr-2*	None	AN8262		AH	P	
V	cAMP Receptor-like	09427	*gpr-3*	None	AN8262		AH	P	

VI	GprK-like/ RGS Domain	09883	*gpr-7*	None	AN7795 (*gprK*)				F
VII	Rat growth hormone releasing factor receptor-like	03253	*gpr-8*	None	AN6680	NA[k]			
VIII	mPR-Like/ PAQR	03238	*gpr-9*	*IZH3*	AN4932				S
VIII	mPR-like/ PAQR	04987	*gpr-10*	*IZH2*	AN4932				F
IX	Microbial Opsin	10055	*nop-1*	*YRO2*, *MRH1*, *HSP30*	AN3361		AH		M
IX	Microbial Opsin	01735	*orp-1*	*YRO2*, *MRH1*, *HSP30*	AN3361		AH		
X	Lung 7TM Superfamily	00182	*gpr-11*	*PTM1*	AN0063				YE
XI	GPCR89/ABA GPCR	00005	*gpr-12*	YHR078w	None				
XII	Family C-like	06629	*gpr-13*	None	AN8601				A
XIII	DUF300 superfamily/Ps GPR11	06987	*gpr-14*	YKR051W	AN2232	NA[k]			

XIV*	Pth11-like	00700	*gpr-15*	None	AN12202	R		PP,P	
	Pth11-like	02903	*gpr-16*	None	AN0178		AH		F
	Pth11-like	04106	*gpr-17*	None	AN7774		AH		
	Pth11-like	04931	*gpr-18*	None	AN10886	NA[k]			
	Pth11-like	05101	*gpr-19*	None	AN1930	NA[k]			
	Pth11-like	05187	*gpr-20*	None	AN8661	NA[k]			
	Pth11-like	05189	*gpr-21*	None	AN8661				
	Pth11-like	05307	*gpr-22*	None	AN0751		AH		
	Pth11-like	05829	*gpr-23*	None	AN0751	R	AH		C,T
	Pth11-like	05854	*gpr-24*	None	AN8971				FL

	Pth11-like	06531	*gpr-25*	None	AN5639				C
	Pth11-like	17171	*gpr-26*	None	AN5664	NA[k]			
	Pth11-like	07538	*gpr-27*	None	AN5664				F
	Pth11-like	16721	*gpr-28*	None	AN2249	NA[k]			
	Pth11-like	07649	*gpr-29*	None	AN8943	R	AH		S,C
	Pth11-like	07769	*gpr-30*	None	AN4452		AH		
	Pth11-like	08429	*gpr-31*	None	None	I	AH		F
	Pth11-like	08431	*gpr-32*	None	AN5664				A
	Pth11-like	08447	*gpr-33*	None	AN5664				
	Pth11-like	08624	*gpr-34*	None	AN0178				

	Pth11-like	08718	*gpr-35*	None	AN8951				
	Pth11-Like	09022	*gpr-36*	None	AN5664				A
	Pth11-like	09201	*gpr-37*	None	AN5664				
	Pth11-like	09796	*gpr-38*	None	AN8328	R			
	Pth11-like	09823	*gpr-39*	None	AN1930		AH		A

Table 3.2 G protein coupled receptor mutants with chemical sensitivity phenotypes

NCU	*N. crassa* Gene	Sorbitol	Peroxide	Menadione	FK506	Cytochalasin A	Fludioxonil	Avicel	Yeast Extract
00300	*gpr-5*					R (+29%)			
09195	*gpr-6*					R (+25%)			
00786	*gpr-1*					S (-13%)			
09883	*gpr-7*				R (+31%)				
03238	*gpr-9*	R (+11%)							
04987	*gpr-10*				R (+15%)				
10055	*nop-1*			R (+26%)					
00182	*gpr-11*								R (+18%)
02903	*gpr-16*				R (+18%)				
05829	*gpr-23*		S (-25%)			S (-29%)			
05854	*gpr-24*						S (-29%)		
06531	*gpr-25*					R (+25%)			
07538	*gpr-27*				R (+19%)				
07649	*gpr-29*	R (+21%)				S (-28%)			
08429	*gpr-31*				R (+16%)				

08431	*gpr-32*							R (+39%)	
09022	*gpr-36*							R (47%)	
09823	*gpr-39*							R (30%)	

R, more resistant than wild type; S, more sensitive than wild type. T-test was performed with a cutoff at $p \leq 0.05$ (for two replicates) and at least $p \leq 0.20$ for the third.

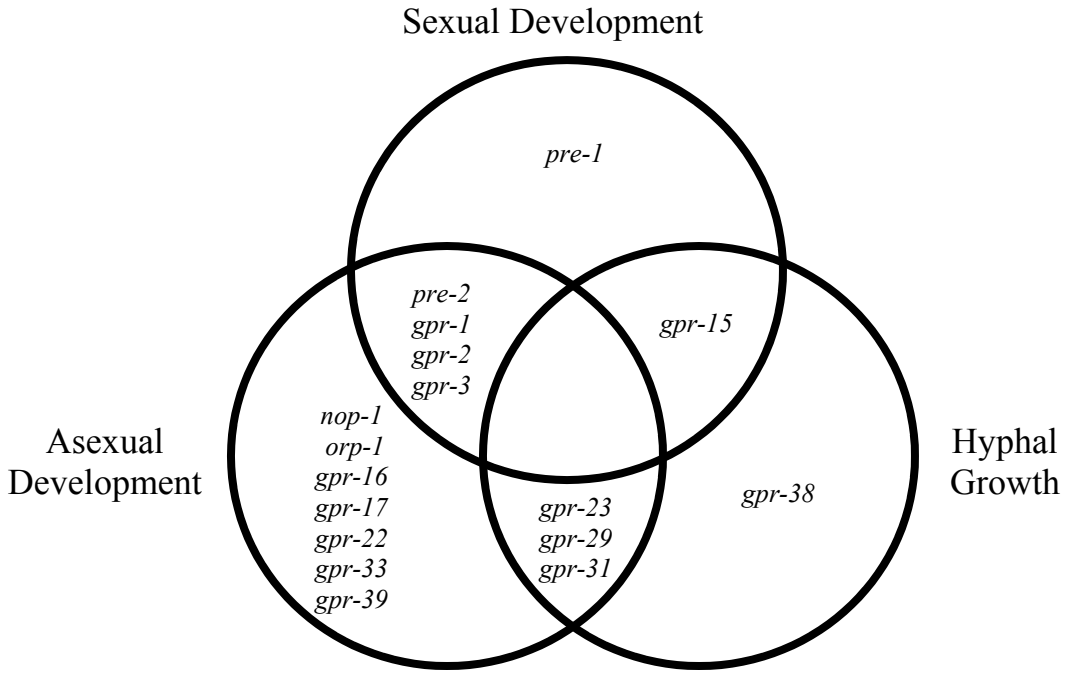

Figure 3.1: Venn diagram displaying GPCR mutants with phenotypes in growth and development.

From the 36 available mutants, 17 (47%) exhibited a defect in at least one assay for hyphal growth or asexual or sexual development, as shown. Mutants with defects are indicated as gene names for the deleted genes.

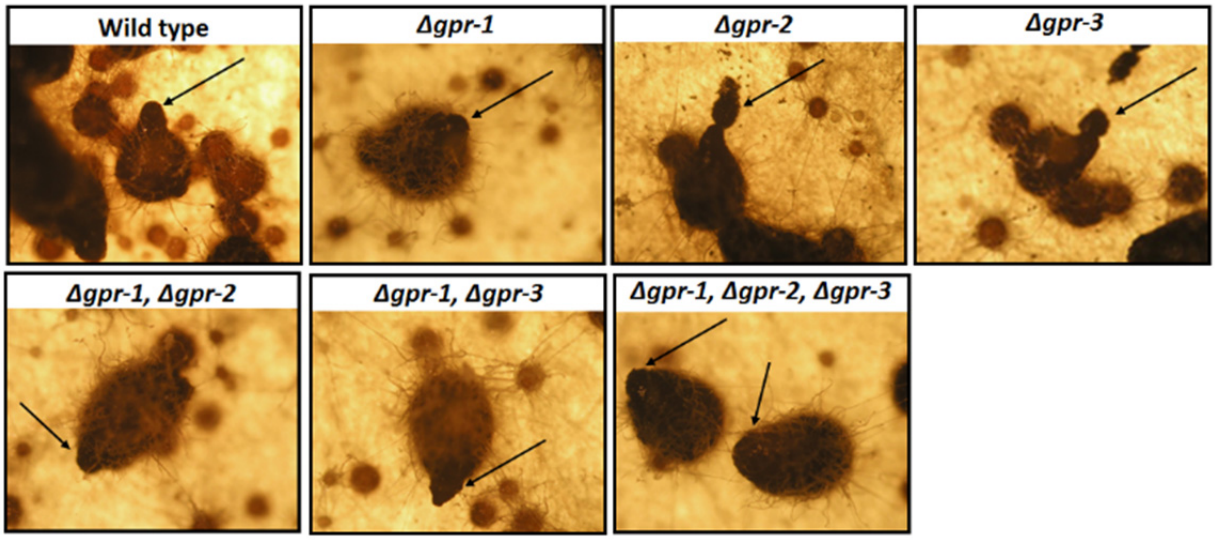

Figure 3.2: Perithecial development in *Δgpr-1*, *Δgpr-2* and *Δgpr-3* mutants lacking CRL class GPCRs.

SCM cultures of the indicated strains containing protoperithecia were fertilized using opposite mating type conidia from a wild type strain. Perithecia were photographed 10 days later. The arrows indicate normal perithecial beaks (wild type), perithecia with beaks that lack ostioles (*Δgpr-1*) or perithecia with beaks that bend downwards or are torn during ascospore ejection (single or double mutants lacking *gpr-2* or *gpr-3*).

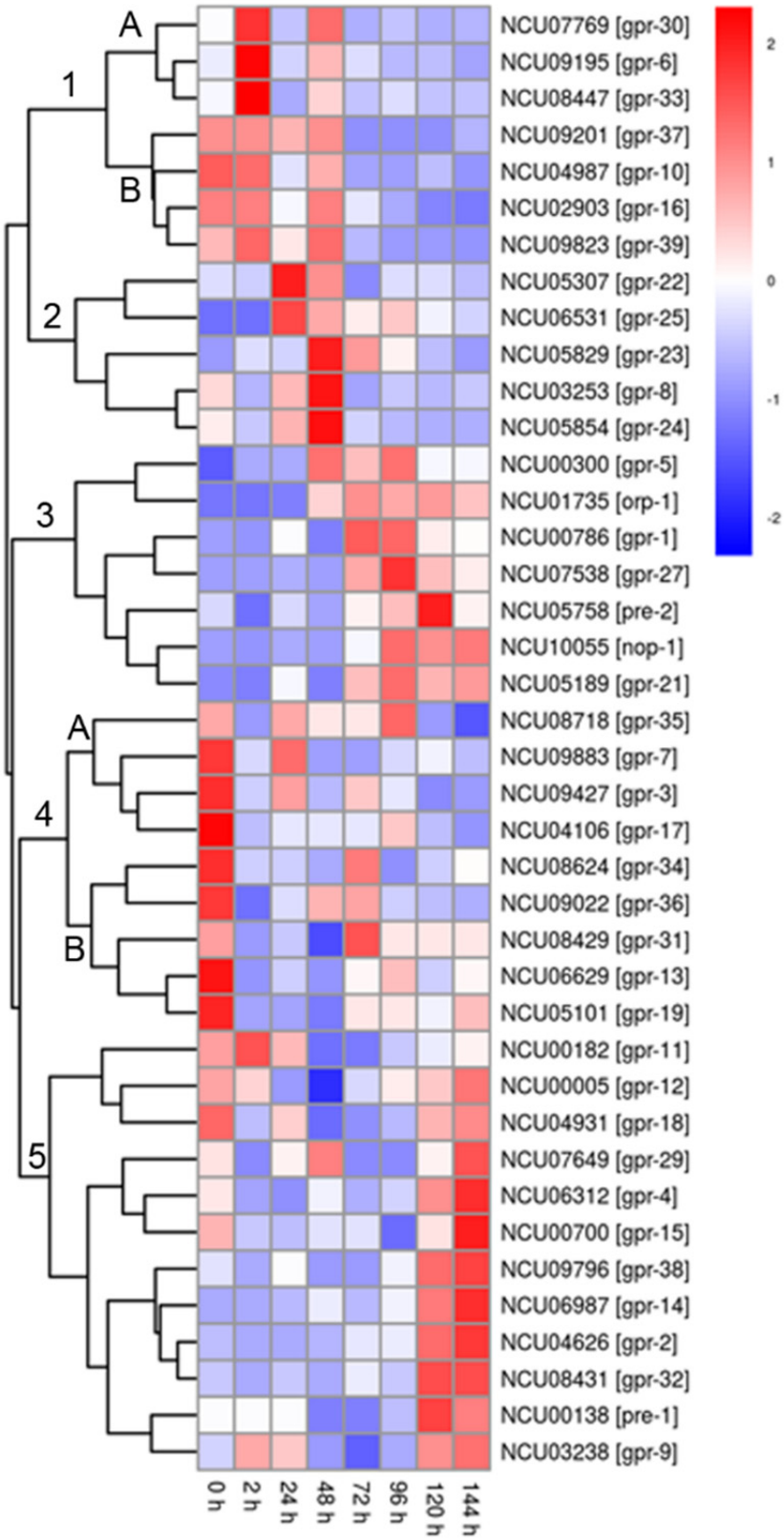
A
1
B
2
3
A
4
B
5
NCU07769 [gpr-30]
NCU09195 [gpr-6]
NCU08447 [gpr-33]
NCU09201 [gpr-37]
NCU04987 [gpr-10]
NCU02903 [gpr-16]
NCU09823 [gpr-39]
NCU05307 [gpr-22]
NCU06531 [gpr-25]
NCU05829 [gpr-23]
NCU03253 [gpr-8]
NCU05854 [gpr-24]
NCU00300 [gpr-5]
NCU01735 [orp-1]
NCU00786 [gpr-1]
NCU07538 [gpr-27]
NCU05758 [pre-2]
NCU10055 [nop-1]
NCU05189 [gpr-21]
NCU08718 [gpr-35]
NCU09883 [gpr-7]
NCU09427 [gpr-3]
NCU04106 [gpr-17]
NCU08624 [gpr-34]
NCU09022 [gpr-36]
NCU08429 [gpr-31]
NCU06629 [gpr-13]
NCU05101 [gpr-19]
NCU00182 [gpr-11]
NCU00005 [gpr-12]
NCU04931 [gpr-18]
NCU07649 [gpr-29]
NCU06312 [gpr-4]
NCU00700 [gpr-15]
NCU09796 [gpr-38]
NCU06987 [gpr-14]
NCU04626 [gpr-2]
NCU08431 [gpr-32]
NCU00138 [pre-1]
NCU03238 [gpr-9]
0 h
2 h
24 h
48 h
72 h
96 h
120 h
144 h
2
1
0
-1
-2

Figure 3.3: Clustering and heatmap generation of mRNA expression data for *N. crassa* GPCR genes during a time course of sexual development.

RNAseq data was mined from (Wang et al. 2014).Expression data for 37 of the 43 predicted GPCR genes was contained in the dataset and a heat map prepared as described in the Materials and Methods. Red color denotes higher levels of expression, while blue corresponds to lower expression.

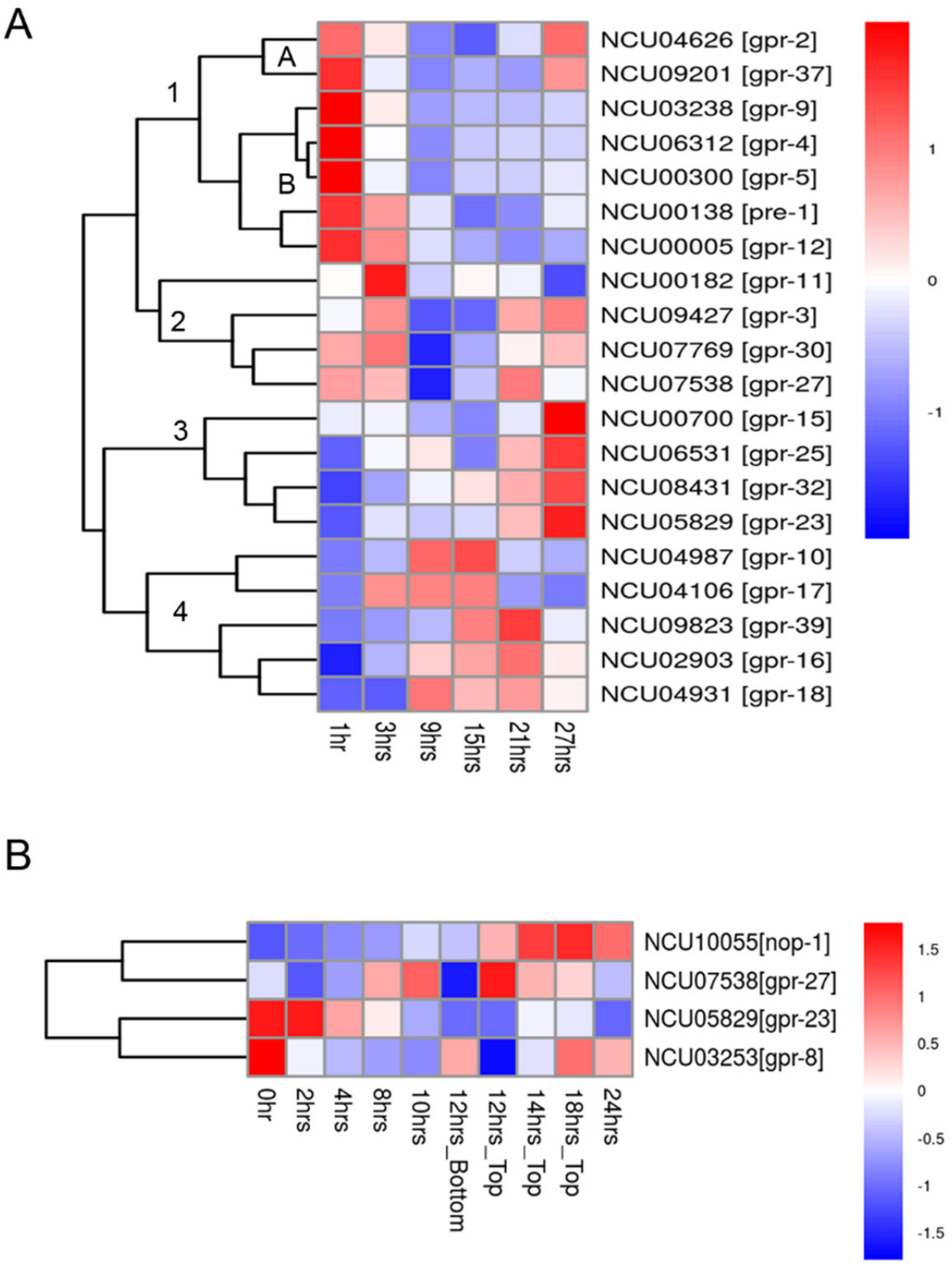
A
A
B
1
2
3
4
NCU04626 [gpr-2]
NCU09201 [gpr-37]
NCU03238 [gpr-9]
NCU06312 [gpr-4]
NCU00300 [gpr-5]
NCU00138 [pre-1]
NCU00005 [gpr-12]
NCU00182 [gpr-11]
NCU09427 [gpr-3]
NCU07769 [gpr-30]
NCU07538 [gpr-27]
NCU00700 [gpr-15]
NCU06531 [gpr-25]
NCU08431 [gpr-32]
NCU05829 [gpr-23]
NCU04987 [gpr-10]
NCU04106 [gpr-17]
NCU09823 [gpr-39]
NCU02903 [gpr-16]
NCU04931 [gpr-18]
1hr
3hrs
9hrs
15hrs
21hrs
27hrs
1
0
-1
B
NCU10055[nop-1]
NCU07538[gpr-27]
NCU05829[gpr-23]
NCU03253[gpr-8]
0hr
2hrs
4hrs
8hrs
10hrs
12hrs_Bottom
12hrs_Top
14hrs_Top
18hrs_Top
24hrs
1.5
1
0.5
0
-0.5
-1
-1.5

Figure 3.4: GPCR genes during time courses of colony growth and asexual development (conidiation).

Data was taken from the indicated sources and heat maps generated as described in the Materials and Methods. Red color denotes higher levels of expression, while blue corresponds to lower expression. **A. Gene expression during colony growth.** Microarray data was obtained from (Kasuga and Glass 2008) for 20 predicted GPCR genes expressed during colony growth**. B. Gene expression during conidiation.** Microarray data was mined from (Greenwald et al. 2010) for four predicted GPCR genes expressed during asexual development (conidiation).

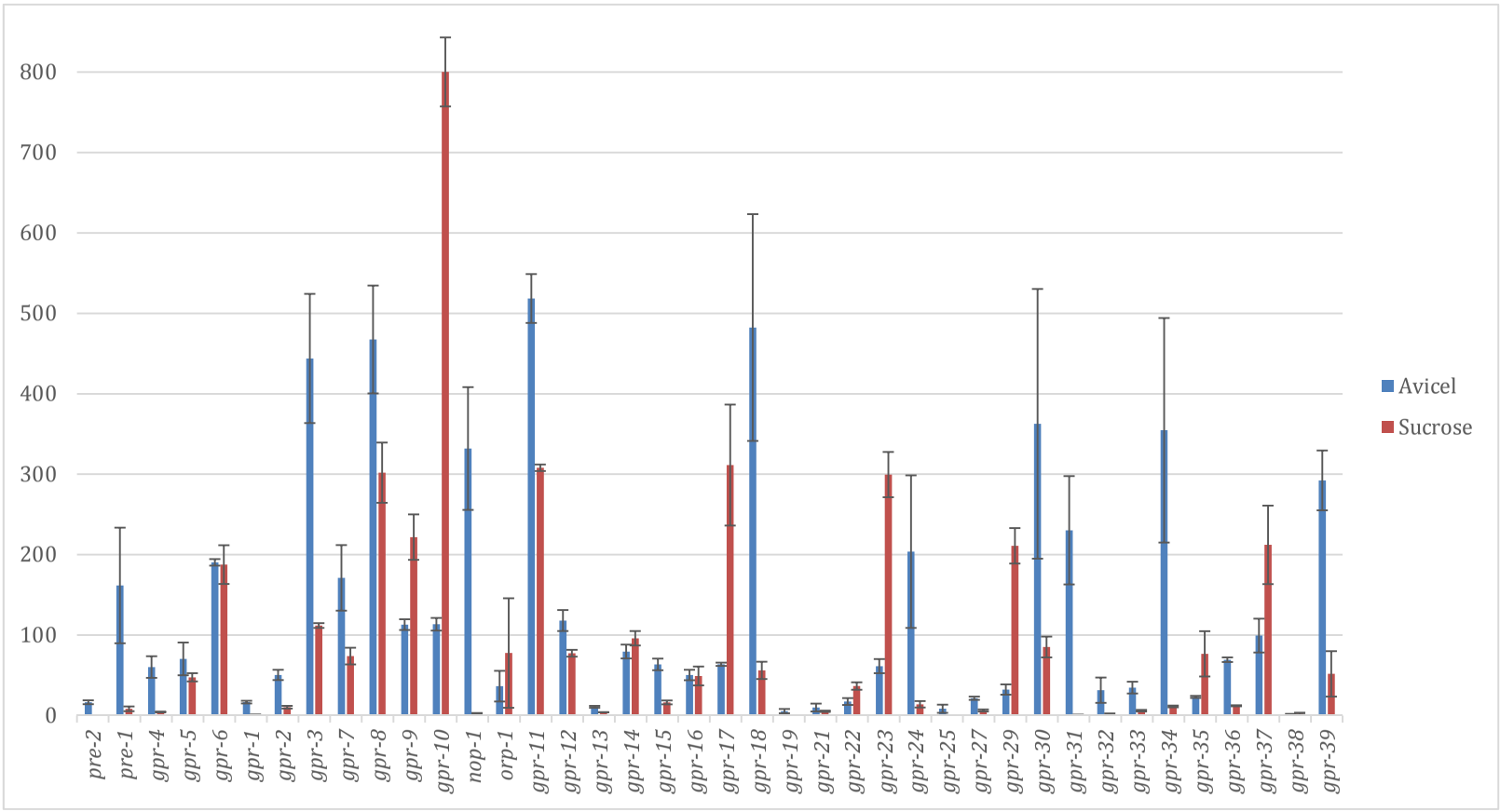

Figure 3.5: Expression patterns for 40 predicted GPCR genes on two different carbon sources.

RNAseq data was obtained from (Coradetti et al. 2012) for genes expressed in tissue grown for 4 hr in liquid medium containing either sucrose (orange bars) or Avicel (crystalline cellulose; blue bars) as a carbon source. Y-axis is reads per kilobase per million mapped reads (RPKM), while x-axis indicates genes.

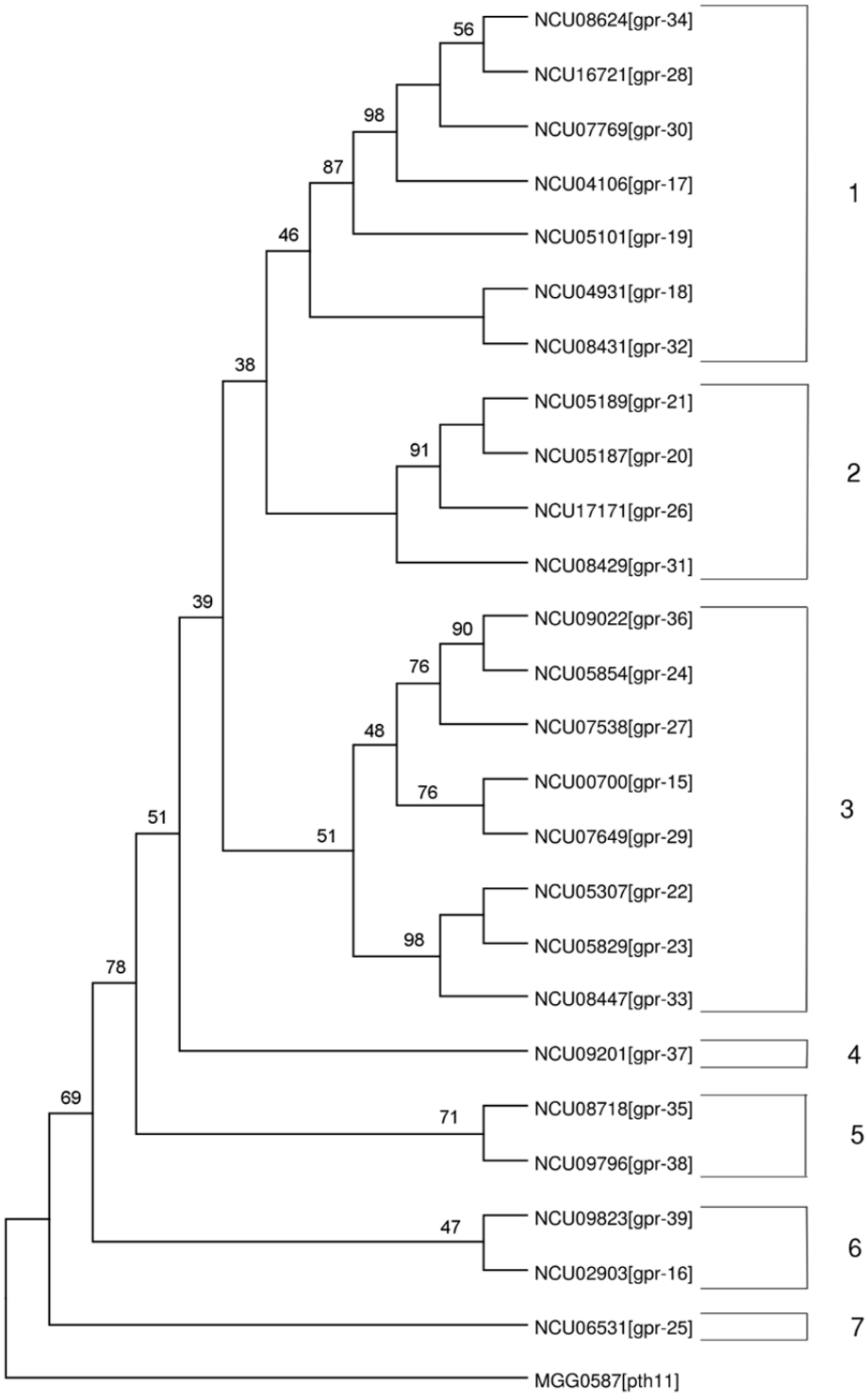
NCU08624[gpr-34]
NCU16721[gpr-28]
NCU07769[gpr-30]
NCU04106[gpr-17]
NCU05101[gpr-19]
NCU04931[gpr-18]
NCU08431[gpr-32]
NCU05189[gpr-21]
NCU05187[gpr-20]
NCU17171[gpr-26]
NCU08429[gpr-31]
NCU09022[gpr-36]
NCU05854[gpr-24]
NCU07538[gpr-27]
NCU00700[gpr-15]
NCU07649[gpr-29]
NCU05307[gpr-22]
NCU05829[gpr-23]
NCU08447[gpr-33]
NCU09201[gpr-37]
NCU08718[gpr-35]
NCU09796[gpr-38]
NCU09823[gpr-39]
NCU02903[gpr-16]
NCU06531[gpr-25]
MGG0587[pth11]
56
98
87
46
38
91
39
90
76
48
76
51
51
98
78
69
71
47
1
2
3
4
5
6
7

Figure 3.6 Phylogenetic analysis of Pth11-related proteins in *N. crassa*.

The protein sequences for the 25 *N. crassa* Pth11-related proteins from (Li et al. 2007) (Table 3.1) and Magnaportheoryzae Pth11 (outgroup) were aligned using T-coffee and trimmed using TrimAl. The consensus parsimony tree produced using 100 bootstrap replicates. See the Materials and Methods for details.

References

Affeldt, K.J., Carrig, J., Amare, M., and Keller, N.P. (2014). Global survey of canonical *Aspergillus flavus* G protein-coupled receptors. mBio 5, e01501-01514.

Altschul, S.F., Gish, W., Miller, W., Myers, E.W., and Lipman, D.J. (1990). Basic local alignment search tool. Journal of molecular biology 215, 403-410.

Attwood, T.K., and Findlay, J.B. (1994). Fingerprinting G-protein-coupled receptors. Protein engineering 7, 195-203.

Baasiri, R.A., Lu, X., Rowley, P.S., Turner, G.E., and Borkovich, K.A. (1997). Overlapping functions for two G protein alpha subunits in *Neurospora crassa*. Genetics 147, 137-145.

Belden, W.J., Larrondo, L.F., Froehlich, A.C., Shi, M., Chen, C.H., Loros, J.J., and Dunlap, J.C. (2007). The band mutation in *Neurospora crassa* is a dominant allele of ras-1 implicating RAS signaling in circadian output. Genes & development 21, 1494-1505.

Bieszke, J.A., Braun, E.L., Bean, L.E., Kang, S., Natvig, D.O., and Borkovich, K.A. (1999). The nop-1 gene of *Neurospora crassa* encodes a seven transmembrane helix retinal-binding protein homologous to archaeal rhodopsins. Proc Natl Acad Sci U S A 96, 8034-8039.

Bieszke, J.A., Li, L., and Borkovich, K.A. (2007). The fungal opsin gene nop-1 is negatively-regulated by a component of the blue light sensing pathway and influences conidiation-specific gene expression in *Neurospora crassa*. Curr Genet 52, 149-157.

Bock, A., Kostenis, E., Trankle, C., Lohse, M.J., and Mohr, K. (2014). Pilot the pulse: controlling the multiplicity of receptor dynamics. Trends in pharmacological sciences 35, 630-638.

Borkovich, K.A., Alex, L.A., Yarden, O., Freitag, M., Turner, G.E., Read, N.D., Seiler, S., Bell-Pedersen, D., Paietta, J., Plesofsky, N., Plamann, M., Goodrich-Tanrikulu, M., Schulte, U., Mannhaupt, G., Nargang, F.E., Radford, A., Selitrennikoff, C., Galagan, J.E., Dunlap, J.C., Loros, J.J., Catcheside, D., Inoue, H., Aramayo, R., Polymenis, M., Selker, E.U., Sachs, M.S., Marzluf, G.A., Paulsen, I., Davis, R., Ebbole, D.J., Zelter, A., Kalkman, E.R., O'Rourke, R., Bowring, F., Yeadon, J., Ishii, C., Suzuki, K., Sakai, W., and Pratt, R. (2004). Lessons from the genome sequence of *Neurospora crassa*: Tracing the path from genomic blueprint to multicellular organism. Microbiology and molecular biology reviews : MMBR 68, 1-108.

Capella-Gutierrez, S., Silla-Martinez, J.M., and Gabaldon, T. (2009). trimAl: a tool for automated alignment trimming in large-scale phylogenetic analyses. Bioinformatics 25, 1972-1973.

Chini, B., Parenti, M., Poyner, D.R., and Wheatley, M. (2013). G-protein-coupled receptors: from structural insights to functional mechanisms. Biochemical Society transactions 41, 135-136.

Chung, K.S., Won, M., Lee, S.B., Jang, Y.J., Hoe, K.L., Kim, D.U., Lee, J.W., Kim, K.W., and Yoo, H.S. (2001). Isolation of a novel gene from *Schizosaccharomyces pombe*: stm1+ encoding a seven-transmembrane loop protein that may couple with the heterotrimeric Galpha 2 protein, Gpa2. J Biol Chem 276, 40190-40201.

Colot, H.V., Park, G., Turner, G.E., Ringelberg, C., Crew, C.M., Litvinkova, L., Weiss, R.L., Borkovich, K.A., and Dunlap, J.C. (2006). A high-throughput gene knockout procedure for *Neurospora* reveals functions for multiple transcription factors. Proc Natl Acad Sci U S A 103, 10352-10357.

Cooper, J.A. (1987). Effects of cytochalasin and phalloidin on actin. The Journal of cell biology 105, 1473-1478.

Coradetti, S.T., Craig, J.P., Xiong, Y., Shock, T., Tian, C., and Glass, N.L. (2012). Conserved and essential transcription factors for cellulase gene expression in ascomycete fungi. Proc Natl Acad Sci U S A 109, 7397-7402.

Davis, R.H., and deSerres, F.J. (1970). Genetic and microbiological research techniques for *Neurospora crassa.* Methods Enzymol. 71A, 79-143.

Davis, R.H., and Perkins, D.D. (2002). Timeline: *Neurospora*: a model of model microbes. Nat Rev Genet 3, 397-403.

DeZwaan, T.M., Carroll, A.M., Valent, B., and Sweigard, J.A. (1999). *Magnaporthe grisea* Pth11p is a novel plasma membrane protein that mediates appressorium differentiation in response to inductive substrate cues. The Plant cell 11, 2013-2030.

Dunlap, J.C., Borkovich, K.A., Henn, M.R., Turner, G.E., Sachs, M.S., Glass, N.L., McCluskey, K., Plamann, M., Galagan, J.E., Birren, B.W., Weiss, R.L., Townsend, J.P., Loros, J.J., Nelson, M.A., Lambreghts, R., Colot, H.V., Park, G., Collopy, P., Ringelberg, C., Crew, C., Litvinkova, L., DeCaprio, D., Hood, H.M., Curilla, S., Shi, M., Crawford, M., Koerhsen, M., Montgomery, P., Larson, L., Pearson, M., Kasuga, T., Tian, C., Basturkmen, M., Altamirano, L., and Xu, J. (2007). Enabling a community to dissect an organism: Overview of the *Neurospora* functional genomics project. Advances in genetics 57, 49-96.

Felsenstein, J. (1989). PHYLIP - Phylogeny Inference Package (Version 3.2). Cladistics 164-166.

Fredriksson, R., Lagerstrom, M.C., Lundin, L.G., and Schioth, H.B. (2003). The G-protein-coupled receptors in the human genome form five main families. Phylogenetic analysis, paralogon groups, and fingerprints. Molecular pharmacology 63, 1256-1272.

Galagan, J.E., Calvo, S.E., Borkovich, K.A., Selker, E.U., Read, N.D., Jaffe, D., FitzHugh, W., Ma, L.J., Smirnov, S., Purcell, S., Rehman, B., Elkins, T., Engels, R., Wang, S., Nielsen, C.B., Butler, J., Endrizzi, M., Qui, D., Ianakiev, P., Bell-Pedersen, D., Nelson, M.A., Werner-Washburne, M., Selitrennikoff, C.P., Kinsey, J.A., Braun, E.L., Zelter, A., Schulte, U., Kothe, G.O., Jedd, G., Mewes, W., Staben, C., Marcotte, E., Greenberg, D., Roy, A., Foley, K., Naylor, J., Stange-Thomann, N., Barrett, R., Gnerre, S., Kamal, M., Kamvysselis, M., Mauceli, E., Bielke, C., Rudd, S., Frishman, D., Krystofova, S., Rasmussen, C., Metzenberg, R.L., Perkins, D.D., Kroken, S., Cogoni, C., Macino, G., Catcheside, D., Li, W., Pratt, R.J., Osmani, S.A., DeSouza, C.P., Glass, L., Orbach, M.J., Berglund, J.A., Voelker, R., Yarden, O., Plamann, M., Seiler, S., Dunlap, J., Radford, A., Aramayo, R., Natvig, D.O., Alex, L.A., Mannhaupt, G., Ebbole, D.J., Freitag, M., Paulsen, I., Sachs, M.S., Lander, E.S., Nusbaum, C., and Birren, B. (2003). The genome sequence of the filamentous fungus *Neurospora crassa*. Nature 422, 859-868.

Ghosh, A., Servin, J.A., Park, G., and Borkovich, K.A. (2014). Global analysis of serine/threonine and tyrosine protein phosphatase catalytic subunit genes in *Neurospora crassa* reveals interplay between phosphatases and the p38 Mitogen-activated protein kinase. G3 4, 349-365.

Gonzalez-Velazquez, W., Gonzalez-Mendez, R., and Rodriguez-del Valle, N. (2012). Characterization and ligand identification of a membrane progesterone receptor in fungi: existence of a novel PAQR in Sporothrix schenckii. BMC microbiology 12, 194.

Greenwald, C.J., Kasuga, T., Glass, N.L., Shaw, B.D., Ebbole, D.J., and Wilkinson, H.H. (2010). Temporal and spatial regulation of gene expression during asexual development of *Neurospora crassa*. Genetics 186, 1217-1230.

Gruber, S., Omann, M., and Zeilinger, S. (2013). Comparative analysis of the repertoire of G protein-coupled receptors of three species of the fungal genus *Trichoderma*. BMC microbiology 13, 108.

Hansberg, W., de Groot, H., and Sies, H. (1993). Reactive oxygen species associated with cell differentiation in *Neurospora crassa*. Free radical biology & medicine 14, 287-293.

Harding, R.W., and Melles, S. (1983). Genetic Analysis of phototropism of *Neurospora crassa* perithecial beaks using white collar and albino mutants. Plant Physiol 72, 996-1000.

Harris, J.L., Howe, H.B., Jr., and Roth, I.L. (1975). Scanning electron microscopy of surface and internal features of developing perithecia of *Neurospora crassa*. Journal of bacteriology 122, 1239-1246.

Hillenmeyer, M.E., Fung, E., Wildenhain, J., Pierce, S.E., Hoon, S., Lee, W., Proctor, M., St Onge, R.P., Tyers, M., Koller, D., Altman, R.B., Davis, R.W., Nislow, C., and Giaever, G. (2008). The chemical genomic portrait of yeast: uncovering a phenotype for all genes. Science 320, 362-365.

Inadome, H., Noda, Y., Adachi, H., and Yoda, K. (2005). Immunoisolaton of the yeast Golgi subcompartments and characterization of a novel membrane protein, Svp26, discovered in the Sed5-containing compartments. Mol Cell Biol 25, 7696-7710.

Ivey, F.D., Hodge, P.N., Turner, G.E., and Borkovich, K.A. (1996). The G alpha i homologue gna-1 controls multiple differentiation pathways in *Neurospora crassa*. Mol Biol Cell 7, 1283-1297.

Jastrzebska, B. (2013). GPCR: G protein complexes--the fundamental signaling assembly. Amino acids 45, 1303-1314.

Johnston, C.A., Taylor, J.P., Gao, Y., Kimple, A.J., Grigston, J.C., Chen, J.G., Siderovski, D.P., Jones, A.M., and Willard, F.S. (2007). GTPase acceleration as the rate-limiting step in *Arabidopsis* G protein-coupled sugar signaling. Proc Natl Acad Sci U S A 104, 17317-17322.

Kasuga, T., and Glass, N.L. (2008). Dissecting colony development of *Neurospora crassa* using mRNA profiling and comparative genomics approaches. Eukaryot Cell 7, 1549-1564.

Kato, A., Akamatsu, Y., Sakuraba, Y., and Inoue, H. (2004). The *Neurospora crassa* mus-19 gene is identical to the qde-3 gene, which encodes a RecQ homologue and is involved in recombination repair and postreplication repair. Curr Genet 45, 37-44.

Kays, A.M., and Borkovich, K.A. (2004). Severe impairment of growth and differentiation in a *Neurospora crassa* mutant lacking all heterotrimeric G alpha proteins. Genetics 166, 1229-1240.

Kays, A.M., Rowley, P.S., Baasiri, R.A., and Borkovich, K.A. (2000). Regulation of conidiation and adenylyl cyclase levels by the Galpha protein GNA-3 in *Neurospora crassa*. Mol Cell Biol 20, 7693-7705.

Kim, H., and Borkovich, K.A. (2004). A pheromone receptor gene, pre-1, is essential for mating type-specific directional growth and fusion of trichogynes and female fertility in *Neurospora crassa*. Mol Microbiol 52, 1781-1798.

Kim, H., and Borkovich, K.A. (2006). Pheromones are essential for male fertility and sufficient to direct chemotropic polarized growth of trichogynes during mating in *Neurospora crassa*. Eukaryot Cell 5, 544-554.

Kim, H., Wright, S.J., Park, G., Ouyang, S., Krystofova, S., and Borkovich, K.A. (2012). Roles for receptors, pheromones, G proteins, and mating type genes during sexual reproduction in *Neurospora crassa*. Genetics 190, 1389-1404.

Kolde, R. (2015). pheatmap: Pretty Heatmaps, vol. 1.0.2 ed.

Krishnan, A., Almen, M.S., Fredriksson, R., and Schioth, H.B. (2012). The origin of GPCRs: identification of mammalian like Rhodopsin, Adhesion, Glutamate and Frizzled GPCRs in fungi. PLoS One 7, e29817.

Krystofova, S., and Borkovich, K.A. (2005). The heterotrimeric G-protein subunits GNG-1 and GNB-1 form a Gbetagamma dimer required for normal female fertility, asexual development, and Galpha protein levels in *Neurospora crassa*. Eukaryot Cell 4, 365-378.

Krystofova, S., and Borkovich, K.A. (2006). The predicted G-protein-coupled receptor GPR-1 is required for female sexual development in the multicellular fungus *Neurospora crassa*. Eukaryot Cell 5, 1503-1516.

Kulkarni, R.D., Thon, M.R., Pan, H., and Dean, R.A. (2005). Novel G-protein-coupled receptor-like proteins in the plant pathogenic fungus Magnaporthe grisea. Genome biology 6, R24.

Lafon, A., Han, K.H., Seo, J.A., Yu, J.H., and d'Enfert, C. (2006). G-protein and cAMP-mediated signaling in aspergilli: a genomic perspective. Fungal Genet Biol 43, 490-502.

Li, L., and Borkovich, K.A. (2006). GPR-4 is a predicted G-protein-coupled receptor required for carbon source-dependent asexual growth and development in *Neurospora crassa.* Eukaryot Cell 5, 1287-1300.

Li, L., Wright, S.J., Krystofova, S., Park, G., and Borkovich, K.A. (2007). Heterotrimeric G protein signaling in filamentous fungi. Annual review of microbiology 61, 423-452.

Liu, W., Xu, D., Yang, H., Xu, H., Shi, Z., Cao, X., Takeshita, S., Liu, J., Teale, M., and Feng, X. (2004). Functional identification of three receptor activator of NF-kappa B cytoplasmic motifs mediating osteoclast differentiation and function. J Biol Chem 279, 54759-54769.

Lyons, T.J., Villa, N.Y., Regalla, L.M., Kupchak, B.R., Vagstad, A., and Eide, D.J. (2004). Metalloregulation of yeast membrane steroid receptor homologs. Proc Natl Acad Sci U S A 101, 5506-5511.

Mende, U., Zagrovic, B., Cohen, A., Li, Y., Valenzuela, D., Fishman, M.C., and Neer, E.J. (1998). Effect of deletion of the major brain G-protein alpha subunit (alpha(o)) on coordination of G-protein subunits and on adenylyl cyclase activity. J Neurosci Res 54, 263-272.

Narasimhan, M.L., Coca, M.A., Jin, J., Yamauchi, T., Ito, Y., Kadowaki, T., Kim, K.K., Pardo, J.M., Damsz, B., Hasegawa, P.M., Yun, D.J., and Bressan, R.A. (2005). Osmotin is a homolog of mammalian adiponectin and controls apoptosis in yeast through a homolog of mammalian adiponectin receptor. Mol Cell 17, 171-180.

Neves, S.R., Ram, P.T., and Iyengar, R. (2002). G protein pathways. Science 296, 1636-1639.

Nordberg, H., Cantor, M., Dusheyko, S., Hua, S., Poliakov, A., Shabalov, I., Smirnova, T., Grigoriev, I.V., and Dubchak, I. (2014). The genome portal of the Department of Energy Joint Genome Institute: 2014 updates. Nucleic Acids Res 42, D26-31.

Notredame, C., Higgins, D.G., and Heringa, J. (2000). T-Coffee: A novel method for fast and accurate multiple sequence alignment. J Mol Biol 302, 205-217.

Ochiai, N., Fujimura, M., Motoyama, T., Ichiishi, A., Usami, R., Horikoshi, K., and Yamaguchi, I. (2001). Characterization of mutations in the two-component histidine kinase gene that confer fludioxonil resistance and osmotic sensitivity in the os-1 mutants of *Neurospora crassa*. Pest management science 57, 437-442.

Pandey, S., and Assmann, S.M. (2004). The Arabidopsis putative G protein-coupled receptor GCR1 interacts with the G protein alpha subunit GPA1 and regulates abscisic acid signaling. The Plant cell 16, 1616-1632.

Park, G., Colot, H.V., Collopy, P.D., Krystofova, S., Crew, C., Ringelberg, C., Litvinkova, L., Altamirano, L., Li, L., Curilla, S., Wang, W., Gorrochotegui-Escalante, N., Dunlap, J.C., and Borkovich, K.A. (2011a). High-throughput production of gene replacement mutants in *Neurospora crassa*. Methods Mol Biol 722, 179-189.

Park, G., Servin, J.A., Turner, G.E., Altamirano, L., Colot, H.V., Collopy, P., Litvinkova, L., Li, L., Jones, C.A., Diala, F.G., Dunlap, J.C., and Borkovich, K.A. (2011b). Global analysis of serine-threonine protein kinase genes in *Neurospora crassa*. Eukaryot Cell 10, 1553-1564.

Prokisch, H., Yarden, O., Dieminger, M., Tropschug, M., and Barthelmess, I.B. (1997). Impairment of calcineurin function in *Neurospora crassa* reveals its essential role in hyphal growth, morphology and maintenance of the apical Ca2+ gradient. Mol Gen Genet 256, 104-114.

Raju, N.B. (1992). Genetic control of the sexual cycle in *Neurospora*. Mycol. Res. 96, 241-262.

Ramanujam, R., Calvert, M.E., Selvaraj, P., and Naqvi, N.I. (2013). The late endosomal HOPS complex anchors active G-protein signaling essential for pathogenesis in *Magnaporthe oryzae*. PLoS pathogens 9, e1003527.

Read, N.D., and Beckett, A. (1996). Ascus and ascospore morphogenesis. Mycol. Res. 100, 1281-1314.

Schioth, H.B., and Fredriksson, R. (2005). The GRAFS classification system of G-protein coupled receptors in comparative perspective. General and comparative endocrinology 142, 94-101.

Sekito, T., Nakamura, K., Manabe, K., Tone, J., Sato, Y., Murao, N., Kawano-Kawada, M., and Kakinuma, Y. (2014). Loss of ATP-dependent lysine uptake in the vacuolar membrane vesicles of *Saccharomyces cerevisiae* ypq1 mutant. Bioscience, biotechnology, and biochemistry 78, 1199-1202.

Shukla, A.K., Singh, G., and Ghosh, E. (2014). Emerging structural insights into biased GPCR signaling. Trends in biochemical sciences 39, 594-602.
Springer, M.L. (1993). Genetic control of fungal differentiation: The three sporulation pathways of *Neurospora crassa*. Bioessays 15, 365-374.

Taddese, B., Upton, G.J., Bailey, G.R., Jordan, S.R., Abdulla, N.Y., Reeves, P.J., and Reynolds, C.A. (2014). Do plants contain g protein-coupled receptors? Plant Physiol 164, 287-307.

Team_RC. (2014). R: A Language and Environment for Statistical Computing, Vienna, Austria.

Tesmer, J.J. (2010). The quest to understand heterotrimeric G protein signaling. Nature structural & molecular biology 17, 650-652.

Thomas, P., Pang, Y., Dong, J., Groenen, P., Kelder, J., de Vlieg, J., Zhu, Y., and Tubbs, C. (2007). Steroid and G protein binding characteristics of the seatrout and human progestin membrane receptor alpha subtypes and their evolutionary origins. Endocrinology 148, 705-718.

Turner, G.E. (2011). Phenotypic analysis of *Neurospora crassa* gene deletion strains. Methods Mol Biol 722, 191-198.

Urano, D., and Jones, A.M. (2014). Heterotrimeric G protein-coupled signaling in plants. Annual review of plant biology 65, 365-384.

Vassilatis, D.K., Hohmann, J.G., Zeng, H., Li, F., Ranchalis, J.E., Mortrud, M.T., Brown, A., Rodriguez, S.S., Weller, J.R., Wright, A.C., Bergmann, J.E., and Gaitanaris, G.A. (2003). The G protein-coupled receptor repertoires of human and mouse. Proc Natl Acad Sci U S A 100, 4903-4908.

Villa, N.Y., Moussatche, P., Chamberlin, S.G., Kumar, A., and Lyons, T.J. (2011). Phylogenetic and preliminary phenotypic analysis of yeast PAQR receptors: potential antifungal targets. Journal of molecular evolution 73, 134-152.

Vogel, H.J. (1964). Distribution of lysine pathways among fungi: Evolutionary implications. Am. Nat. 98, 435-446.

Wang, Z., Lopez-Giraldez, F., Lehr, N., Farre, M., Common, R., Trail, F., and Townsend, J.P. (2014). Global gene expression and focused knockout analysis reveals genes associated with fungal fruiting body development in *Neurospora crassa*. Eukaryot Cell 13, 154-169.

Westergaard, M., and Mitchell, H.K. (1947). Neurospora V. A synthetic medium favoring sexual reproduction. Amer. J. Bot. 34, 573-577.

White, B., and Woodward, D. (1995). A simple method for making disposable race tubes. Fungal Genetics Newsletter 42, 79.

Willhite, C.C. (1983). Benomyl. Journal of applied toxicology : JAT 3, 261-264.

Won, S., Michkov, A.V., Krystofova, S., Garud, A.V., and Borkovich, K.A. (2012). Genetic and physical interactions between Galpha subunits and components of the Gbetagamma dimer of heterotrimeric G proteins in *Neurospora crassa*. Eukaryot Cell 11, 1239-1248.

Zheng, H., Zhou, L., Dou, T., Han, X., Cai, Y., Zhan, X., Tang, C., Huang, J., and Wu, Q. (2010). Genome-wide prediction of G protein-coupled receptors in *Verticillium spp*. Fungal biology 114, 359-368.

Chapter 4

The guanine nucleotide exchange factor RIC8 regulates conidial germination through Gα proteins in *Neurospora crassa*

Abstract

Heterotrimeric G protein signaling is essential for normal hyphal growth in the filamentous fungus *Neurospora crassa*. We have previously demonstrated that the non-receptor guanine nucleotide exchange factor RIC8 acts upstream of the Gα proteins GNA-1 and GNA-3 to regulate hyphal extension. Here we demonstrate that regulation of hyphal extension results at least in part, from an important role in control of asexual spore (conidia) germination. Loss of GNA-3 leads to a drastic reduction in conidial germination, which is exacerbated in the absence of GNA-1. Mutation of RIC8 leads to a reduction in germination similar to that in the Δ*gna-1*, Δ*gna-3* double mutant, suggesting that RIC8 regulates conidial germination through both GNA-1 and GNA-3. Support for a more significant role for GNA-3 is indicated by the observation that expression of a GTPase-deficient, constitutively active *gna-3* allele in the Δ*ric8* mutant leads to a significant increase in conidial germination. Localization of the three Gα proteins during conidial germination was probed through analysis of cells expressing fluorescently tagged proteins. Functional TagRFP fusions of each of the three Gα subunits were constructed through insertion of TagRFP in a conserved loop region of the Gα subunits. The results demonstrated that GNA-1 localizes to the plasma membrane and vacuoles,

and also to septa later during hyphal development. GNA-2 and GNA-3 localize to both the plasma membrane and vacuoles during early germination, but are then found in intracellular vacuoles later during hyphal growth.

Introduction

G proteins have been found to play key roles in diverse fungal processes ranging from asexual and sexual development to pathogenicity of animal and phytopathogenic fungi (Li *et al.*, 2007). Most fungi possess three Gα subunits and a single Gβ and Gγ protein, therefore allowing for the assembly of three different heterotrimers. These three Gα subunits can act independently to regulate separate pathways, leading to differing phenotypes for single Gα mutants. For example, *Neurospora crassa* GNA-1 is required for normal vegetative growth, aerial hyphae formation and female fertility (Ivey *et al.*, 1996), whereas GNA-3 is required for normal production of asexual spores (conidia) and maturation of sexual spores (ascospores) (Kays *et al.*, 2000). In contrast, the *N. crassa* Δgna-2 mutant displays only a mild phenotype during growth on poor carbon sources (Li and Borkovich, 2006). However, loss of GNA-2 exacerbates phenotypes of the *Δgna-1* and *Δgna-3* mutants, indicating that GNA-2 shares overlapping functions with the other two Gα subunits (Baasiri *et al.*, 1997; Kays and Borkovich, 2004). Indeed, all three G proteins are thought to act together to regulate some processes, as mutants lacking GNA-1 and GNA-3 or all three Gα subunits are severely impaired in growth on solid medium,

inappropriately conidiate in submerged liquid culture and do not produce female reproductive structures (Kays and Borkovich, 2004).

G protein coupled receptors (GPCRs), act as guanine nucleotide exchange factors (GEFs) for Gα subunits, facilitating exchange of GDP for GTP, thereby leading to activation and dissociation from the Gβγ dimer (Li *et al.*, 2007). However, recently a non-receptor GEF capable of activating Gα proteins, RIC8, has been identified in both animals and some fungi (Li *et al.*; Wilkie and Kinch, 2005; Wright *et al.*, 2011). In *N. crassa*, loss of ric8 leads to a severe growth impairment phenotype similar to that in mutants lacking both *gna-1* and *gna-3* or all three Gα subunit genes (Wright *et al.*, 2011). Expression of GTPase-deficient *gna-1* or *gna-3* alleles rescued many of the defects of the Δ*ric8* mutant during asexual growth on solid medium, and biochemical analyses showed that RIC8 can act as a GEF for both GNA-1 and GNA-3 in vitro, suggesting RIC8 acts upstream of both GNA-1 and GNA-3, particularly during regulation of asexual growth on solid medium (Wright *et al.*, 2011). Asexual hyphal growth is important for nutrient scavenging and for the organism to spread throughout the environment. In addition, it is important for encountering a mate of the opposite mating type, which allows the sexual cycle to proceed and produce the environmentally resistant sexual spores (ascospores).

Using a strain expressing a functional RIC8-GFP fusion, we have previously shown that RIC8 is a cytoplasmic protein (Wright *et al.*, 2011). Production of Gα-fluorescent protein fusions is problematic, as an N or C-terminal tag can interfere with normal functioning of the Gα protein. However, *Dictyostelium discoideum* Gα2 and mammalian Gαo have been successfully tagged by insertion of GFP in a fold where it

does not interfere with Gαo function (Janetopoulos *et al.*, 2001; Azpiazu and Gautam, 2004).

In this study we further probe the role of RIC8, GNA-1 and GNA-3 in asexual hyphal growth and development. We produce strains expressing GNA-1, GNA-2 and GNA-3 proteins as internal TagRFP fusions. We present here the first use of this internal tagging method for localization of Gα proteins in filamentous fungi. Using these strains, we determine the localization pattern of Gα proteins in conidia and during conidial germination and test for colocalization of RIC8 with GNA-1 and GNA-3 with RIC8.

The text of Chapter 4 of this dissertation is a reprint of a paper published in *PLoS One* with authors; Carla J. Eaton, Ilva E. Cabrera, Jacqueline A. Servin, Sara J. Wright, Murray P. Cox and Katherine A. Borkovich, entitled, "The guanine nucleotide exchange factor RIC8 regulates conidial germination through Gα proteins in *Neurospora crassa*," with minor changes. I would like to acknowledge the contributions of the other authors. Dr. Carla Eaton, my co-first author on the *PLoS One* paper, generated the fluorescently tagged strains used in the study. Dr. Jacqueline Servin assisted in optimizing the conditions for fluorescent dyes. I would also like to acknowledge Katherine A. Borkovich, whom supervised this project.

Materials and Methods

Strains and growth conditions:

Neurospora strains used in this study are listed in Table 4.1. For vegetative growth analysis, strains were grown on Vogel's minimal (VM) medium (Vogel, 1964). Cultures were inoculated with conidia and grown as described previously (Krystofova and Borkovich, 2006; Li and Borkovich, 2006) .

Gα-TagRFP strain construction:

To observe the cellular localization of GNA-1, GNA-2 and GNA-3, TagRFP (Berepiki *et al.*, 2010) was inserted into a conserved loop region within the Gα protein. This conserved loop region was found to be optimal for insertion of tags with conservation of Gα protein function in *Dictyostelium discoideum* Gα2 (Janetopoulos *et al.*, 2001) and chinese hamster Gnao (Azpiazu and Gautam, 2004). Primers were designed to prepare the Gα-TagRFP fusion constructs using yeast recombinational cloning. TagRFP was amplified from pAL3-Lifeact (Berepiki *et al.*, 2010); provided by Nick Read, University of Edinburgh) and the appropriate Gα N- and C-terminal fragments were amplified from cDNA clones. These fragments were inserted into pRS426 using yeast recombinational cloning (Colot *et al.*, 2006). The Gα-TagRFP fusion construct was then subcloned from pRS426 into pMF272 (Freitag *et al.*, 2004) as

an *Eco*RI/*Xba*I fragment, resulting in replacement of *sgfp* from pMF272 with the Gα-TagRFP fusion and placing it under the control of the *ccg-1* promoter. The fusion constructs were then transformed into *his-3* Δ*gna-1*, Δ*gna-2* or Δ*gna-3* gene replacement mutants. Transformants were then screened by Southern blotting to ensure correct integration of the construct (data not shown).

Western blot analysis:

Western blotting was used to detect Gα-TagRFP fusion proteins in whole-cell extracts prepared from macroconidia. Conidia from 6-7 day flask cultures were collected using sterile water, pelleted and stored at -80°C. After thawing on ice, the conidia were resuspended using 1 ml of extraction buffer (10 mM HEPES, pH 7.5, 0.5mM EDTA, 0.5 mM PMSF, 1 mM DTT and 0.1% v/v of fungal protease inhibitor (Cat# T8215, Sigma-Aldrich, St. Louis, MO) and then transferred to a mortar. The conidia were vigorously crushed using a mortar and pestle under liquid nitrogen. Roughly equal amounts of ground tissue were then transferred to 2 ml screw cap tubes, and topped off with additional extraction buffer if necessary. Samples were spun at 3,300 RPM (1,000Xg) for 10 minutes at 4°C in a microcentrifuge and the supernatants (whole cell extracts) retained.

Protein concentration was determined using the Bradford Protein Assay (Bio-Rad, Hercules, CA). Samples containing 50 µg of whole-cell protein were subjected to SDS-PAGE using 10% gels and gels transferred to nitrocellulose membranes as described

previously (Krystofova and Borkovich, 2005). Western analysis was performed using a polyclonal RFP antibody (#R10367, Invitrogen, Carlsbad, CA) as the primary antibody at a dilution of 1:2000. A horseradish peroxidase conjugate antibody (Bio-Rad) was used as the secondary antibody at a dilution of 1:5000 and chemiluminescent detection was performed as described previously (Krystofova and Borkovich, 2005).

Microscopy:

For analysis of conidial germination, 8 x 10^6 conidia were spread on 100 mm 10 ml VM agarose plates and incubated at 30°C for 0, 4, 6 or 8h. Cells were then visualized using differential interference contrast (DIC) microscopy using an Olympus IX71 inverted microscope (Olympus America, Center Valley, PA) with a 60x oil immersion objective (NA = 1.42). Images were captured using a QIClickTM digital CCD camera (QImaging, Surrey, British Columbia, Canada) and analyzed using Metamorph software (Molecular Devices Corporation, Sunnyvale, CA). For analysis of conidial anastomosis tubes, conidia were spread on VM agarose, and imaged after 5-16 h at 30°C as detailed above.

For observation of Gα localization, VM agarose plate cultures were prepared as described above. Germinating conidia were analyzed using a Leica TCS SP5 II confocal microscope with a 63x oil objective (NA= 1.40; Leica Microsystems Inc., Buffalo Grove, IL). The Gα-RFP strains were visualized with the Hybrid Detection system (HyD) laser at an excitation of 543nm, and emission of 565-665 nm.

To confirm vacuolar localization, conidia from the Gα-TagRFP strains were inoculated onto VM agarose plates and incubated as described above. An aliquot containing 30 µl of a 20 µg/ml solution of Oregon Green® 488 carboxylic acid diacetate (Carboxy-DFFDA; catalog number O6151; Molecular Probes) was applied to a coverslip. An agarose block containing germinating conidia was inverted onto the coverslip and incubated for 5 minutes at room temperature in the dark. Images were obtained using the Leica TCS SP5 II confocal microscope described above. GFP images were obtained by excitation at 488 nm, with emission collected from 500-535 nm. RFP images were obtained with excitation at 543 nm and emission from 555-700 nm. Images were captured sequentially in order to prevent crosstalk among samples.

The vacuolar and plasma membrane localization of GNA-1-TagRFP was further explored by imaging a heterokaryon that expresses GNA-1-TagRFP and a GFP fusion of the Ca^{2+} ATPase, NCA-3 (Bowman *et al.*, 2009). NCA-3-GFP is known to localize to the vacuolar and plasma membranes (Bowman *et al.*, 2009). The two strains were co-inoculated onto a VM slant in order to produce a heterokaryon with conidia expressing both fluorescent proteins. Conidia were inoculated onto VM agarose plates as described above and imaged 6 h later using a 543nm HyD laser and 488nm laser on the Leica TCS SP5 II confocal microscope. Images were captured sequentially.

Possible co-localization of RIC8 and GNA-1 or GNA-3 was investigated through co-culturing of the RIC8-GFP strain with the GNA-1-TagRFP or GNA-3-TagRFP strains on a VM slant to produce a heterokaryon expressing two fluorescent proteins. Conidia from the heterokaryons were inoculated onto VM agarose plates as described above,

followed by incubation at 30°C for 0 or 6h for GNA-1-TagRFP/RIC8-GFP and 0 or 4h for the GNA-3-TagRFP/RIC8-GFP fusion strain. Images were obtained by confocal microscopy, as described above.

Results

Having demonstrated that Gα proteins are important for conidial germination, we next investigated the subcellular localization of these proteins during this process. For these experiments, we took advantage of previous studies in *Dictyostelium* and mammalian cells demonstrating that insertion of a fluorescent tag in a loop region of the Gα subunit does not disrupt the interaction with the Gβγ dimer or interfere with Gα function (Janetopoulos *et al.*, 2001; Azpiazu and Gautam, 2004).

We expressed all three Gα-TagRFP fusions under control of the highly expressed *ccg-1* promoter from the *his-3* locus in the corresponding Gα mutant strain. Expression of GNA-1-TagRFP complemented the conidial germination and female fertility defects and partially complemented the growth rate phenotype of the Δ*gna-1* mutant (data not shown). Expression of GNA-3-TagRFP in the Δ*gna-3* mutant restored conidial germination back to wild-type levels at all-time points investigated.

We confirmed that the three TagRFP constructs are expressed as full-length fusion proteins in conidia using Western analysis with an RFP antiserum (Figure 4.1). TagRFP is 27 kD and each Gα is approximately 41 kD. Correspondingly, each of the

three Gα fusion proteins migrated close to their predicted molecular mass of 68 kD. Interestingly, although all three genes are expressed under control of the same promoter from a common genomic site, levels of GNA-1 are much higher than those of GNA-2 and GNA-3. This suggests some post-transcriptional regulation of Gα protein levels, with GNA-1 accumulating to higher levels in *N. crassa*. In addition, potential degradation products were observed for all three proteins (Figure 4.1; asterisks), suggesting at least some of the variation in protein levels may be due to differences in protein turnover.

We examined the strains expressing TagRFP fusion proteins during conidial germination using confocal fluorescent microscopy. Conidia were plated on solid medium and examined at four time points (0, 4, 6 and 8 h). At 0 h, all three Gα proteins localized to the plasma membrane and vacuoles (Figure 4.2, 4.3A). The plasma-membrane localization is consistent with results previously observed during cell fractionation studies in our laboratory (Ivey *et al.*, 1996; Baasiri *et al.*, 1997; Kays and Borkovich, 2004); data not shown). The vacuolar localization of GNA-1-TagRFP, GNA-2-TagRFP, and GNA-3-TagRFP was validated by the overlapping signal observed between TagRFP and the carboxy-DFFDA vacuolar dye during confocal microscopy (Figure 4.3A). In addition, a strain containing a GFP-tagged protein, NCA-3, a Ca^{2+} ATPase known to localize to vacuoles and the plasma membrane was combined with the GNA-1-RFP strain to produce a heterokaryon (Bowman *et al.*, 2009). Many conidia and germinating hyphae from these heterokaryons exhibit green and red fluorescence, indicative of the presence of both NCA-3-GFP and GNA-1-TagRFP. Confocal microscopy of conidia from this heterokaryon confirmed that GNA-1 localizes to the

plasma membrane and vacuoles (Figure 4.3B). It is unclear whether the vacuolar fluorescence represents a functional localization or a site of protein turnover.

At 4 h of conidial germination, GNA-1 continued to display plasma membrane and vacuolar localization, while GNA-2 and GNA-3 were predominantly found in vacuoles, with less apparent plasma membrane localization (Figure 4.2). At 6 h, GNA-1 was present in the plasma membrane vacuoles, and the first septum separating the conidium and the developing hypha (Figure 4.2). GNA-2 exhibited a similar localization as observed at 4 h. Interestingly, in addition to vacuolar localization, GNA-3 was also found in distinct patches on the plasma membrane of the original conidium (Figure 4.2). These patches were observed in 50% or more of the cells being sampled. At 6 h, the plasma membrane patches were even more easily observed in GNA-3-TagRFP strains, as the fluorescence in vacuoles and other regions of the plasma membrane began to dim (Figure 4.2). At 8 h, GNA-1-TagRFP fluorescence was still relatively strong in plasma membrane, vacuoles and septa (Figure 4.2). In contrast, GNA-2- and GNA-3-TagRFP fluorescence was too dim to analyze in 8 h germlings (data not shown).

We have previously demonstrated that RIC8 exhibits cytosolic localization in conidia and mature hyphae using fluorescent microscopy with an inverted compound microscope (Wright *et al.*, 2011). In this study, we utilized the more discriminating method of confocal fluorescence microscopy to explore possible co-localization of GNA-1-TagRFP and/or GNA-3-TagRFP with RIC8-GFP in cellular compartments during conidial germination. For these experiments, we cultured strains carrying the RIC8-GFP and GNA-1-TagRFP constructs together to produce heterokaryons expressing both

fluorescent proteins. Similar to previous results, RIC8-GFP is cytosolic and excluded from vacant areas that appear to be vacuoles (Figure 4.4). In contrast, GNA-1-TagRFP is located in the plasma membrane and vacuoles (Figure 4.4) and the merged image did not reveal co-localization with RIC8-GFP in conidia or young germlings (Figure 4.4). Similarly, co-localization was also not observed between GNA-3-TagRFP and RIC8-GFP (Figure 4.4). In addition, there was no evidence for co-localization between the GNA-3 fluorescent patches and RIC8 (Figure 4.4).

Discussion

G proteins regulate nearly every facet of growth and development in fungi. During asexual development, in particular, they have been found to regulate both the timing and level of conidiation (rev. in (Li *et al.*, 2007), and in recent years have also been shown to regulate conidial germination (Zuber *et al.*, 2003; Chang *et al.*, 2004; Doehlemann *et al.*, 2006; García-Rico *et al.*, 2009; García-Rico *et al.*, 2011). Here, we report evidence showing that in *N. crassa* G protein signaling regulates both conidial development and germination, and this is regulated through the non-receptor GEF RIC8.

In this study we pioneered the use of an internal Gα tagging method in filamentous fungi based on a successful approach used in *Dictyostelium* and mammalian cells, inserting TagRFP into a conserved loop region in the Gα subunits (Janetopoulos *et al.*, 2001; Azpiazu and Gautam, 2004). Using this approach we were able to localize GNA-1, GNA-2 and GNA-3 during conidial germination, revealing that all three Gα

proteins localize to the plasma membrane in ungerminated conidia and young germlings and that GNA-1 can be detected in septa in older hyphae. All three Gα subunits were also detected in vacuoles, however, it is unclear if this is functional localization as proteins are often targeted for degradation by the vacuole (Klionsky *et al.*, 1990). Perhaps the most intriguing finding was the observation of patches of GNA-3-TagRFP on the plasma membrane at later time points during germination of conidia. This change in localization during the transition from conidium to germling may be related to the requirement for GNA-3 during conidial germination; further analysis is necessary to explore this hypothesis.

Using purified proteins in *in vitro* assays, we have previously demonstrated that RIC8 can bind to and act as a GEF for GNA-1 and GNA-3 (Wright *et al.*, 2011). However, confocal microscopy of strains expressing GNA-1-TagRFP or GNA-3-TagRFP and RIC8-GFP did not reveal any evidence for co-localization of either Gα protein with RIC8 in conidia or hyphae, suggesting the interaction may be transient. Studies in *Drosophila* neuroblasts have demonstrated cytoplasmic localization of Ric-8, while $G\alpha_i$ was found in the apical cortex (Wang *et al.*, 2005). Ric-8 was also observed in 'spot-like' structures close to the apical cortex that partially colocalized with $G\alpha_i$, indicating that their interaction may take place on the cytoplasmic face of the plasma membrane or in the cytoplasm (Wang *et al.*, 2005).

Interestingly, the GNA-1-TagRFP signal was stronger than that of GNA-2 and GNA-3, and detectable over a longer period, suggesting this protein fusion may be more

stable. This conclusion is also supported by the results from western analysis using RFP antibodies. In yeast, the Ste2 GPCR is ubiquitinated and targeted to the vacuole for degradation (Hicke and Riezman, 1996). Analysis of *N. crassa* GNA-1, GNA-2 and GNA-3 using UbPred (http://www.ubpred.org/) predicts that GNA-1 and GNA-2 contain potential ubiquitination target sites, which may explain the vacuolar localization of these proteins. Future studies will explore whether this vacuolar localization is functional, and if so investigate the importance of G protein signaling in the vacuole.

Table 4.1: ***N. crassa* strains used in Chapter 4.**

Strain	Relevant genotype	Comments	Source
74-OR23-IVA	Wild type, *mat A*	FGSC 2489[a]	FGSC
2-1	Δ*gna-1::hph*$^+$*, gna-1-TagRFP::his-3*$^+$ *mat A*	Expresses GNA-1-TagRFP	This Study
5-1	Δ*gna-2::hph*$^+$*, gna-2-TagRFP::his-3*$^+$ *mat a*	Expresses GNA-2-TagRFP	This Study
12-1	Δ*gna-3::hph*$^+$*, gna-3-TagRFP::his-3*$^+$ *mat A*	Expresses GNA-3-TagRFP	This Study
R8GFP	Δ*ric8::hph*$^+$*, ric8-GFP::his-3*$^+$*, mat a*	Expresses RIC8-GFP	Wright, S. J., R. Inchausti, et al. (2011)

[a]FGSC, Fungal Genetics Stock Center, Kansas City, MO.

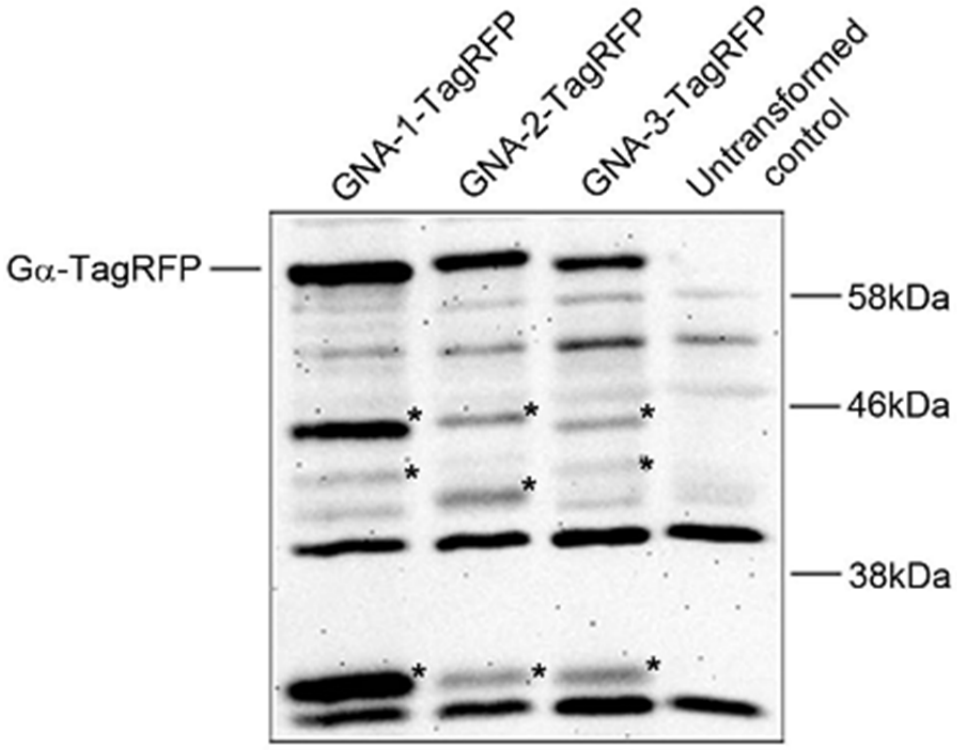

Figure 4.1 Western blot detection of Gα-TagRFP fusion proteins.

Samples containing 50 µg of protein from conidial extracts were subjected to western blot analysis with a RFP primary antiserum. Strains are Δ*gna-1*, *gna-1-TagRFP* (2.1), Δ*gna-2*, *gna-2-TagRFP* (5.1), Δ*gna-3*, *gna-3-TagRFP* (12.1) and wild type (untransformed control; 74-OR23-IVA). TagRFP is 27 kD, while the predicted size of the three TagRFP fusion proteins is 68 kD. Potential degradation products for each RFP fusion are noted with asterisks.

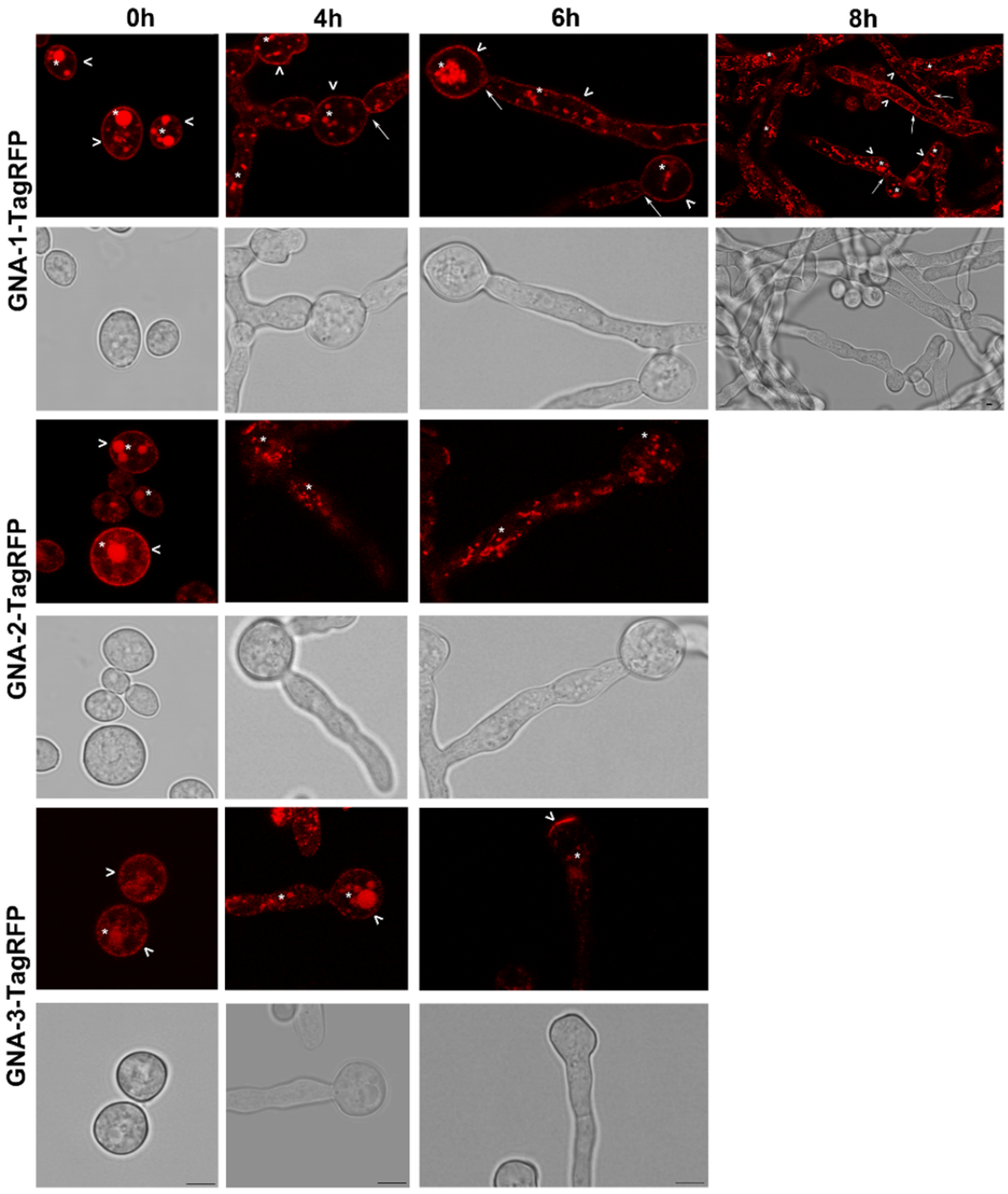
0h
4h
6h
8h
GNA-1-TagRFP
GNA-2-TagRFP
GNA-3-TagRFP

Figure 4.2 Localization of Gα proteins in germinating conidia.

Conidia from strains expressing GNA-1-TagRFP, GNA-2-TagRFP, GNA-3-TagRFP and untransformed controls were inoculated on solid medium and analyzed after 0, 4, 6 and 8 h of growth. Images were captured by bright field and the 543 nm HyD laser using the Leica TCS SP5 II inverted confocal microscope. The arrowhead, asterisk and solid arrow correspond to plasma membrane, vacuole and septa localization, respectively. Panels are only shown for time points in which fluorescence can be detected above background. All panels are 4× zoom, with the exception of GNA-1 at 8 h, which is 2×. Scale bar = 5 μm.

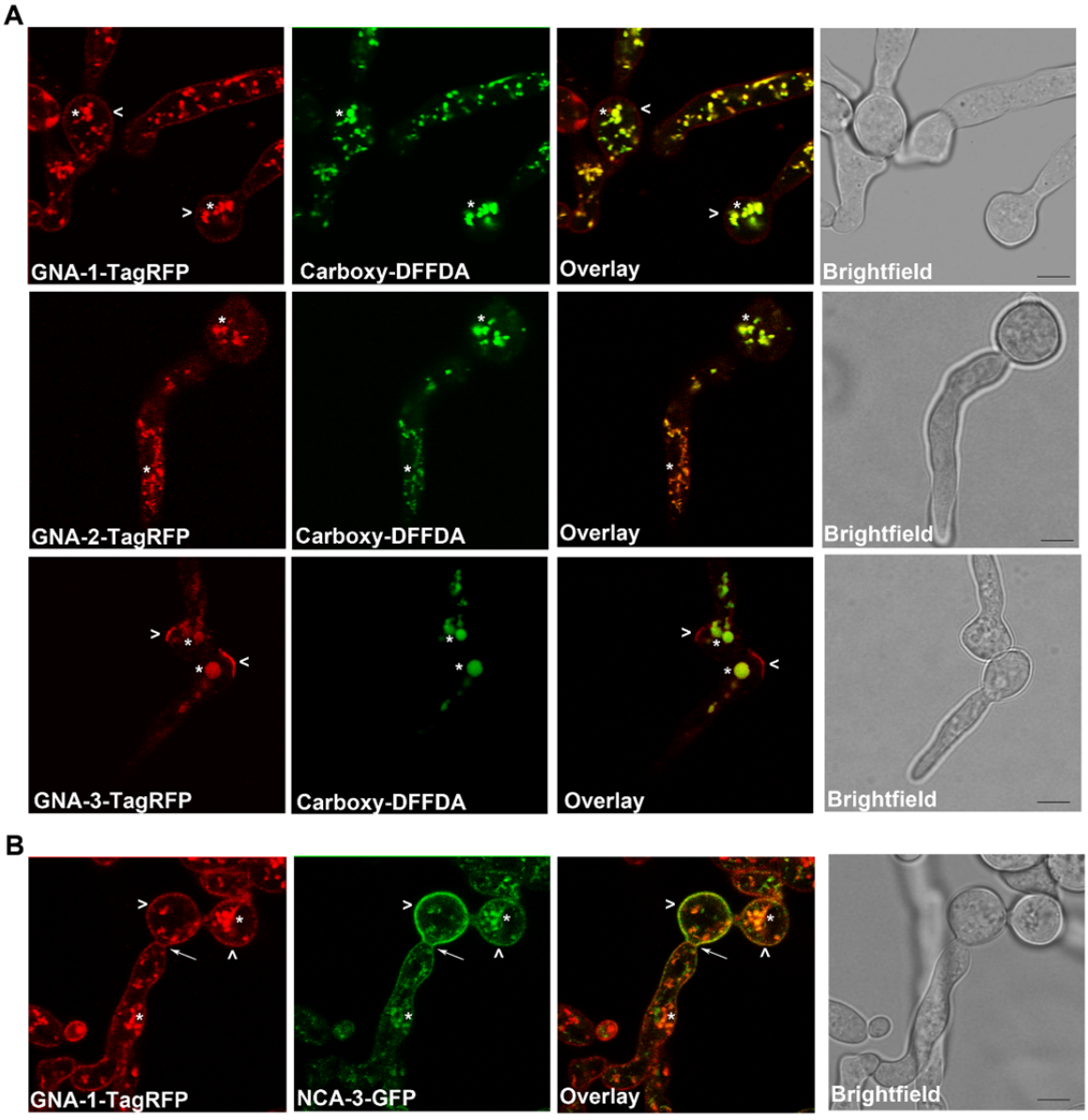
A
GNA-1-TagRFP
Carboxy-DFFDA
Overlay
Brightfield
GNA-2-TagRFP
Carboxy-DFFDA
Overlay
Brightfield
GNA-3-TagRFP
Carboxy-DFFDA
Overlay
Brightfield
B
GNA-1-TagRFP
NCA-3-GFP
Overlay
Brightfield

Figure 4.3: All three Gα proteins localize to vacuoles.

A. Conidia expressing the corresponding Tag-RFP Gα were inoculated onto 100 mm solid VM at a concentration of 8×106 conidia per plate. Plates were incubated at 30°C for 4 h (GNA-2 and GNA-3) or 6 h (GNA-1). The vacuolar dye Carboxy-DFFDA was applied at a concentration of 20 μg/ml. Images were captured using the Leica TCS SP5 II inverted confocal microscope. The RFP and GFP panels were merged to create the overlay. B. Conidia expressing both GNA-1-TagRFP and NCA-3-GFP were inoculated onto 100 mm solid VM at a concentration of 8×106 conidia per plate. Plates were incubated at 30°C for 6 h. Images were captured using the Leica TCS SP5 II inverted confocal microscope. The RFP and GFP panels were merged to create the overlay. All panels are 4× zoom. Bar = 5 μm.

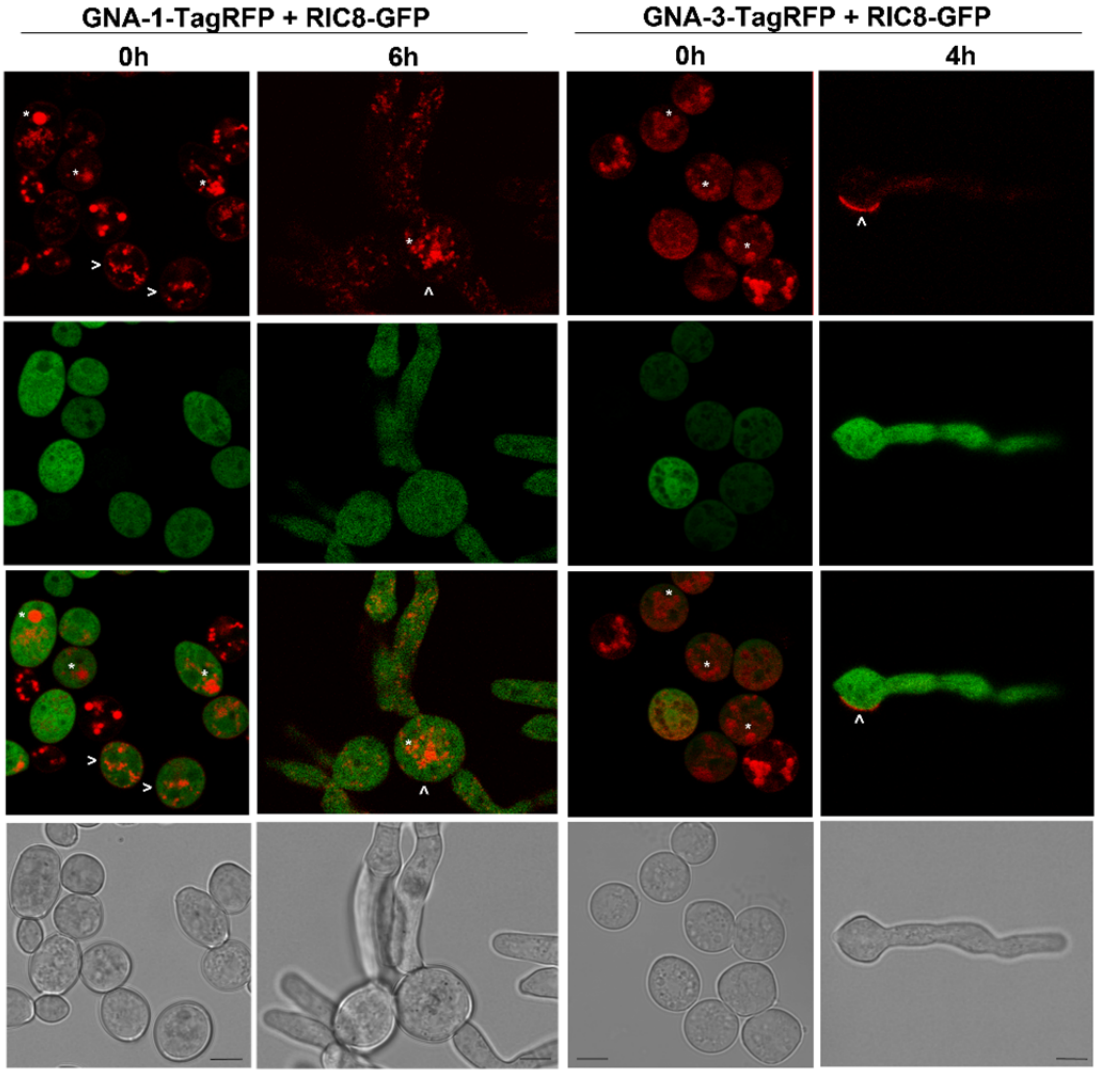
GNA-1-TagRFP + RIC8-GFP
GNA-3-TagRFP + RIC8-GFP
0h
6h
0h
4h

Figure 4.4 Localization of GNA-1-TagRFP and GNA-3-TagRFP with RIC8-GFP in germinating conidia.

Conidia from a fused strain expressing GNA-1-TagRFP or GNA-3-TagRFP and RIC-8-GFP were harvested as described in the Materials and Methods. An aliquot containing 8×10^6 conidia was spread on a 100 mm VM solid medium plate. Images were captured using a Leica TCS SP5 II inverted confocal microscope. Conidia were imaged immediately after inoculation on the solid medium plate. Conidia were allowed to germinate for 6 h or 4 h at 30°C before imaging. The first two panels were merged to create the third panel. All panels are 4× zoom. Scale bar = 5 μm.

References

Azpiazu, I., and Gautam, N. (2004). A fluorescence resonance energy transfer-based sensor indicates that receptor access to a G protein is unrestricted in a living mammalian cell. J Biol Chem *279*, 27709-27718.

Baasiri, R.A., Lu, X., Rowley, P.S., Turner, G.E., and Borkovich, K.A. (1997). Overlapping functions for two G protein alpha subunits in *Neurospora crassa*. Genetics *147*, 137-145.

Berepiki, A., Lichius, A., Shoji, J.Y., Tilsner, J., and Read, N.D. (2010). F-actin dynamics in *Neurospora crassa*. Eukaryot Cell *9*, 547-557.

Bowman, B.J., Draskovic, M., Freitag, M., and Bowman, E.J. (2009). Structure and distribution of organelles and cellular location of calcium transporters in *Neurospora crassa*. Eukaryot Cell *8*, 1845-1855.

Chang, M.H., Chae, K.S., Han, D.M., and Jahng, K.Y. (2004). The GanB Gα-protein negatively regulates asexual sporulation and plays a positive role in conidial germination in *Aspergillus nidulans*. Genetics *167*, 1305-1315.

Colot, H.V., Park, G., Turner, G.E., Ringelberg, C., Crew, C.M., Litvinkova, L., Weiss, R.L., Borkovich, K.A., and Dunlap, J.C. (2006). A high-throughput gene knockout procedure for *Neurospora* reveals functions for multiple transcription factors. PNAS *103*, 10352-10357.

Doehlemann, G., Berndt, P., and Hahn, M. (2006). Different signalling pathways involving a Gα protein, cAMP and a MAP kinase control germination of *Botrytis cinerea* conidia. Mol Microbiol *59*, 821-835.

Freitag, M., Hickey, P.C., Raju, N.B., Selker, E.U., and Read, N.D. (2004). GFP as a tool to analyze the organization, dynamics and function of nuclei and microtubules in *Neurospora crassa*. Fungal Genet Biol *41*, 897-910.

García-Rico, R.O., Chavez, R., Fierro, F., and Martin, J.F. (2009). Effect of a heterotrimeric G protein α subunit on conidia germination, stress response, and roquefortine C production in *Penicillium roqueforti*. Int Microbiol *12*, 123-129.

García-Rico, R.O., Martin, J.F., and Fierro, F. (2011). Heterotrimeric Gα protein Pga1 from *Penicillium chrysogenum* triggers germination in response to carbon sources and affects negatively resistance to different stress conditions. Fungal Genet Biol *48*, 641-649.

Hicke, L., and Riezman, H. (1996). Ubiquitination of a yeast plasma membrane receptor signals its ligand-stimulated endocytosis. Cell *84*, 277-287.

Ivey, F.D., Hodge, P.N., Turner, G.E., and Borkovich, K.A. (1996). The G alpha i homologue gna-1 controls multiple differentiation pathways in *Neurospora crassa*. Mol Biol Cell *7*, 1283-1297.

Janetopoulos, C., Jin, T., and Devreotes, P. (2001). Receptor-mediated activation of heterotrimeric G-proteins in living cells. Science *291*, 2408-2411.

Kays, A.M., and Borkovich, K.A. (2004). Severe impairment of growth and differentiation in a *Neurospora crassa* mutant lacking all heterotrimeric G alpha proteins. Genetics *166*, 1229-1240.

Kays, A.M., Rowley, P.S., Baasiri, R.A., and Borkovich, K.A. (2000). Regulation of conidiation and adenylyl cyclase levels by the Galpha protein GNA-3 in *Neurospora crassa*. Mol Cell Biol *20*, 7693-7705.

Klionsky, D.J., Herman, P.K., and Emr, S.D. (1990). The fungal vacuole: composition, function, and biogenesis. Microbiol Rev *54*, 266-292.

Krystofova, S., and Borkovich, K.A. (2005). The heterotrimeric G-protein subunits GNG-1 and GNB-1 form a Gβγ dimer required for normal female fertility, asexual development, and galpha protein levels in *Neurospora crassa*. Eukaryot cell *4*, 365-378.

Krystofova, S., and Borkovich, K.A. (2006). The predicted G-protein-coupled receptor GPR-1 is required for female sexual development in the multicellular fungus *Neurospora crassa*. Eukaryot cell *5*, 1503-1516.

Li, L., and Borkovich, K.A. (2006). GPR-4 is a predicted G-protein-coupled receptor required for carbon source-dependent asexual growth and development in *Neurospora crassa*. Eukaryot Cell *5*, 1287-1300.

Li, L., Wright, S.J., Krystofova, S., Park, G., and Borkovich, K.A. (2007). Heterotrimeric G protein signaling in filamentous fungi. Annu Rev Microbiol *61*, 423-452.

Li, Y., Yan, X., Wang, H., Liang, S., Ma, W.B., Fang, M.Y., Talbot, N.J., and Wang, Z.Y. MoRic8 Is a novel component of G-protein signaling during plant infection by the rice blast fungus *Magnaporthe oryzae*. Mol Plant Microbe Interact *23*, 317-331.

Vogel, H.J. (1964). Distribution of lysine pathways among fungi - Evolutionary implications. Am Nat *98*, 435-446.

Wang, H., Ng, K.H., Qian, H., Siderovski, D.P., Chia, W., and Yu, F. (2005). Ric-8 controls *Drosophila* neural progenitor asymmetric division by regulating heterotrimeric G proteins. Nature cell biology *7*, 1091-1098.

Wilkie, T.M., and Kinch, L. (2005). New roles for Galpha and RGS proteins: communication continues despite pulling sisters apart. Curr Biol *15*, R843-854.

Wright, S.J., Inchausti, R., Eaton, C.J., Krystofova, S., and Borkovich, K.A. (2011). RIC8 is a guanine-nucleotide exchange factor for Galpha subunits that regulates growth and development in *Neurospora crassa*. Genetics *189*, 165-176.

Zuber, S., Hynes, M.J., and Andrianopoulos, A. (2003). The G-protein α-subunit GasC plays a major role in germination in the dimorphic fungus *Penicillium marneffei*. Genetics *164*, 487-499.

Chapter 5

The guanine nucleotide exchange factor RIC8 and STE50 influence Erk class mitogen activated protein kinase activity in *Neurospora crassa*

Abstract

Heterotrimeric G proteins are essential components of signal transduction pathways that regulate environmental sensing, growth, and development in eukaryotes. RIC8 is a cystolic protein that can serve as a guanine nucleotide exchange factor (GEF) for G alpha proteins. A *ric8* homologue is present within the *Neurospora crassa* genome. Using a yeast two hybrid screen, a previous graduate student identified STE50 as a protein that interacted with RIC8. STE50 has been demonstrated to function as a regulator of MAPK signaling in other fungi. *N. crassa* contains three different mitogen activated protein kinase (MAPK) cascades. Two of the pathways contain Erk class MAPKs (MAK-1 and MAK-2), while the third cascade has a terminal p38 MAP kinase (OS-2). I constructed strains expressing tagged RIC8 or STE50 in order to confirm the interaction between the two proteins using co-immunoprecipitation. I also analyzed Δ*ste50* and Δ*ric8* single and double mutants for growth and developmental defects and for effects on the activity of the Erk class MAPKs. Mutants lacking *ric8*, *ste50*, *ric8ste50*, or the MAPK genes, *mak-1* and *mak-2,* exhibited slow hyphal extension, and short aerial hyphae with conidiation close to the agar surface. Δ*ste50* had no detectable phosphorylated MAK-2 in liquid or solid VM cultures. Similar to *ste50* single mutants,

the Δ*ric8* Δ*ste50* double mutant did not have detectable MAK-2-phosphate on liquid VM cultures. However levels of MAK-2-phosphate in the Δ*ric8* Δ*ste50* double mutant were similar to wild type and Δ*ric8* strains on solid VM cultures, thus demonstrating that the dependence of MAK-2-phosphate on *ste50* varies in the *ric8* background under different media conditions.

Introduction

Recent studies have identified a cytosolic protein (RIC8) that is able to bypass the GPCR mechanism, and promote exchange of GDP for GTP on Gα subunits (Miller *et al.*, 2000; Tall *et al.*, 2003; Afshar *et al.*, 2004; Couwenbergs *et al.*, 2004; David *et al.*, 2005; Wright *et al.*, 2011). RIC8 is absent from plants and yeast, but is found in animals and fungi (Wilkie and Kinch, 2005). *N. crassa* has one copy of *ric8* in its genome (Wright *et al.*, 2011). The Δ*ric8* mutant is viable, but has a severe growth defect and is impaired in all developmental pathways, including sexual and asexual development (Wright *et al.*, 2011).

A schematic of the MAPK pathways can be found in Figure 1.2. MAPK pathways are key components in signal transduction, relaying important information in the cell. *N. crassa* has three MAPK cascades. Two of the MAPK pathways contain Erk class MAPKs, MAK-1 and MAK-2 (Pandey *et al.*, 2004; Li *et al.*, 2005; Maerz *et al.*, 2008; Park *et al.*, 2008), while the third cascade has a terminal p38 MAPK (OS-2) (Zhang *et al.*, 2002). The MAK-1 and MAK-2 pathways are implicated in control of cell growth

and integrity, formation of aerial hyphae and conidia, fusion of conidial anastomosis tubes, conidial germination and female fertility (Pandey *et al.*, 2004; Li *et al.*, 2005; Roca *et al.*, 2005; Maerz *et al.*, 2008; Park *et al.*, 2008; Fu *et al.*, 2011). The OS-2 cascade is essential for resistance to hyperosmotic stress, resistance to fungicides, cell integrity and female fertility (Fujimura *et al.*, 2000, Zhang *et al.*, 2002; Jones *et al.*, 2007).

STE50 is a conserved fungal adaptor protein that regulates MAPK signaling. The STE50 protein in *Saccharomyces cerevisiae* (ScSte50p) has been extensively studied, revealing its function in mating response, filamentous growth, and osmosensing (Posas and Saito, 1998; Ramezani Rad *et al.*, 1998; Ramezani-Rad, 2003). STE50 is composed of three characterized domains: an N-terminal Sterile-Alpha Motif (SAM) domain, a central serine/threonine rich region and a Ras Association (RA) domain at the C-terminus (Grimshaw *et al.*, 2004; Qiao and Bowie, 2005). *N. crassa* contains one STE50 homolog (NCU00455) and MAK-2 phosphorylation cannot be detected when *ste50* is absent (Dettmann *et al.*, 2014).

A previous graduate student, James Kim, demonstrated a yeast two-hybrid interaction between *N. crassa* STE50 and RIC8. This chapter supplements his work with additional assays to confirm the interaction. In addition, Δ*ste50* and Δ*ric8* single and double mutants were assayed for growth and developmental defects. Lastly, effects on the activity of the ERK MAP kinases in the different strains were determined during different developmental stages and conditions.

Materials and Methods

N. crassa culture conditions:

N. crassa strains used in this study are listed in Table 5.1. For vegetative growth analysis, strains were grown on Vogel's minimal (VM) medium (Vogel, 1964). For producing female reproductive structures for crossing, synthetic crossing medium (SCM) was used (Westergaard and Mitchell, 1947). For isolation of ascospore progeny, spores were plated on Fructose, Glucose, Sorbose (FGS) plates (Case *et al.*, 1979). Hygromycin B (Calbiochem, San Diego, CA) was added to media at 200 μg/ml where indicated.

Plate diameter phenotype:

In order to assess overall hyphal growth and morphology, 25ml-VM plates were inoculated in the center with 1 μl of a conidial suspension and then incubated at room temperature in the dark for 24 hrs. Four plate replicates were obtained for each mutant.

An independent experiment was conducted for colony morphology assays were conducted using 25ml- VM plates by inoculating 1 μl of a conidial suspension in the center. Plates were incubated at room temperature in the dark for 32 hrs and then photographed.

Co-immunoprecipitation trials:

For co-immunoprecipitation experiments, cells were collected from 1) 16-hr liquid cultures inoculated at a concentration of $1x10^6$ conidia/ml; 2) conidia isolated from 500 ml slanted flasks containing 100ml of VM medium; 3) 3-day liquid SCM cultures (inoculated using $1x10^6$ conidia/ml), and 4) SCM medium plates overlaid with cellophane. VM liquid cultures were grown for 16 hr with shaking at 200 rpm at 30°C, while liquid SCM cultures were shaken at 50 rpm at room temperature under constant light. After collection by vacuum filtration, cheesecloth filtration, or scraping tissue from cellophane, tissue was ground in liquid nitrogen and transferred to an Oakridge centrifuge tube containing ice-cold co-immunoprecipitation (Co-IP) buffer (20 mM TrisCl pH 7.4, 200mM NaCl, 1 mM EDTA, 0.5 mM PMSF, and 1 µl/ml Fungal Protease Inhibitor Cocktail (Cat #T8215, Sigma-Aldrich, St. Louis, MO). Detergent (0.5% Nonidet P40, NC 9375914- Fisher Scientific) was added for some experiments. After thorough mixing, tubes were centrifuged at 1,000 x g, at 4˚C for 10 min. (whole cell extract) or initially at 1,000 x g, at 4˚C for 10 min. with a subsequent centrifugation at 46,000 x g at 4˚C for 30 min. (cytosolic fraction). The supernatant was transferred to a new tube and protein concentration measured using the Bradford assay (Bio-Rad, Hercules, CA).

A volume of extract containing 1.5-6 mg of total protein was transferred to a new tube and mixed with buffer to give a total volume of 0.5-1 ml. This sample was gently mixed with 20 µl packed volume of V5 antibody-coupled agarose-antibody slurry (agarose immobilized goat anti-V5 antibody, S190-119, Bethyl laboratories,

Montgomery, TX.) or 20 µl packed volume of FLAG antibody-coupled (ANTI-FLAG® M1 Agarose Affinity Gel, Cat# A4596, Sigma-Aldrich, St. Louis, MO) or 5 µl of GFP-trap agarose beads (Cat# gta-20, ChromoTek, Planegg-Martinsried, Germany) or 1:500 or 1:1000 rabbit anti-RIC8 antibody. The tube was placed on a rotating shaker overnight at 4˚C. For the RIC8 antibody, 20 µl of Protein A beads were incubated for 20 min-1 hr. After centrifugation at 200 x g for 5 min., the supernatant was removed. The beads were washed three times by suspension in 0.5 ml ice-cold 1x Tris-buffer saline (TBS), 10-30 µl of 2x sample buffer [125 mM Tris-Cl (pH 6.8), 4% SDS, 20% glycerol, and 0.005% bromphenol blue] and heated at 90°C for 5 min and then separated from the agarose beads by centrifuging at 3,000 rpm for 5 min in a microcentrifuge at room temperature. Supernatants were analyzed using SDS-PAGE and then subjected to western analysis (Table 5.2 for summary).

MAPK phosphorylation assays:

Stimulated phosphorylation of MAK-1 using lysing enzymes:

Conidia were used to inoculate 20 ml VM liquid cultures at a concentration of $1x10^7$ cells/ml. Cultures were incubated with shaking at 200 rpm for 16 hr at 30˚C. For induction, lysing enzymes (*Trichoderma harzianum*; Cat# L1412; Sigma-Aldrich, St. Louis, MO) were added to a final concentration of 20 mg/ml for the last 15 minutes of incubation. Tissue was collected by vacuum filtration and then flash-frozen with liquid

nitrogen. The protein extraction method was as described (Pandey *et al.*, 2004). Protein concentration was determined using the BCA Protein Assay (Pierce Chemical, Rockford, IL) using Bovine Serum Albumin (BSA) as the protein standard (Cat# P5619, Sigma-Aldrich, St. Louis, MO). Samples containing 50 μg of protein were subjected to a 10% poly-acrylamide gel and then transferred to a 0.45 μm nitrocellulose membrane (Cat# EP4HY00010, GE Water and Process Technologies, Trevose, PA). A duplicate gel stained with Coomassie was used to confirm even loading. Membrane was blocked with 5% dry milk in TBST (Tris-buffer saline with 0.05% Tween 20) for 1 hr at room temperature, and subsequently washed 3x with TBST for 5 min each. Phosphorylated MAK-1 (51 kDa) and MAK-2 (41 kDa) were detected using a 1:500 dilution of anti-phospho p44/42 antibody (cat. #4370, Cell Signaling Technology, Danvers, MA) and incubated overnight at 4°C on a shaker. Membrane was washed 3x with TBST for 5 min each. Secondary antibody reaction was with Goat anti-rabbit (H+L)-HRP conjugate (cat. # 170-6515, Biorad, Hercules, CA) at a 1:1000 dilution. Chemiluminescent detection was as described (Krystofova and Borkovich, 2005) (Cat# 34079, Themo Scientific, Grand Island, NY).

MAK-1 and MAK-2 phosphorylation assays using different types of media:

Conidia from 8-day old cultures (4 days in the dark at 25°C and 4 days in ambient light at room temperature) were used to inoculate 25 ml VM and SCM plates overlaid with cellophane. A sample containing $8x10^6$ cells in 100μl was spread on the plates.

Cultures were allowed to grow for 6 days at 25°C in constant light. Tissue was scraped from the cellophane and flash frozen. Samples were processed as described above for the lysing enzymes induction experiment.

Results

An interaction between RIC8 and STE50 could not be confirmed using co-immunoprecipitation

As mentioned in the Introduction, a direct interaction between RIC8 and STE50 was demonstrated by James Kim using a yeast two hybrid screen. I attempted to follow up on these results using another method, co-immunoprecipitation. For these experiments, I constructed a homokaryotic strain that expresses STE50-FLAG tag. In addition, I crossed STE50-gfp with Δ*ric8* to obtain progeny that were STE50-gfp, Δ*ric8*. I also utilized James Kim's RIC8-V5, STE50-FLAG strain in these experiments. More detailed information for the strains can be found in Table 5.1.

The conditions tested in this study did not demonstrate a protein-protein interaction between RIC8 and STE50. I was able to immunoprecipitate each protein using antibody to its tag every time. However, the putative interactor was never detected (Table 5.2).

Δ*ric8*, Δ*ste50*, and Δ*ric8* Δ*ste50* mutants have short aerial hyphae

Figure 5.1 shows that Δ*ric8*, Δ*ste50* and Δ*ric8* Δ*ste50* mutants have short hyphae, thus giving a "flat" appearance when compared to wild type. Previous research confirms these findings, as the *ric8* and *mak-1* and *mak-2* MAPK mutants have short aerial hyphae and conidiate close to the agar surface (Park *et al.*, 2008; Wright *et al.*, 2011). Due to hyperconidiation, the Δ*ric8* strain produces a bright orange pigmentation, differing from Δ*ste50*, Δ*mak-1*, or Δ*mak-2,* which have less abundant conidia. The morphology of the double mutant Δ*ric8* Δ*ste50* resembled that of the strain lacking only *ric8* in terms of pigmentation.

Plate growth assays (Figure 5.2A) showed that the Δ*ric8*, Δ*ste50*, Δ*ric8*Δ*ste50*, Δ*mak-1* and Δ*mak-2* mutants have very small colony diameters when compared to wild type. Quantitative data was obtained by measuring the diameter of the colonies after a period of 24 hr (Figure 5.2B). All mutants grew less than 30% of wild type: Δ*ric8* (12.9%), Δ*ste50* (27.6%), Δ*ric8* Δ*ste50* (14.3%), Δ*mak-1* (21.0%), and Δ*mak-2* (24.3%) (Figure 5.2B). The similar diameter of Δ*ric8* and Δ*ric8* Δ*ste50* mutants suggests that *ric8* is epistatic to *ste50* for growth rate.

STE50 is required for normal phosphorylation of MAK-2, while RIC8 is required for normal basal phosphorylation of MAK-1 in liquid VM cultures

MAK-1 and MAK-2 phosphate levels were measured before and after addition of lysing enzymes to liquid VM (Figure 5.3). Lysing enzymes have been previously shown to induce phosphorylation of the cell wall integrity MAPK (MAK-1) in *N. crassa* (Park *et al.*, 2008). MAK-2 phosphate levels were normal in Δ*ric8* strains, but not detected in Δ*ste50* and Δ*ste50* Δ*ric8* mutants in liquid VM cultures (Figure 5.3). These findings indicate that STE50 is required for MAK-2 phosphorylation, which has been previously shown in liquid VM cultures (Dettmann *et al.*, 2014). Interestingly, Δ*ric8* mutants exhibited elevated basal MAK-1 phosphorylation, but levels were normal after addition of lysing enzymes (Figure 5.3). Δ*ste50* mutants possessed normal basal and induced levels of MAK-1-phosphate. Relatively normal MAK-1-phosphate levels were also observed in Δ*ric8* Δ*ste50* double mutants (Figure 5.3), thus negating the increased MAK-1 phosphorylation in the single Δ*ric8* mutant. These results suggests that *ste50* acts downstream of *ric8* to affect MAK-1 phosphorylation.

MAK-1 phosphorylation levels are normal in Δ*ste50* mutants on low nitrogen SCM solid medium

MAK-1- and MAK-2-phosphate levels were measured in extracts isolated from VM and SCM plate cultures (Figure 5.4). SCM is a low nitrogen medium that induces formation of female reproductive structures (Westergaard and Mitchell, 1947). The

results show that Δ*ric8* and Δ*ric8* Δ*ste50* mutants have normal levels of MAK-1-Pi and MAK-2-Pi on SCM. The Δ*ste50* mutant has undetectable MAK-1 or MAK-2-phosphate levels on high nitrogen VM plates. However, MAK-1 phosphate levels were normal on SCM medium (low nitrogen source). There was detectable MAK-2 phosphate in the Δ*ste50* mutant on SCM medium. However, this amount was not comparable to wild type. These results suggests that STE50 is required for MAK-2 phosphorylation on VM plate cultures, which supports earlier findings using conditions with high nitrogen liquid VM (Dettmann *et al.*, 2014). However, the results also showed that Δ*ric8* and Δ*ric8* Δ*ste50* strains had wild type levels of MAK-1 and MAK-2 phosphorylation.

Discussion

I was not able to detect an interaction between STE50 and RIC8 using co-immunoprecipitation approaches. This result suggests further investigation of 1) other growth conditions that may provide interaction between the two proteins, 2) fixation of the sample which may reveal a transient interaction or 3) that the yeast two-hybrid interaction is an artifact and RIC8 and STE50 do not interact *in vivo*. Analyzing SCM cultures, as both mutants affects the female fertility pathway, is an ideal condition to test. Looking at a time-course will reveal if the interaction occurs late in the sexual cycle.

Morphological assays were conducted in order to reveal significant phenotypes for strains lacking *ric8*, *ste50* or the MAPK genes *mak-1* and *mak-2*. All of these mutants exhibited a "flat" phenotype on the agar surface, with short aerial hyphae and conidiation

close to the agar surface. All mutants have a slower growth rate than wild type. Thus, RIC8 and STE50 are both required for normal conidiation and hyphal extension in *N. crassa*. However, the hyper-conidiation phenotype observed for both Δ*ric8* and Δ*ric8* Δ*ste50* strains suggests that *ric8* is epistatic to *ste50* with regards to colony morphology. This hypothesis is also supported by the growth rate measurements, as the Δ*ric8* Δ*ste50* double mutant resembles Δ*ric8*.

MAPK Assays: Liquid Cultures

MAPK assays were a biochemical approach towards understanding the underlying mechanisms involving these genes. The experiments revealed that *ste50* is necessary for phosphorylation of MAK-2 in 16 hr VM liquid cultures. This finding suggests that *ste50* is acting as a positive regulator in the MAK-2 MAPK cascade. Removing *ste50* influences the MAK-2-phosphorylation in a negative manner.

MAK-1-phosphylation levels appeared normal in the *ste50* mutant, however basal MAK-1-P_i was elevated in the *ric8* mutant. The double mutant, Δ*ric8* Δ*ste50*, resembled the Δ*ste50* single mutant. This finding suggest that STE50 may be functioning downstream of RIC8 to phosphorylate MAK-1 in liquid VM cultures.

MAPK Assays: Plate Cultures

Δste 50 appeared to have very low MAK-1 and MAK-2 phosphorylation in 6 day old VM plate cultures, again suggesting that STE50 is a positive regulator of not only MAK-2-phosphorylation, but MAK-1-phosphorylation as well. The results also showed that Δ*ric8* and Δ*ric8* Δ*ste50* mutants had wild type levels of MAK-1 and MAK-2 phosphorylation, suggesting that *ric8* is epistatic to *ste50* with regards to MAPK phosphorylation on VM plate cultures. Similarly to liquid cultures, STE50 behaves as a positive regulator of both MAK-1 and MAK-2 phosphorylation on solid media. The double mutant results suggest that RIC8 is a negative regulator of MAK-2 phosphorylation when STE50 is absent.

Future directions

Further investigation is needed to decipher the regulatory circuit controlling MAK-1 and MAK-2 phosphorylation in the Δ*ric8* and Δ*ste50* mutants. Preliminary genetic analysis did not reveal a conclusive result for epistatic relationships. Genetic studies over-expressing *ric8* and/or *ste50* are necessary to reveal epistasis between these genes regarding the effect on MAK-1 and MAK-2 phosphorylation. For example, if *ric8* is a negative regulator of MAK-2 phosphorylation in SCM cultures, overexpression of *ric8* in the wild type background should lead to lower levels of MAK-2-phosphate. Other possible future directions would be to analyze the effects of the Δ*ric8* and Δ*ste50* mutations on *mak-1* and *mak-2* transcription and/or protein levels. Transcript levels of the

mak-1 and *mak-2* genes can be measured using Northern analysis. For more quantitative results, qPCR would be required. However, if *ric8* and *ste50* affect MAK-1 and MAK-2 phosphorylation indirectly, RNAseq would be a route to take in order to analyze the effect on transcription on a genome-wide scale. RNAseq experiments should include the single and double mutants.

Table 5.1: ***N. crassa* strains used in Chapter 5.**

Strain	Relevant genotype	Comments	Source
74-OR23-IVA	Wild type, *mat A*	FGSC 2489[a]	FGSC
R81a	Δ*ric8::hph*$^+$*, mat a*		Wright et al., 2011
S50A	Δ*ste-50::hph*$^+$*, mat A*	FGSC 17041[a]	FGSC
S50R8	Δ*ste-50::hph*$^+$ Δ*ric8::hph*$^+$*, mat A*		James Kim
Ric8-V5-1	*ric8-V5*::*nat*$^+$, *mat a*		Patrick Schacht
STE50-FLAG	*ste-50-FLAG*::*nat*$^+$	Homokaryon obtained from STE50-FLAG x Ric8-V5 #17	Collaboration with James Kim
R8V5, S50F	*ric8-V5*::*nat*$^+$, *ste-50-FLAG*::*nat*$^+$		James Kim
9-F1	Δ*ste50::hph*$^+$*, ste-50-gfp::his-3*$^+$		James Kim
S50-gfp	Δ*ste50::hph*$^+$, *ste50-gfp::his-3*$^+$		James Kim
S50-gfp,R8	Δ*ste-50::hph*$^+$*, ste50-gfp::his-3*$^+$ Δ*ric8::hph*$^+$	Obtained from STE50-GFP x Δ*ric8* #62	This study
mak1	Δ*mak-1::hph*$^+$ *mat a*	FGSC 11320 [a]	FGSC
mak2	Δ*mak-2::hph*$^+$ *mat A*	#660	Dan Ebbole

[a]FGSC, Fungal Genetics Stock Center, Kansas

C

Wild type *Δric8* *Δste50*

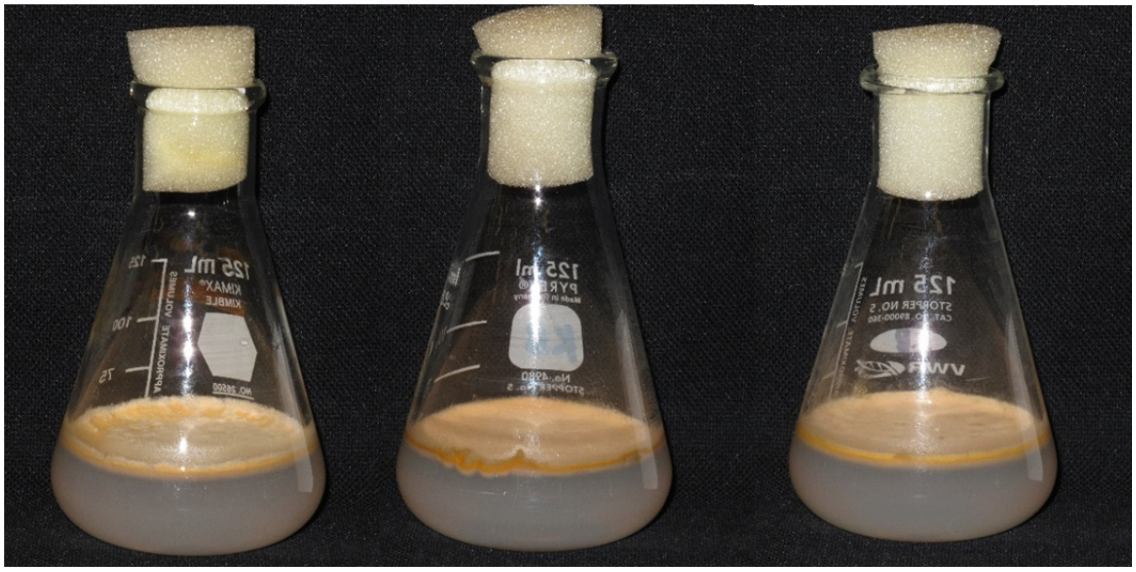

Δric8, *Δste50* *Δmak-1* *Δmak-2*

Figure 5.1: Flask morphology of mutants in *N. crassa*.

Cultures were grown on 50ml VM agar flasks and incubated at 25°C in the dark for 5 days.

A

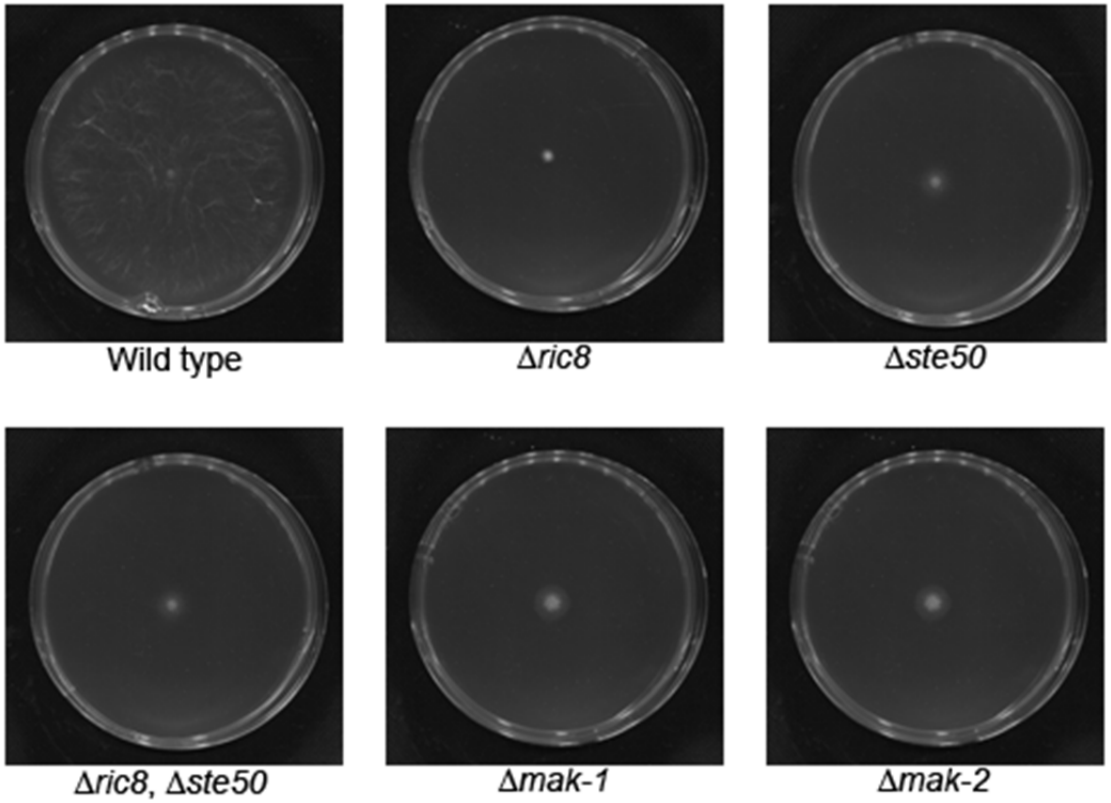
Wild type
Δric8
Δste50
Δric8, Δste50
Δmak-1
Δmak-2

B

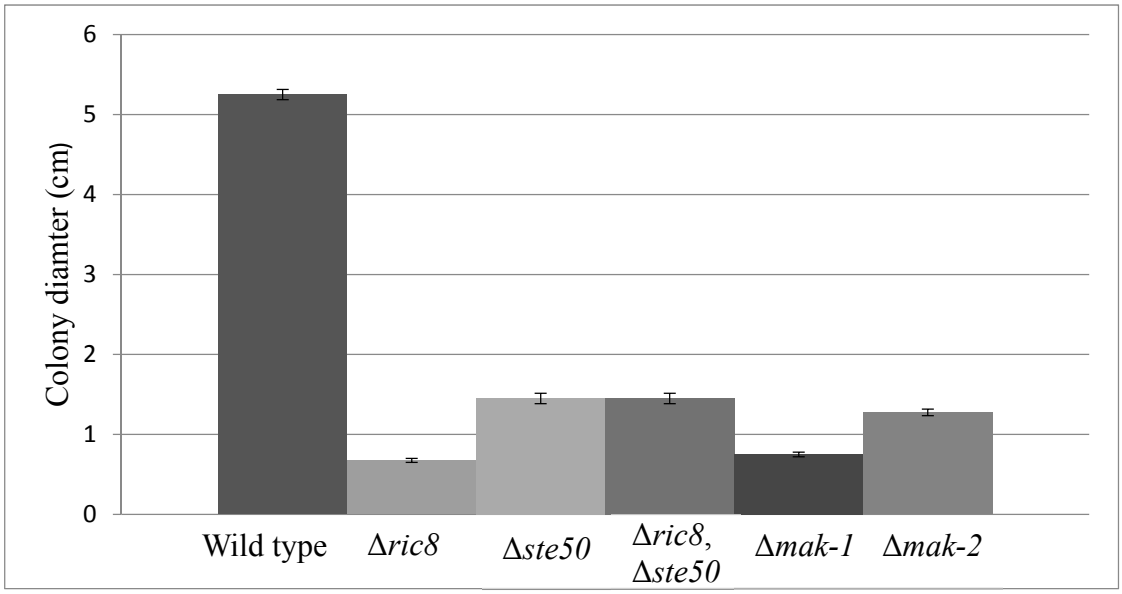
Colony diamter (cm)
0
1
2
3
4
5
6
Wild type
Δric8
Δste50
Δric8, Δste50
Δmak-1
Δmak-2

Figure 5.2: Colony morphology of mutants in *N. crassa*.

A conidial suspension (1 μl) of a conidial suspension was placed on the center a VM plate, and allowed to grow at room temperature in the dark for 32 hours (A). Diameters were measured in centimeters at 24 hours of incubation. Four plate replicates were conducted for each mutant. The standard error was determined for each strain (B).

A

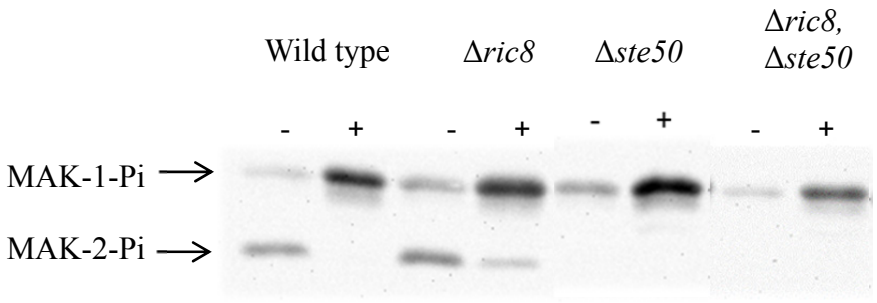
Wild type
Δ*ric8*
Δ*ste50*
Δ*ric8*, Δ*ste50*
- + - + - + - +
MAK-1-Pi
MAK-2-Pi

B

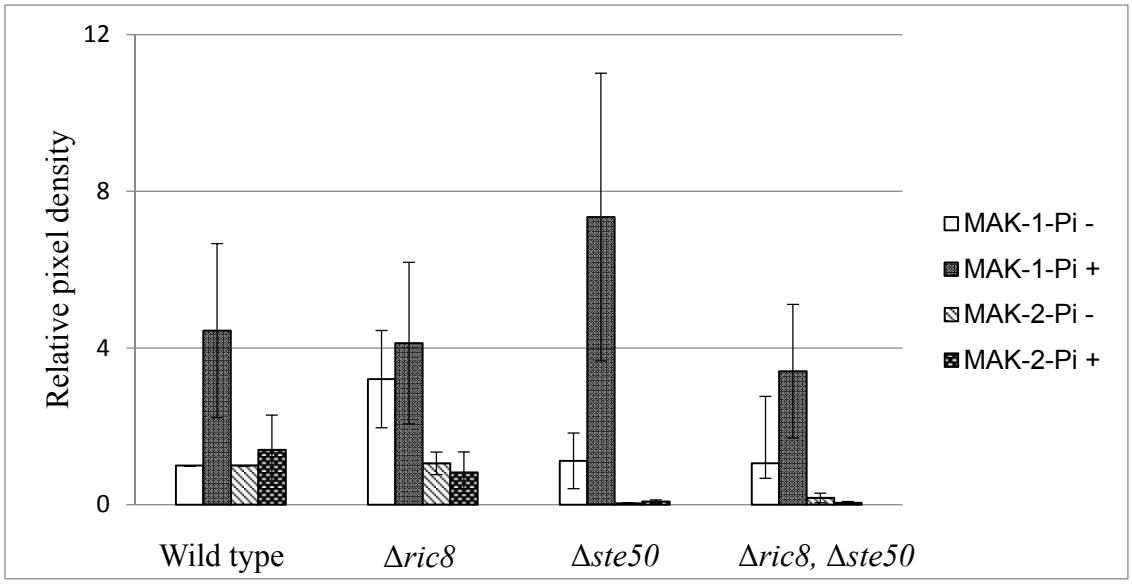
12
8
4
0
Relative pixel density
MAK-1-Pi -
MAK-1-Pi +
MAK-2-Pi -
MAK-2-Pi +
Wild type
Δ*ric8*
Δ*ste50*
Δ*ric8*, Δ*ste50*

Figure 5.3: Lysing enzymes MAPK assay.

16-hr shaken liquid cultures from the indicated strains were treated with water (-) or induced using 20 mg/ml lysing enzymes (+) (A, B). Band intensities were quantitated using LabWorks software. Pixel densities were normalized to the wild type uninduced samples. Data are from 4 independent experiments (B).

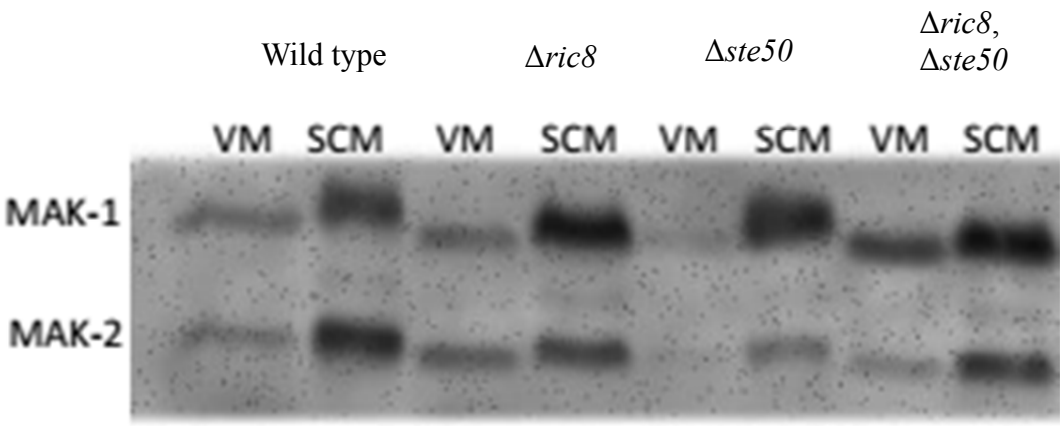

Figure 5.4: MAPK assay on VM and SCM plate cultures.

Basal MAK-1 and MAK-2 phosphorylation levels were detected in 6 day old VM and SCM plates cultures on plates. Cell extracts were prepared and 50 µg total protein subjected to western analysis using a phospho-ERK antibody.

Table 5.2: **Co-immunoprecipitation conditions**

Strain	Tissue	Buffer/Detergent	Beads	Primary antibody
R8V5, S50F	16hr liquid VM	Co-IP	Bethyl- V5	DYKDDDK Tag Rabbit, Cell Signaling
R8V5, S50F	16hr liquid VM	Co-IP	Bethyl-FLAG	Mouse anti-V5, Invitrogen
R8V5, S50F	16hr liquid VM	Co-IP	Sigma-FLAG	Mouse anti-V5, Invitrogen
R8V5, S50F	16hr liquid SCM	Co-IP + 6mM $MgCl_2$, 200µM GDP/ 0.5% NP40	Sigma-FLAG	Rabbit anti-V5, Bethyl
R8V5, S50F	16hr liquid VM	Co-IP + 6mM $MgCl_2$, 200µM GDP/ 0.5% NP40	Sigma-FLAG	Rabbit anti-V5, Bethyl
R8V5, S50F	24hr liquid SCM	Co-IP + 6mM $MgCl_2$, 200µM GDP	Sigma-FLAG	Rabbit anti-V5, Bethyl
R8V5, S50F	16hr liquid VM	Co-IP + 100µM GDP	Sigma-FLAG	Rabbit anti-V5, Bethyl
S50-gfp	16hr liquid VM	Co-IP	GFP-Trap	Rabbit anti-RIC8
S50-gfp	16hr liquid VM	Co-IP	RIC8 antibody+ Protein A beads	DYKDDDK Tag Rabbit, Cell Signaling
S50-gfp	Conidia	Co-IP	GFP-Trap	Rabbit anti-RIC8
S50-gfp	Conidia	Co-IP	RIC8 antibody	DYKDDDK Tag Rabbit, Cell Signaling
S50-gfp	24hr liquid SCM	Co-IP	RIC8 antibody+ Protein A beads	DYKDDDK Tag Rabbit, Cell Signaling

References

Afshar, K., Willard, F.S., Colombo, K., Johnston, C.A., McCudden, C.R., Siderovski, D.P., and Gonczy, P. (2004). RIC-8 is required for GPR-1/2-dependent Galpha function during asymmetric division of *C. elegans* embryos. Cell *119*, 219-230.

Case, M.E., Schweizer, M., Kushner, S.R., and Giles, N.H. (1979). Efficient transformation of *Neurospora crassa* by utilizing hybrid plasmid DNA. Proc Natl Acad Sci U S A *76*, 5259-5263.

Couwenbergs, C., Spilker, A.C., and Gotta, M. (2004). Control of embryonic spindle positioning and Galpha activity by *C. elegans* RIC-8. Curr Biol *14*, 1871-1876.

David, N.B., Martin, C.A., Segalen, M., Rosenfeld, F., Schweisguth, F., and Bellaiche, Y. (2005). Drosophila Ric-8 regulates Galphai cortical localization to promote Galphai-dependent planar orientation of the mitotic spindle during asymmetric cell division. Nat Cell Biol *7*, 1083-1090.

Dettmann, A., Heilig, Y., Valerius, O., Ludwig, S., and Seiler, S. (2014). Fungal communication requires the MAK-2 pathway elements STE-20 and RAS-2, the NRC-1 adapter STE-50 and the MAP kinase scaffold HAM-5. PLoS Genet *10*, e1004762.

Fu, C., Iyer, P., Herkal, A., Abdullah, J., Stout, A., and Free, S.J. (2011). Identification and characterization of genes required for cell-to-cell fusion in *Neurospora crassa*. Eukaryot Cell *10*, 1100-1109.

Fujimura, M., Ochiai, N., Ichiishi, A., Usami, R., Horikoshi, K., and Yamaguchi, I. (2000). Fungicide resistance and osmotic stress sensitivity in *os* mutants of *Neurospora crassa*. Pestic. Biochem. Physiol. *67*, 125-133.

Grimshaw, S.J., Mott, H.R., Stott, K.M., Nielsen, P.R., Evetts, K.A., Hopkins, L.J., Nietlispach, D., and Owen, D. (2004). Structure of the sterile alpha motif (SAM) domain of the *Saccharomyces cerevisiae* mitogen-activated protein kinase pathway-modulating protein STE50 and analysis of its interaction with the STE11 SAM. J Biol Chem *279*, 2192-2201.

Jones, C.A., Greer-Phillips, S.E., and Borkovich, K.A. (2007). The response regulator RRG-1 functions upstream of a mitogen-activated protein kinase pathway impacting asexual development, female fertility, osmotic stress, and fungicide resistance in *Neurospora crassa*. Mol Biol Cell *18*, 2123-2136.

Krystofova, S., and Borkovich, K.A. (2005). The heterotrimeric G-protein subunits GNG-1 and GNB-1 form a Gbetagamma dimer required for normal female fertility, asexual development, and galpha protein levels in *Neurospora crassa*. Eukaryot Cell *4*, 365-378.

Li, D., Bobrowicz, P., Wilkinson, H.H., and Ebbole, D.J. (2005). A mitogen-activated protein kinase pathway essential for mating and contributing to vegetative growth in *Neurospora crassa*. Genetics *170*, 1091-1104.

Maerz, S., Ziv, C., Vogt, N., Helmstaedt, K., Cohen, N., Gorovits, R., Yarden, O., and Seiler, S. (2008). The nuclear Dbf2-related kinase COT1 and the mitogen-activated protein kinases MAK1 and MAK2 genetically interact to regulate filamentous growth, hyphal fusion and sexual development in *Neurospora crassa*. Genetics *179*, 1313-1325.

Miller, K.G., Emerson, M.D., McManus, J.R., and Rand, J.B. (2000). RIC-8 (Synembryn): a novel conserved protein that is required for G(q)alpha signaling in the *C. elegans* nervous system. Neuron *27*, 289-299.

Pandey, A., Roca, M.G., Read, N.D., and Glass, N.L. (2004). Role of a mitogen-activated protein kinase pathway during conidial germination and hyphal fusion in *Neurospora crassa*. Eukaryot Cell *3*, 348-358.

Park, G., Pan, S., and Borkovich, K.A. (2008). Mitogen-activated protein kinase cascade required for regulation of development and secondary metabolism in *Neurospora crassa*. Eukaryot Cell *7*, 2113-2122.

Posas, F., and Saito, H. (1998). Activation of the yeast SSK2 MAP kinase kinase kinase by the SSK1 two-component response regulator. EMBO J *17*, 1385-1394.

Qiao, F., and Bowie, J.U. (2005). The many faces of SAM. Sci STKE *2005*, re7.

Ramezani-Rad, M. (2003). The role of adaptor protein Ste50-dependent regulation of the MAPKKK Ste11 in multiple signalling pathways of yeast. Curr Genet *43*, 161-170.

Ramezani Rad, M., Jansen, G., Buhring, F., and Hollenberg, C.P. (1998). Ste50p is involved in regulating filamentous growth in the yeast *Saccharomyces cerevisiae* and associates with Ste11p. Mol Gen Genet *259*, 29-38.

Roca, M.G., Arlt, J., Jeffree, C.E., and Read, N.D. (2005). Cell biology of conidial anastomosis tubes in *Neurospora crassa*. Eukaryot Cell *4*, 911-919.

Tall, G.G., Krumins, A.M., and Gilman, A.G. (2003). Mammalian Ric-8A (synembryn) is a heterotrimeric Galpha protein guanine nucleotide exchange factor. J Biol Chem *278*, 8356-8362.

Vogel, H.J. (1964). Distribution of lysine pathways among fungi - Evolutionary implications. Am Nat *98*, 435-446.

Westergaard, M., and Mitchell, H.K. (1947). *Neurospora* . A Synthetic Medium Favoring Sexual Reproduction. American Journal of Botany *34*, 573-577.

Wilkie, T.M., and Kinch, L. (2005). New roles for Galpha and RGS proteins: communication continues despite pulling sisters apart. Curr Biol *15*, R843-854.

Wright, S.J., Inchausti, R., Eaton, C.J., Krystofova, S., and Borkovich, K.A. (2011). RIC8 is a guanine-nucleotide exchange factor for Ga subunits that regulates growth and development in *Neurospora crassa*. Genetics *189*, 165-176.

Zhang, Y., Lamm, R., Pillonel, C., Lam, S., and Xu, J.R. (2002). Osmoregulation and fungicide resistance: the *Neurospora crassa* os-2 gene encodes a HOG1 mitogen-activated protein kinase homologue. Appl Environ Microbiol *68*, 532-538.

Chapter 6

Conclusions and Future Directions

The main objective of this dissertation was to expand the knowledge of G protein signaling components and their effects on growth and development in filamentous fungi.

In Chapter 2, the analysis of G protein signaling components revealed *ric* 8, *gna-1*, *gna-3*,*gnb-1*, *gng-1*, and *rgs-1* to play a role in hyphal growth. This was the first in-depth study for qualitative and quantitative features in the negative regulators of G protein signaling. The development of novel image processing tools allowed the analysis of aspects in vegetative hyphal development never detected before. In addition, the expanding field of Video Bioinformatics allows development of faster and more accurate data from videos. These techniques were used to supplement other quantitative phenotypic data for G protein signaling components.

The results revealed several novel phenotypes, including larger cell compartment size in Δ*rgs-3*, Δ*rgs-4*, and Δ*rgs-5* mutants. Smaller compartment size was detected in Δ*gna-1* and Δ*ric8* mutants. These findings suggest that *rgs-3*, *rgs-4*, and *rgs-5* are the negative regulators, on *gna-1* and *ric8* in regulating cell size. Analyzing cell compartment size on *gna-1* and these *rgs* double mutants will reveal if the opposing effects restores the phenotype to wild type. The development of these tools can allow other groups of mutants to be analyzed, thus revealing novel information. Another future direction for this project would be to obtain strains expressing the GTPase deficient Gα alleles as well as all other double mutant combination (Gα and *rgs*) and analyze their hyphal

compartment size. For example, if observation of GTPase deficient GNA-1 led to larger cell compartment size, then one can assume that GNA-1 can be linked to RGS-3, -4, or -5. This hypothesis stems from knocking out any of these three *rgs*' leads to a large cell. Linking RGS and Gα genes will allow us to construct a regulatory mechanism for this complex pathway.

In Chapter 3, the phenotypic analysis of available G protein coupled receptor (GPCR) mutants was performed in an efficient manner by undergraduate students. Morphological as well as chemical assays were conducted. In addition, publically available data was used to determine expression patterns of the GPCR's during growth and development. A special interest was taken on the Pth11-related class of GPCRs. This study has expanded the knowledge of GPCRs, especially for the gene family related to pathogenesis (Pth11). Future directions consist of construction of double (or more) mutants that share expression patterns in order to observe other phenotypes, not visible before due to gene redundancy. In addition, performing RNAseq (RNA sequencing) on mutants, especially the Pth11-related mutants, will reveal which genes are affected, thus building an inter-related network.

In Chapter 4, we were the first fungal research group to fluorescently tag the Gα subunits and study their localization during early development. Using this approach, we were able to localize GNA-1, GNA-2 and GNA-3 during conidial germination, revealing that all three Gα proteins localize to the plasma membrane in ungerminated conidia and young germlings. GNA-1 was also detected in septa in older hyphae. Further studies will look at other proteins also known to function in septa formation, such as cytoskeletal

components. Actin cables were found to associate with Tropomyosin and class II myosin at septa (Delgado-Alvarez *et al.*, 2014). Current GFP Lifeact-fused cytoskeletal protein strains are currently available (Delgado-Alvarez *et al.*, 2014). GNA-1-TagRFP strain can be fused with the GFP Lifact proteins to confirm co-localization to the septa. In addition, protein-protein interaction studies can be conducted via co-immunoprecipitation using GFP trap agarose beads (Cat# gta-20, ChromoTek, Planegg-Martinsried, Germany), and probing for the presence of GNA-1. All three Gα subunits were also detected in vacuoles, therefore further investigation is needed to decipher the function in vacuoles; are the proteins being degraded or do they serve a function? In addition, the most intriguing finding was the observation of patches of GNA-3-TagRFP on the plasma membrane at later time points during germination of conidia. This change in localization during the transition from conidium to germling may be related to the requirement for GNA-3 during conidial germination; further analysis is necessary to explore this hypothesis.

Lastly, in Chapter 5, two genes- *ric8* and *ste50* were further investigated for interaction, morphological phenotypes, and downstream effects on the mitogen-activated protein kinase (MAPK) cascade. Although, I was unable to confirm protein-protein interaction via co-immunoprecipitation, other conditions may be sought in order to find interaction. Further investigation, such as fixing the sample, for example using formaldehyde, may aid in seeing a transient interaction. Different buffers may be also utilized to stabilize the protein complex. Another approach to confirm protein-protein interaction would be to visualize their interaction *in vivo*, by the means of bimolecular fluorescence complementation (BiFC). BiFC utilizes a system, where two interacting

proteins will bring together a fully intact fluorescent protein, thus visualizing the interaction in real time. This system has been successfully used in *N. crassa* to confirm interaction amongst proteins (Bardiya *et al.*, 2008).

References

Bardiya, N., Alexander, W.G., Perdue, T.D., Barry, E.G., Metzenberg, R.L., Pukkila, P.J., and Shiu, P.K. (2008). Characterization of interactions between and among components of the meiotic silencing by unpaired DNA machinery in *Neurospora crassa* using bimolecular fluorescence complementation. Genetics *178*, 593-596.

Delgado-Alvarez, D.L., Bartnicki-Garcia, S., Seiler, S., and Mourino-Perez, R.R. (2014). Septum development in *Neurospora crassa*: the septal actomyosin tangle. PLoS One *9*, e96744.

Appendix A: Phenotypic analyses on the regulators of G protein signaling mutants

Overview

The focus of this study is phenotypic analysis of the negative regulators in the G protein signaling pathway. Regulators of G protein signaling (RGS) proteins are the major components for the inactivation of the G protein cycle. There is currently no published data on the characterization of the RGS genes in *N. crassa*. Phenotypic studies on growth, female fertility, and germination were conducted. Previous work in our group has shown that loss of the Gβ, Gɣ subunit or *ric8* leads to lower levels of Gα proteins (Krystofova and Borkovich, 2005; Wright *et al.*, 2011) . Since RGS proteins negatively regulate Gα subunits, it was possible that RGS mutants might have elevated levels of Gα proteins. Therefore, I also checked levels of two Ga proteins in the plasma membrane fraction of the RGS mutants.

Materials and Methods

Phenotypic analysis: Phenotypic assays were conducted as described in the legends to figures. Media were inoculated with conidia from 5-7 day old VM flask cultures.

rgs knock-out mutants were obtained as homokaryons from the FGSC. Southern analysis was conducted by former graduate student Sara Wright to confirm the proper

gene knockout. The Δ*rgs-5* knockout strain was confirmed via Southern analysis by former graduate student Liande Li.

Western analysis: Strains were cultured in VM flasks for a 8 days, after which conidia were collected using a cheesecloth filter affixed to a flask. Conidia were subjected to two independent washes, with a 5 minute spin at 2500 RPM in between. Conidia were then counted using a hemacytometer and inoculated at a concentration of $1x10^6$ cells/mL in a 250mL flask containing 100 mL of VM liquid medium and then grown with shaking at 250 RPM for 16 hours at 30°C. The Δ*rgs*-2 mutant did not produce enough conidia to inoculate, therefore it was not included in this study. Subsequent experiments revealed no changes in GNA-1 protein levels were present in the Δ*rgs*-2 mutant background (data not shown). Tissue was collected and frozen using liquid nitrogen. Tissue was then placed in the bead beater with approximately 30% of the container packed with glass beads. Tissue was blended 3x for 30 seconds with 1 minute rests in between. A series of centrifugations were performed to obtain the plasma membrane fraction (Figure A.3). The plasma membrane extract containing 50 µg of protein in sample buffer (62.5 mM Tris-HCl [pH 6.8], 10% glycerol, 2% SDS, 1% β-mercaptoethanol, 0.005% bromphenol blue), was subjected to a 10% acrylamide sodium dodecyl sulfate-polyacrylamide gel electrophoresis (SDS-PAGE), then transferred to a 0.45µm nitrocellulose membrane and probed with the GNA-1 or GNA-2 antibody. The Western blot protocol was as described in Wright et al. 2011.

RGS knockout mutants were crossed to Δ*gna-1,* Δ*gna-2,* and Δ*gna-3* Gα mutants, using as the RGS mutant as the female, except in the case of Δ*rgs*-1 and Δ*rgs*-2, where they were used as males. See Table 2.1 for details. The Δ*gna-1* helper strain was used as the female when both strains were female sterile (see Table 2.1). Additionally, RGS mutants were crossed with other *rgs* knockout mutants, in order to make *rgs* double mutants. Table A.1 summarizes all the completed crosses with confirmed double mutants in silica storage. Primers used for diagnostic PCRs are listed in Table A.2.

Results

A 24 hour growth assay revealed that all but one of the *rgs* mutants demonstrates a growth defect (Figure A.1). Δ*rgs-5* showed the smallest growth defect amongst the *rgs* mutants, most resembling the wild type (Figure. A.1). Δ*gna-2* is the only Gα mutant which resembles wild type. Δ*gna-1* and Δ*gna-3* have a smaller colony than wild type (Wright *et al.*, 2011). Analyzing GTPase deficient alleles will give further insight to which *rgs* mutant it resembles. A female fertility assay revealed that Δ*rgs-1* does not produce protoperithecia, thus causing it to be female-sterile, while Δrgs-*2* produces fewer perithecia than wild type (Figure. 2.2, Figure 2.3). This finding suggests roles for both *rgs-1* and *rgs-2* in the female reproductive cycle, due to both genes affecting the presence and abundance of protoperithecia respectively.

Microscopic analysis revealed that spore germination is affected in all RGS mutants (Figure. A.3). Formation of conidial anastomosis tubes (CATs) is a major event

that occurs during conidial germination (Fleissner *et al.*, 2009). Neighboring conidia sense one another via these CATs. CATs fuse with each other, thus exchanging nuclei and other cytoplasmic material, which includes nutrients. Δ*rgs-3* and Δ*rgs-4* mutants produce significantly amount of CATs than wild-type (Figure. A.2). In addition to CAT defects, Δ*rgs-1*, Δ*rgs-2*, and Δ*rgs-5* mutants have a wider germ tube than wild-type. Although, in (Eaton *et al.*, 2012) quantification of germ tubes were not conducted, both Δ*gna-1* and Δ*gna-3* did have a germination defect, as they grew slower than wild type.

Protein levels for GNA-1 and GNA-2 were checked in the plasma membrane fraction of the RGS mutants. There are no obvious differences in GNA-2 protein levels in any of the RGS mutants. However, Δ*rgs-1* appears to have a slight increase in GNA-1 protein levels compared to wild type, thus suggesting possible regulation of RGS-1 on GNA-1 (Figure A.4).

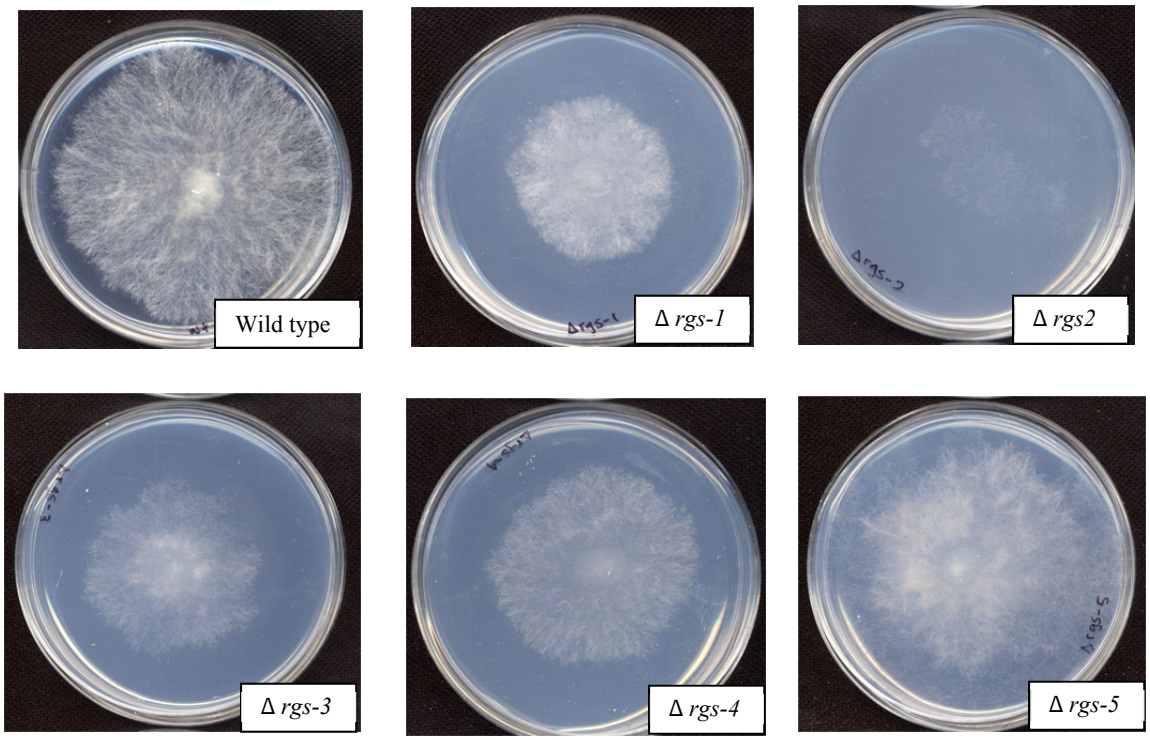

Figure A.1: Growth analysis assay.

Strains were inoculated in the center of the VM agar plate, and allowed to grow for 24 hours at 30°C in the dark. *rgs-1*, Δ*rgs-2*, Δ*rgs-3* and Δ*rgs-4* mutants have a smaller colony diameter than wild type.

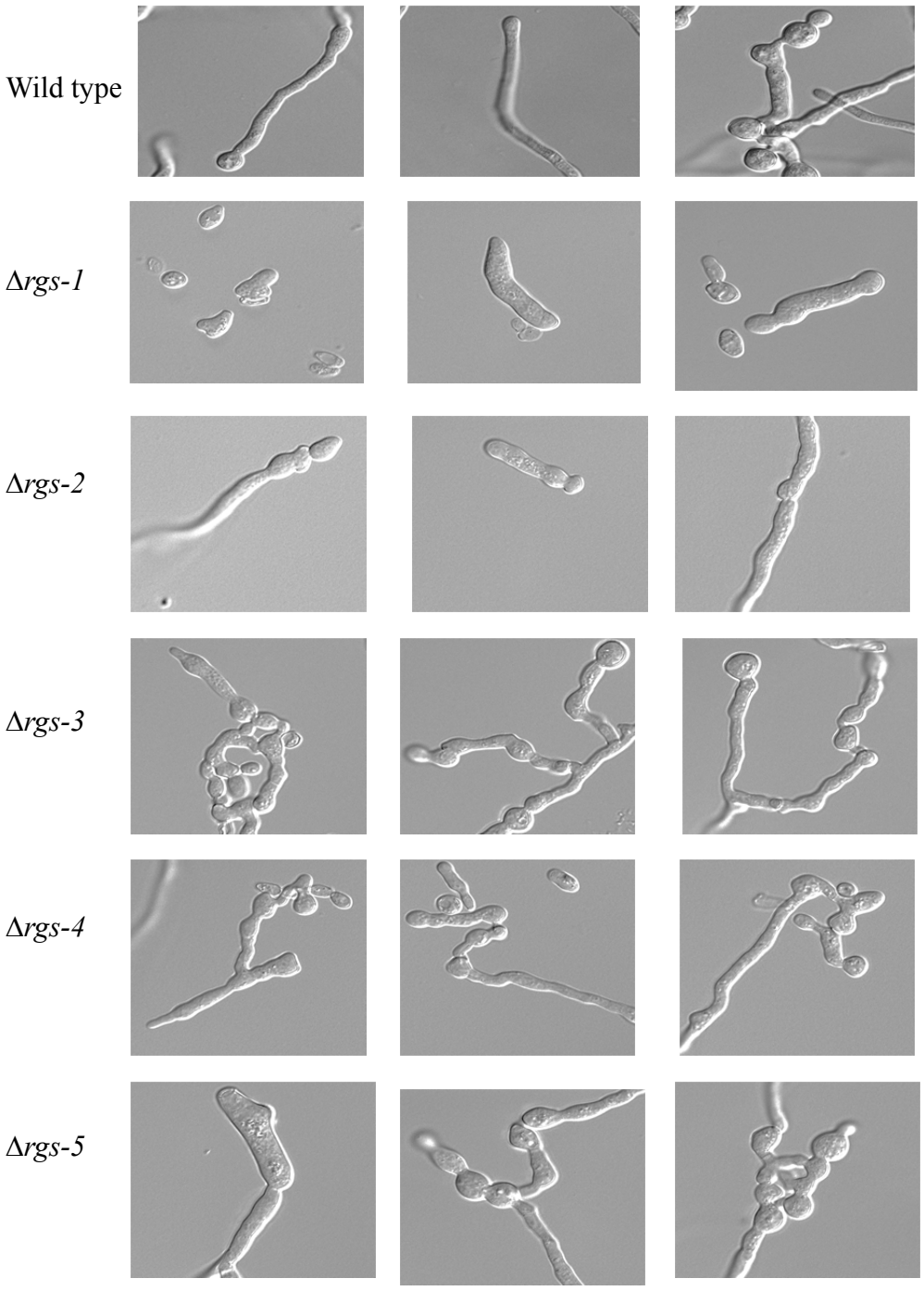
Wild type
Δrgs-1
Δrgs-2
Δrgs-3
Δrgs-4
Δrgs-5

Figure A.2: Spore germination analysis.

Conidia were collected from all strains (wild type and five RGS mutants), and plated on VM-agarose plates. Plates were incubated for 8 hours at 30°C in the dark. Differential interference contrast (DIC) images were taken using an Olympus 1X71 inverted microscope. *rgs-1*, *rgs-2*, and *rgs-5* mutants appear to have a thicker germ tube than wild-type. Other noticeable phenotypes were that *rgs-3* and *rgs-4* mutants produce a greater amount of conidial anastomosis tubes (CATs) than wild type.

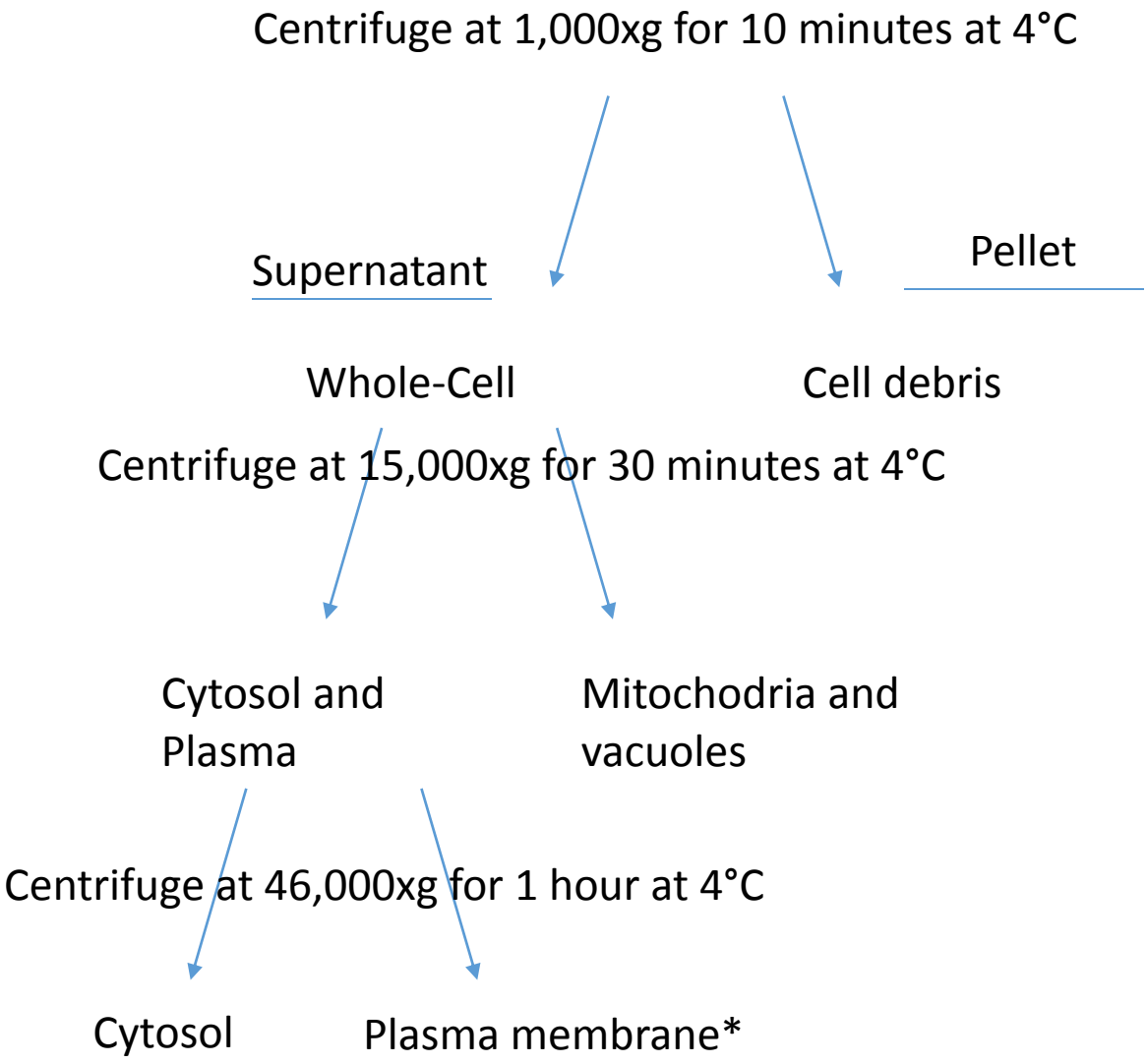

Figure A.3: Schematic of the centrifugation process used to obtain the plasma membrane fraction.

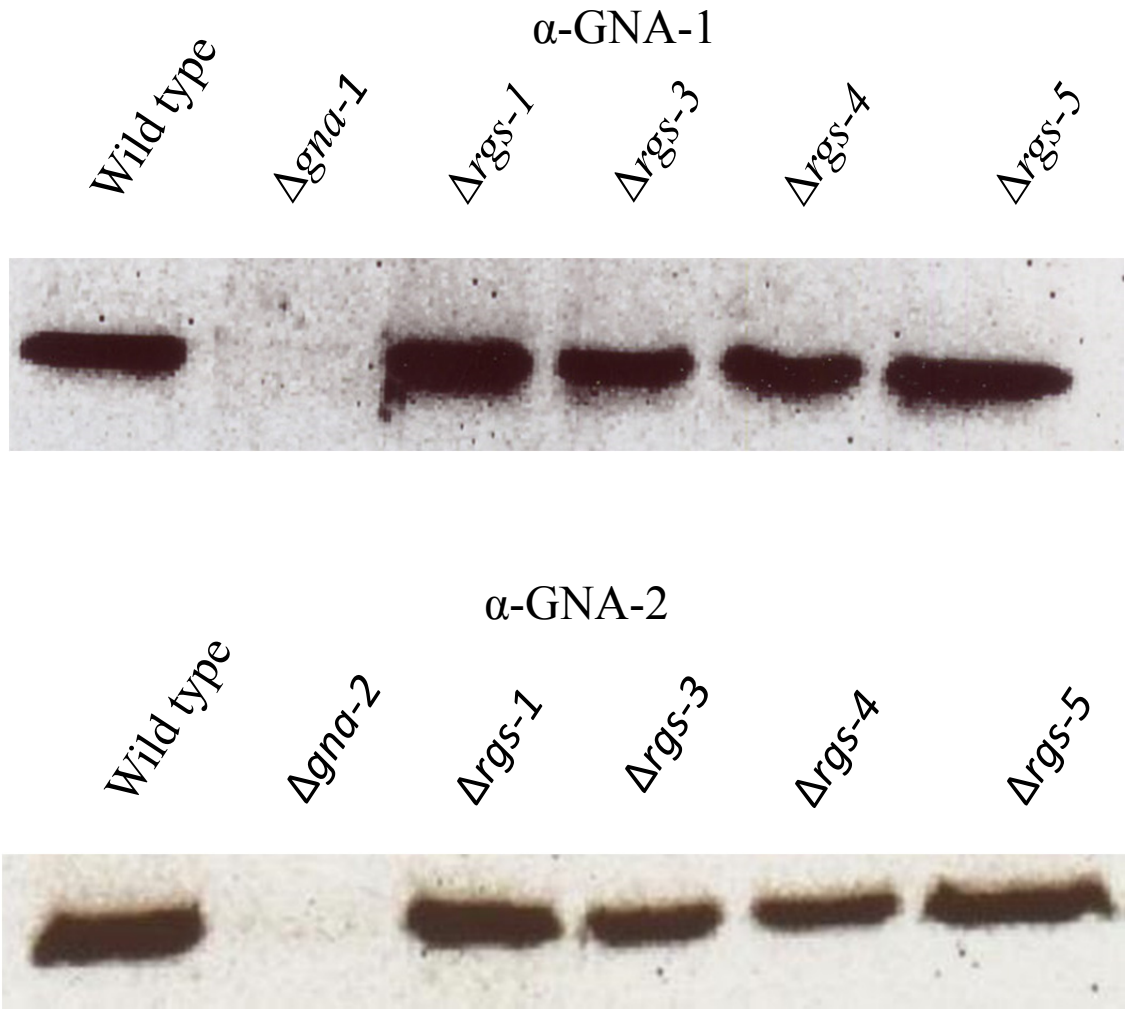

Figure A.4: Gα Protein levels.

Samples containing 50 micrograms of plasma membrane protein extract were electrophoresed on a 10% SDS-PAGE gel. The gel was blotted on to nitrocellulose and subjected to Western analysis with a rabbit anti-GNA-1 (top panel) or rabbit-anti-GNA-2 (bottom panel) antibody. Strains used are found in Table 2.1.

Table A.1: Summary of double mutants. Highlighted boxes are confirmed double mutants. NA are not currently available strains. X denote already made strains by KAB lab members.

	Δ*rgs-1*	Δ*rgs-2*	Δ*rgs-3*	Δ*rgs-4*	Δ*rgs-5*	Δ*gna-1*	Δ*gna-2*	Δ*gna-3*
Δ*rgs-1*	-							
Δ*rgs-2*		-						
Δ*rgs-3*			-					
Δ*rgs-4*				-				
Δ*rgs-5*			NA		-			
Δ*gna-1*					NA	-		
Δ*gna-2*				NA		X	-	
Δ*gna-3*				NA		X	X	-

Table A.2: Primers used for confirmation PCRs.

Gene	Primer Name	Sequence (5'-3')
rgs-1	rgs-1 FW diagnostic	TTCAGAAAGCCCCAGACCGCGACG
rgs-1	rgs-1 RV diagnostic	CCCTGGGGTGATTGATACACTCATC
rgs-2	rgs-2 FW diagnostic	GAAACCTTGGCTCTTGTCTTGTCG
rgs-2	rgs-2 RV diagnostic	GTCCGGTATGGAAAGCAGTC
rgs-3	rgs-3 FW diagnostic	GTAAGCGAACTCCTTGATCTCCTTG
rgs-3	rgs-3 RV diagnostic	GACAGGCTCGTGTGACTTTCTCATC
rgs-4	rgs-4 FW diagnostic	GGCTCATGCCAACCCTTTCTCCG
rgs-4	rgs-4 RV diagnostic	CTCCCGTTTCACTACTACATGCCC
rgs-5	rgs-5 FW diagnostic	CCTGTCCCTGGAGAAAGTCCGTC
rgs-5	rgs-5 RV diagnostic	ATGATCTTCGGTGTCTGTCCCCCG
gna-1	gna-1 FW diagnostic	ATAGAGAGGGTCTCGAAGG
gna-1	gna-1 RV diagnostic	CCTAGTGGCTTGAAGG
gna-2	gna-2 FW diagnostic	CAGAAATGGAACCTACCAGG
gna-2	gna-2 RV diagnostic	GCAGTCGCTTACAACC
gna-3	gna-3 FW diagnostic	CGACTTTTCTTCCTTCCAGC
gna-3	gna-3 RV diagnostic	GATACGGAAACCAGGCTGC
*hph**	hph end FW	CGCCCCAGCACTCGTCCGAGGGC
*hph**	hph end RV	GGCATTCATTGTTGACCTCCA

**hph* primers were designed for use by the Neurospora genome project.

References

Eaton, C.J., Cabrera, I.E., Servin, J.A., Wright, S.J., Cox, M.P., and Borkovich, K.A. (2012). The guanine nucleotide exchange factor RIC8 regulates conidial germination through Galpha proteins in *Neurospora crassa*. PLoS One *7*, e48026.

Fleissner, A., Diamond, S., and Glass, N.L. (2009). The Saccharomyces cerevisiae PRM1 homolog in Neurospora crassa is involved in vegetative and sexual cell fusion events but also has postfertilization functions. Genetics *181*, 497-510.

Krystofova, S., and Borkovich, K.A. (2005). The heterotrimeric G-protein subunits GNG-1 and GNB-1 form a Gbetagamma dimer required for normal female fertility, asexual development, and galpha protein levels in *Neurospora crassa*. Eukaryot Cell *4*, 365-378.

Wright, S.J., Inchausti, R., Eaton, C.J., Krystofova, S., and Borkovich, K.A. (2011). RIC8 is a guanine-nucleotide exchange factor for Galpha subunits that regulates growth and development in *Neurospora crassa*. Genetics *189*, 165-176.

Appendix B: Prediction of gene functions using phenomics in the model filamentous fungus, *Neurospora crassa*

Overview

Neurospora crassa has 9733 predicted genes. The goal of the Neurospora Genome project, funded by a NIH P01, was to knockout all of the genes within its genome. Mutants for nearly 9000 genes are currently available at the Fungal Genetics Stock Center (http://www.fgsc.net/). All knockout mutants contain deletions of the gene open reading frame, with replacement by an *hph* marker, conferring resistance to hygromycin (Colot *et al.*, 2006; Collopy *et al.*, 2010).

A second goal of the Neurospora Genome Project was to perform phenotypic characterization of knockout mutants. An undergraduate research program at the University of California, Los Angeles, pioneered methods for phenotyping mutants, with 1,200 mutants analyzed (Turner, 2011). This data is available on the Neurospora Broad Database, but has not been otherwise analyzed or interpreted using statistical clustering methods.

In our laboratory, we have used the phenotypic methods developed by the UCLA project to analyze additional mutants lacking serine/threonine protein kinases, serine/threonine and tyrosine protein phosphatases, G protein coupled receptors and transcription factors (unpublished; Park *et al.*, 2011; Ghosh *et al.*, 2014; Cabrera, 2015). Our goal was to determine whether unknown information about gene

relationships could be obtained through statistical clustering approaches, such as Principal Components Analysis (PCA). PCA manipulates a set of variables (observations) into an orthogonal transformation, in order to visualize correlations based on variance (Jollife, 2002). In our study, quantitative and qualitative features for the kinases, phosphatases, G protein coupled receptors, and transcription factors were organized and analyzed using PCA.

Quantitative phenotypes for mutants are linear growth rate, aerial hyphae height on VM and aerial hyphae height on VM supplemented with yeast extract. Qualitative phenotypes are conidia abundance, protoperithecia production, perithecia production, and ascospore production. Three known Mitogen-Activated Protein Kinase (MAPK) pathway components (MAK-1, MAK-2, and OS-2) were used as positive controls in our study.

Materials and Methods

Growth and Morphological Phenotypes:

Phenotypic methods were as described for the group of knockout mutants published at the Broad Neurospora Database (Turner, 2011). We collected morphological and developmental phenotypes for all available transcription factors, [251 genes; (Colot *et al.*, 2006); unpublished], serine-threonine protein kinases [86 genes; (Park *et al.*,

2011)], serine- threonine and tyrosine protein phosphatases [30 genes; (Ghosh *et al.*, 2014)] and G protein coupled receptors [GPCRs; 33 genes; (Cabrera, 2015)].

Principal Components Analysis:

Statistical analysis was conducted with Minitab 17 software (2010). Qualitative morphological phenotypes were converted into numerical values, with normal = 1, abnormal = 0.5 and none = 0. Each quantitative data set (growth rate and aerial hyphae on VM and YE) was divided by its wild type, in order to obtain the data as relative to its wild type in growth. The dataset was then mean-centered, thus resulting in the mean of that sample being equal to zero. Mean centering involves taking the average of that dataset, and then subtracting the mean from the original data point. A correlation matrix was used, as all variables used were considered equally important (Chatfield, 1980).

Results

Table B.1 shows how much the variance is explained by each component. With four components, one can explain over 90% of the variance in the sample, an ideal situation. Due to limited visualization capabilities, the score plot (Figure B.1) is portrayed as a two-dimensional image.

The internal control for this study was to make sure that the three individual components of each MAPK cascade group together. The *mak-1*/*mek-1*/*mik1*; *mak-*

2/*mek-2*/*nrc-1* and *os-2*/*os-4*/*os-5* groups comprise the three MAPK cascades (Zhang *et al.*, 2002; Pandey *et al.*, 2004; Li *et al.*, 2005; Maerz *et al.*, 2008; Park *et al.*, 2008). We know from previous work that mutating one gene in each pathway results in the same phenotype as any other mutant in the same cascade. It is clear that the MAPK cascade components for the same pathway group together in the PCA plot, with the MAK-2 and MIK-1 components overlapping (left) and the OS-2 cascade separated. Wild type is labeled (right side, Figure B.1). As seen in Figure B.1, the majority of mutants cluster near wild type due to the fact that they do not have a distinguishable phenotype. All GPCRs are underneath the wild type cluster. There are two large distinct groups with a third group that include Protein Kinase A (pkac-1; bottom), (Figure B.1). Also, studies have found possible interaction of PP-1 and MAK-2 (Li *et al.*, 2005). Both mutants have slow growth rate, short aerial hyphae, and are female sterile (red arrow). Both *mak-2* and *pp-1* are in the large cluster to the left.

Mutants that cluster nearby the MAPK components have similar phenotypes, thus implying possible function in the same pathway. Follow up studies must be conducted in order to confirm this hypothesis. Molecular analyses, such as assays, that measure phosphorylation of the three terminal MAPK proteins (discussed in Chapter 5) could be used to link a particular mutant to a MAPK pathway. Additional studies could include constructing double mutants with genes that cluster with one another. The hypothesis is that a double mutant lacking two genes functioning in the same pathway will have a similar phenotype as both single mutants, whereas a double

mutant with genes functioning in different pathways may have a more severe phenotype. Lastly, other multi-variate tools can be used for statistical analysis such as Unsupervised Random Forests. Unsupervised Random Forests does not require a training set, generates classes of observations (trees) and then uses majority voting to assign observations to each tree (Shi T., 2006; Dinsdale, 2013). Results can be visualized using a two-dimensional plot.

Table B.1: Total variance for each component

	Component 1	Component 2	Component 3	Component 4	Component 5	Component 6	Component 7
Variance Explained	57.10%	77.40%	86.20%	92.20%	95.60%	98.80%	100%

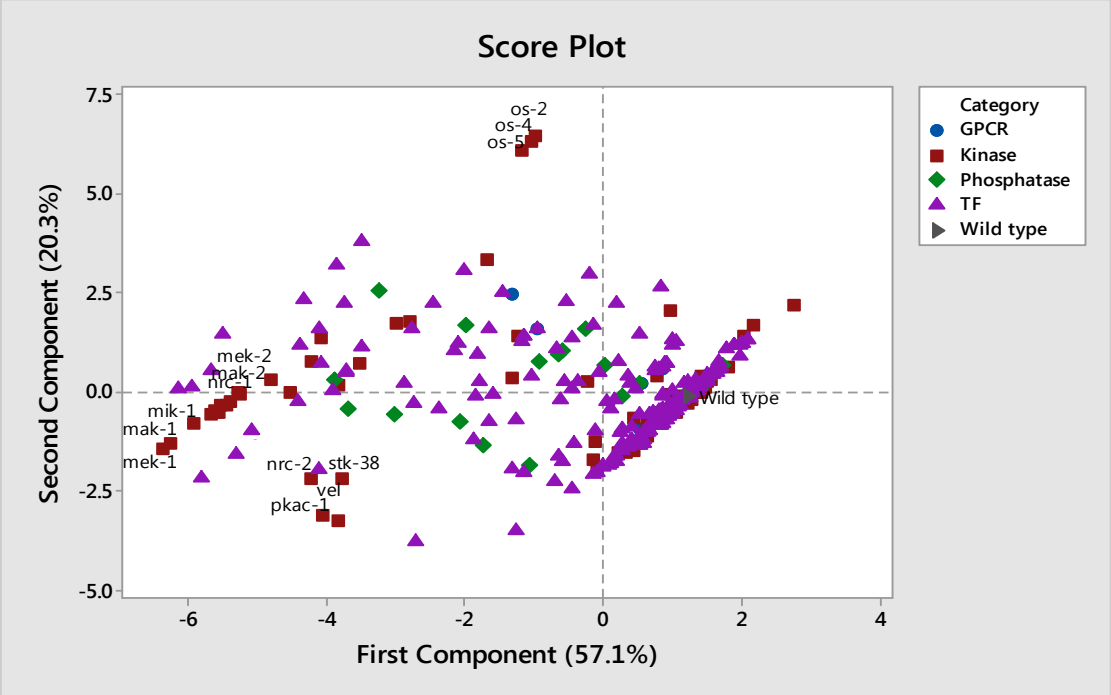

Figure B.1: Principal component analysis score plot.

Analysis of results showing the first two components for of all mutants.

References

(2010) Minitab 17 Software. State College, PA: Minitab, Inc. (www.minitab.com)

Cabrera, I.E., Itallia V. Pacentine , Andrew Lim , Nayeli Guerrero , Svetlana Krystofova , LIande Li , Alexander V. MIchkov , Jacqueline A. Servin , Mr. Steven R. Ahrendt , Alexander J. Carrillo , Liza M. Davidson , Andrew H. Barsoum , Jackie Cao , Ronald Castillo , Wan-Ching Chen , Alex Dinkchian , Stephanie Kim , Sho M. Kitada , Taffani H. Lai , Ashley Mach , Cristin Malekyan , Toua R. Moua , Carlos Rojas Torres , Alaina Yamamoto, and Katherine A. Borkovich. (2015). Global analysis of predicted G protein coupled receptor genes in the filamentous fungus, *Neurospora crassa*. Submitted.

Chatfield, A.a.C., A.J. (ed.) (1980). Introduction to Multivariate Analysis. Chapman and Hall Association with Methuen, Inc.: New York, NY.

Collopy, P.D., Colot, H.V., Park, G., Ringelberg, C., Crew, C.M., Borkovich, K.A., and Dunlap, J.C. (2010). High-throughput construction of gene deletion cassettes for generation of *Neurospora crassa* knockout strains. Methods Mol Biol *638*, 33-40.

Colot, H.V., Park, G., Turner, G.E., Ringelberg, C., Crew, C.M., Litvinkova, L., Weiss, R.L., Borkovich, K.A., and Dunlap, J.C. (2006). A high-throughput gene knockout procedure for *Neurospora* reveals functions for multiple transcription factors. Proc Natl Acad Sci U S A *103*, 10352-10357.

Dinsdale, E.A., Edwards R.A., Bailey B.A., Tuba I., Akhter S., McNair K., Schmieder R., Apkarian N., Creek M., Guan E., Hernandez M., Isaacs K., Peterson C., Regh T., Ponomarenko V. . (2013). Multivariate analysis of functional metagenomes. . Frontiers in genetics *4*.

Ghosh, A., Servin, J.A., Park, G., and Borkovich, K.A. (2014). Global analysis of serine/threonine and tyrosine protein phosphatase catalytic subunit genes in *Neurospora crassa* reveals interplay between phosphatases and the p38 mitogen-activated protein kinase. G3 (Bethesda) *4*, 349-365.

Jollife, I.T. (2002). Principal Component Analysis. Springer: NY.

Li, D., Bobrowicz, P., Wilkinson, H.H., and Ebbole, D.J. (2005). A mitogen-activated protein kinase pathway essential for mating and contributing to vegetative growth in *Neurospora crassa.* Genetics *170*, 1091-1104.

Maerz, S., Ziv, C., Vogt, N., Helmstaedt, K., Cohen, N., Gorovits, R., Yarden, O., and Seiler, S. (2008). The nuclear Dbf2-related kinase COT1 and the mitogen-activated protein kinases MAK1 and MAK2 genetically interact to regulate filamentous growth, hyphal fusion and sexual development in *Neurospora crassa*. Genetics *179*, 1313-1325.

Pandey, A., Roca, M.G., Read, N.D., and Glass, N.L. (2004). Role of a mitogen-activated protein kinase pathway during conidial germination and hyphal fusion in *Neurospora crassa*. Eukaryot Cell *3*, 348-358.

Park, G., Pan, S., and Borkovich, K.A. (2008). Mitogen-activated protein kinase cascade required for regulation of development and secondary metabolism in *Neurospora crassa*. Eukaryot Cell *7*, 2113-2122.

Park, G., Servin, J.A., Turner, G.E., Altamirano, L., Colot, H.V., Collopy, P., Litvinkova, L., Li, L., Jones, C.A., Diala, F.G., Dunlap, J.C., and Borkovich, K.A. (2011). Global analysis of serine-threonine protein kinase genes in *Neurospora crassa*. Eukaryot Cell *10*, 1553-1564.

Shi T., H.S. (2006). Unsupervised learning with random forest predictors. J. Comput. Graph Stat. , 118-138.

Turner, G.E. (2011). Phenotypic analysis of *Neurospora crassa* gene deletion strains. Methods Mol Biol *722*, 191-198.

Zhang, Y., Lamm, R., Pillonel, C., Lam, S., and Xu, J.R. (2002). Osmoregulation and fungicide resistance: the *Neurospora crassa* os-2 gene encodes a HOG1 mitogen-activated protein kinase homologue. Appl Environ Microbiol *68*, 532-538.